Experimental Evaluation of a Trailing-Arm Suspension for Heavy Trucks

Jeffrey L. Glass

Thesis submitted to the Faculty of the Virginia Polytechnic Institute and State University in partial fulfillment of the requirements for the degree

Master of Science
in
Mechanical Engineering

Approved:

_____
Mehdi Ahmadian
Chairman

_____ _____
Daniel J. Inman Donald J. Leo

May 8, 2001
Blacksburg, Virginia

Keywords: Trailing-Arm Suspension, Heavy Truck, Dynamic, Kinematics, Test Analysis, Ride

Experimental Evaluation of a Trailing-Arm Suspension for Heavy Trucks

by

Jeffrey L. Glass

Mehdi Ahmadian, Chairman

Mechanical Engineering

This study includes an experimental evaluation of a prototype trailing-arm suspension for heavy trucks. The primary goal of this new suspension is to match or improve the kinematics and dynamic performance of an existing "Z-bar" suspension. Significant reductions in cost, weight, and number of parts are the main reasons for this redesign.

A permanent facility is constructed to support the testing of different heavy truck suspensions. For actuation of the vehicle suspension, hydraulic actuators are used in the kinematics tests in a quasi-dynamic manner. For the dynamic tests, the vehicle is excited using two hydrodynamic actuators. A collection of forces, displacements, velocities, and accelerations are measured during the tests using transducers that were installed on the suspension and test vehicle. The test measurements are analyzed in both time and frequency domains and then the results of the two suspensions were compared to establish the dynamic merits of the prototype suspension.

The kinematics tests include vertical stiffness, roll stiffness, and roll steer measurements for each suspension. The results from the kinematics tests show that the trailing-arm suspension exhibits kinematics traits that are quite similar to the "Z-bar" suspension, within the context of the tests conducted in the study.

The dynamic testing consists of three input signals commonly used for such tests, namely: a chirp signal input, a step signal input, and a range of pure tone inputs. The test results show that the resonant frequencies of the two primary suspensions differ by an amount that is most likely too small to affect ride dynamics. The two suspensions, however, exhibit significantly different damping characteristics. The new suspension has much less frictional damping than the existing suspension. This is expected to provide better ride characteristics, assuming that the primary dampers (shock absorbers) are properly tuned for the vehicle that the new suspension was designed for.

Acknowledgments

Without the significant help and support of my advisor, Dr. Mehdi Ahmadian, this project would never have succeeded in so many ways. His guidance helped me to become more confident in my own abilities and develop the independence that I now enjoy. My apologies extend to him for his brief, yet thrilling, ride on an errant hydraulic actuator.

My graduate committee members, Drs. Daniel Inman, Alfred Wicks, and Donald Leo, deserve special thanks as well. Dr. Inman's much appreciated sense of humor never faltered through even the most demanding class lectures. As long as his Mother-in-Law does not see the class tapes, everything should be fine. Dr. Wicks always challenged my understanding of class material and never let me get away with nodding in blissful ignorance. Unfortunately, complications arose that prevented Dr. Wicks from remaining a member of my committee. Dr. Leo graciously accepted our request for him to replace Dr. Wicks at such a late stage of the program. Many thanks for his help; he is a valuable addition to my committee.

I would also like to thank Volvo Heavy Trucks for providing the major project funding and the drive behind this research. Generous contributions from Unimeasure, PCB, and Futek provided us with the additional hardware that we needed. Also, Dave, Nando, and the other guys in the AVDL and VTTI really made this project work.

On a personal note, Jen, you are my favorite sister and you know I think the world of you. Many thanks go to my parents, Wayne and Kathy Glass, for their immense support. Drew Zima also needs special recognition for putting up with me for the last two years, but at least the abuse was mutual. Thanks to my good friends B.J. Dabney and Kris Mount, and to everyone else that has helped make these last two years so great...

Contents

List of Tables

List of Figures

Chapter 1
Introduction

1.1 Overview

This study is an experimental evaluation of a prototype trailing-arm suspension for heavy trucks. The intent of this new suspension is to reproduce the same kinematics and dynamic performance of the current "Z-bar" suspension. Significant reductions in cost, weight, and number of parts are the main driving forces behind this major redesign.

A vehicle's primary suspension, which is responsible for supporting the substantial static loads, is the system that most significantly affects ride quality. Ride quality is the combination and compromise of stability and comfort for a vehicle. This quality is the overall "feel" of the vehicle. Methods for obtaining ride quality are some of the most guarded secrets of a suspension designer. Ride quality can be linked, directly or indirectly, to driver fatigue, tire wear, maximum payload capabilities, pavement damage, and myriad other factors that concern designers. Once a manufacturer has established the ride quality for a given vehicle, the customers identify it with the brand, just as they identify manufacturing quality, service, and the overall look of a vehicle.

Other significant aspects of the suspension, such as roll stiffness and roll steer (both of which relate directly to vehicle safety), are inherent in the kinematics of the suspension. The physical dimensions of a suspension and the stiffness of its components define a suspension's kinematics traits.

For all of these reasons, it is important that the new trailing-arm suspension exhibits the same kinematics and dynamic characteristics as the current production

suspension. By testing the kinematics and the dynamics of both suspensions, this study will show whether or not the trailing-arm suspension successfully achieves this goal.

1.2 Goals

There are several overall goals of this study:

1) build a permanent facility capable of supporting the necessary tests for this study as well as any future work,
2) perform sufficient kinematics and dynamic comparisons of the two suspensions to determine any differences and record results, and
3) provide a well-documented set of procedures so that the same tests can be performed on other trucks at a later date.

1.3 Approach

In order to achieve these goals, a facility must be available with enough space to accommodate a Class 8 road tractor. Figure 1-1 shows an example of such a vehicle in our facility. There must also be room for the required test equipment. This equipment includes a suitable structure to ground the vehicle's frame for the kinematics testing. Adding and removing weight from the vehicle is performed using this structure, as well. This structure is visible in the background of Figure 1-1, but is more clearly seen in Figure 1-2. The weights simulate trailer load at the fifth wheel of the truck for dynamic testing.

Once the formats for the suspension tests are finalized, required equipment not already on hand must be purchased. As long as all equipment necessary to support the tests is available, the facility will suit the needs of this study.

Figure 1-1 Class 8 Road Tractor in Test Facility.

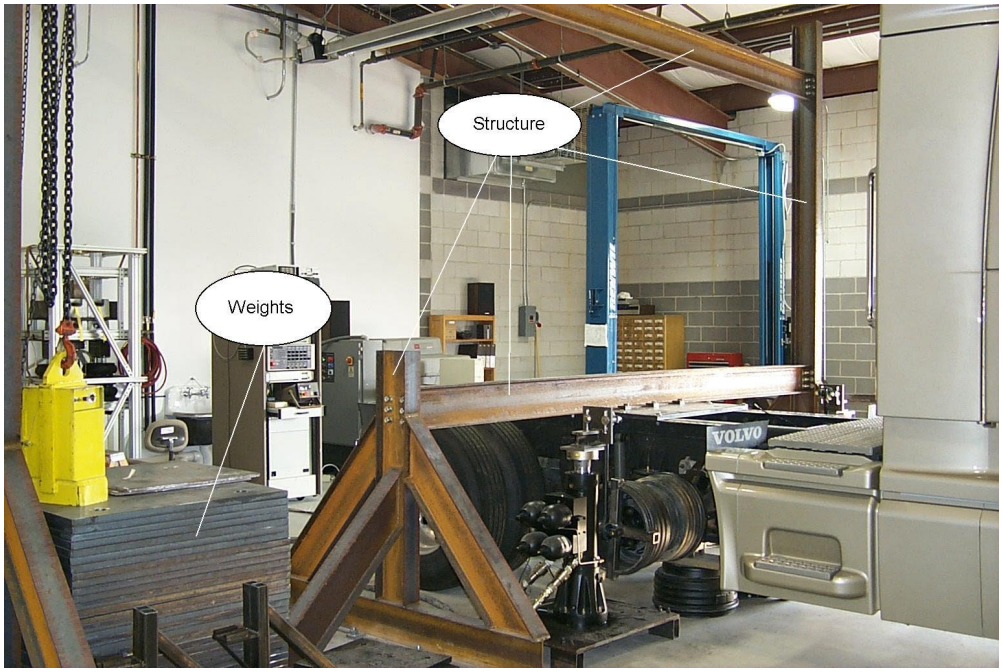

Figure 1-2 Structure for Kinematics Tests and Moving Weights.

After the test facility is established, the testing will be performed. First, the testing of the kinematics of the "Z-bar" suspension will be completed. Next, the trailing-arm suspension will be tested. The results of both sets of tests will be compared and recorded. The tests of each suspension's dynamic characteristics will be conducted in the same manner.

As the tests progress, the procedures undertaken in both the kinematics and dynamic tests will be documented. This documentation will provide a detailed set of instructions should someone want to recreate the tests on another truck or some other vehicle.

1.4 Outline

This thesis consists of six chapters. Chapter 2 provides background information significant to this project. This includes a description of the tests conducted in this study, as well as detailed definitions of vehicle ride, the current "Z-bar" suspension, and the prototype trailing-arm suspension. In addition, Chapter 2 includes a literature review of research in several areas of vehicle testing. Chapter 3 includes all the details of the test setup. This chapter goes into sufficient depth to allow someone to recreate the setup if desired. All of the results for the kinematics tests are discussed in Chapter 4. Further, Chapter 4 includes the kinematics test arrangements, the data that was collected, the reduction of the data, and the significant findings of the kinematics tests. In a similar manner, Chapter 5 covers all of the dynamic testing results and their supporting information. Chapter 6, the final chapter of this study, presents concluding remarks and suggests possible future studies.

Chapter 2

Background

The information contained in Chapter 2 lends support that may be necessary to the understanding of this study. For a mapping of the chapter, refer to Figure 2-1. Vehicle ride is covered in depth, prior to a description of "Z-bar" and trailing-arm suspensions. In addition, a discussion of the tests conducted in this study precedes review of literature concerning other research that has been conducted on heavy vehicle suspensions.

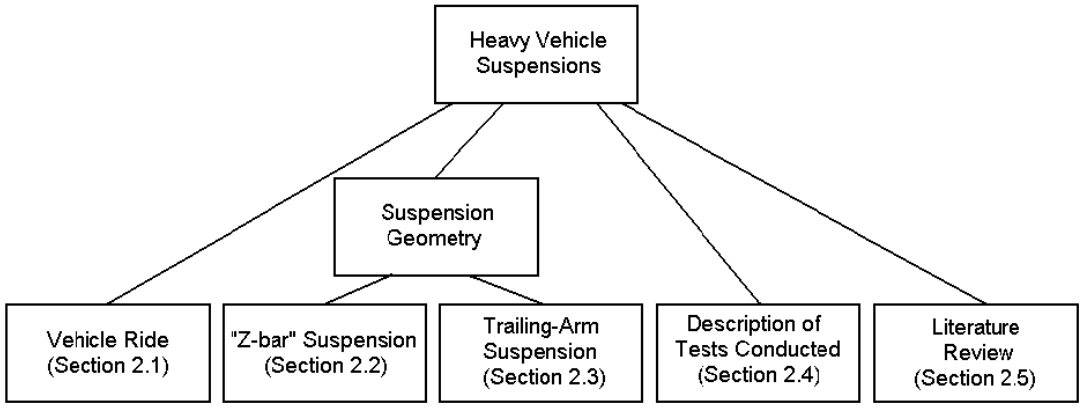

Figure 2-1 Map of Chapter 2, Background of the Study.

2.1 Vehicle Ride

Before discussing the testing, it is important to develop a good understanding of vehicle ride. Section 2.1 defines ride and describes its relationship to the vehicle's primary suspension. The section goes on to identify important vehicle vibration modes and discuss how ride affects the driver.

2.1.1 Definition of Ride

Vibrations from the road and other sources reach the driver by tactile, visual, or aural paths [1]. Generally, vibrations with frequencies less than 25 Hz fall under the definition of ride and those audible to humans (25-20,000 Hz) are termed noise. Although noise and ride are both of significant concern to a suspension designer, the testing performed in this study was limited to investigating ride quality. Since all test frequencies in this study are below 25 Hz, this limitation is valid.

Ride is a subjective quality of a vehicle, combining aspects of both vehicle stability (safety) and driver comfort (feel). In any vehicle with a non-adjustable suspension, there will always be some compromise between these two aspects. On one hand, a suspension that is very soft may give a good ride, as far as the driver is concerned, but the vehicle could become unstable or exhibit excessive roll in a corner. On the other hand, a suspension that is very stiff will maintain the vehicle's stability in a corner, but it may transmit intolerable vibration (a harsh ride) to the driver or cargo.

2.1.2 Primary Suspension of a Vehicle

A vehicle's primary suspension is the system that most affects ride quality. The suspension connects the axle assembly to the vehicle frame, supports the substantial loads present, and provides a means of isolating the frame from road roughness. Shown in Figure 2-2 is a simplified model of a primary suspension. The model, which is commonly referred to as a "quarter-car model," represents the sprung and unsprung body dynamics for a single suspension. Due to its simplicity, the quarter-car model is widely used for studying the fundamental aspects of vehicle suspensions.

The sprung mass represents the mass of the vehicle frame, as well as other components of the vehicle isolated from the road by the primary suspension. Representing the mass of the axle, brakes, wheels, and tires is the unsprung mass. Any irregularities in the road not absorbed in the primary suspension can reach the driver, or cargo, in the form of vibrations.

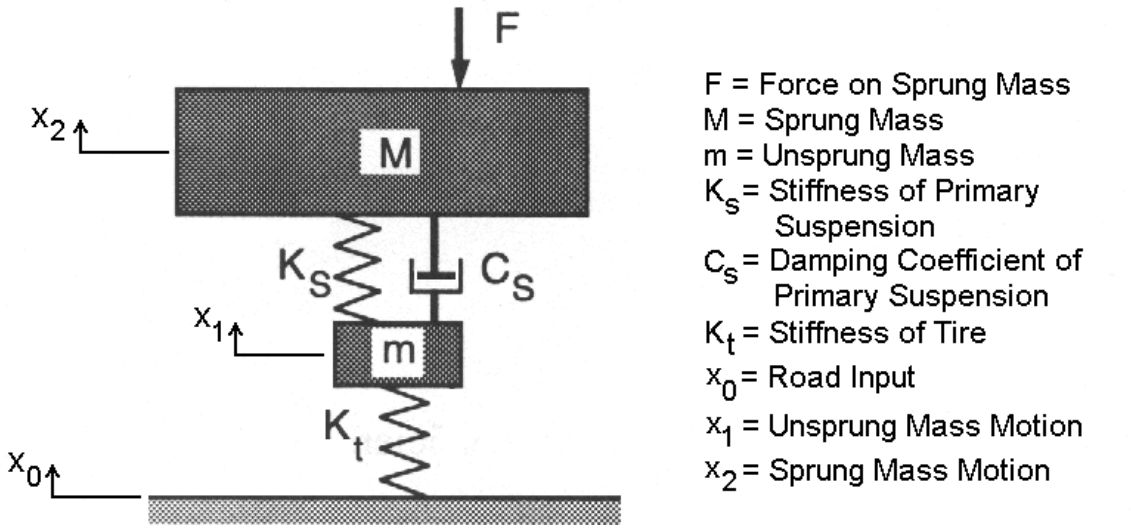

Figure 2-2 Quarter-Car Model of a Vehicle's Primary Suspension (adapted from Fig. 5.14 [1]).

A vehicle's ride quality depends strongly on the resonant (natural) frequency of the primary suspension. For a given frequency range, a resonant frequency is defined as when the ratio of the output signal to the input signal is maximized. Using the equations listed below, suspension designers specify a vehicle's primary suspension stiffness and damping to achieve the desired ride quality. The governing equation for the natural frequency of a primary suspension without damping or tire interaction can be approximated as:

$$\omega_n = \sqrt{\frac{K_s}{M}}, \tag{2-1}$$

where ω_n is the natural frequency (undamped) of the primary suspension in rad/s, K_s is the vertical stiffness of the primary suspension in kN/mm, and M is the sprung mass of the vehicle in kg.

Even though damping and tire interactions are present in practice, Equation 2-1 provides an estimate of the vehicle suspension natural frequency that can be used effectively in many studies [1]. For more accurate results, one may choose to include the suspension damping in the calculation of the suspension's natural frequency. The damped natural frequency can be calculated as:

$$\omega_d = \omega_n \sqrt{\left(1 - \xi^2\right)}, \tag{2-2}$$

where ω_d is the damped natural frequency of the primary suspension in rad/s and ξ is the damping ratio (dimensionless). The damping ratio is defined as:

$$\xi = \frac{C_s}{\sqrt{\left(4 K_s M\right)}}, \tag{2-3}$$

where C_s is the damping coefficient of the primary suspension in N*s/m.

2.1.3 Vibration Modes

A vibration mode occurs when an input frequency passes through one of a component's resonant frequencies. Every component system of a vehicle has a specific resonant frequency, and many of those systems reach resonance below 25 Hz. Although all modes of vehicle vibration are of concern to suspension designers, there are just too many modes to study individually. Those of primary importance include primary suspension modes, rigid-body modes (the whole vehicle translates), frame bending (beaming) modes, and other modes that affect either the driver or component reliability.

In the specific case of this study, the resonance of the primary suspension, the frame beaming, and the excitation of the exhaust stack(s) are of interest.

The first resonant frequency (mode) of the primary suspension was calculated in the previous section. This mode is identified when the motion across the primary suspension (the difference between x_1 and x_2 in the quarter-car model in Figure 2-2) reaches a maximum. Although a primary suspension natural frequency of 1 Hz is considered a "design optimum for highway vehicles, "according to Gillespie [2], most trucks will be closer to the 1.3-1.7 Hz range. This difference is because some comfort must be sacrificed in order to achieve better vehicle stability. As far as importance goes, the primary suspension mode is one of the most noticeable elements of a vehicle's ride quality. Therefore, this mode must be examined closely in the design and analysis of any new suspension.

The frame beaming mode is reached when the vertical bending of the frame reaches a maximum amplitude in a given frequency range. The 5-8 Hz range is where this mode is expected to occur. Variations in components mounted to the frame account for the wide frequency range between different vehicles. Significant excitations in the cab in this frequency range, especially the pitching effect, can be attributed to frame beaming.

The mode of the exhaust stack(s) is also important in our specific study. In addition to the effects of exhaust stack vibrations on ride quality, failures in the mounting brackets of both the single and dual exhaust configurations can be of concern to the manufacturer.

2.1.4 Effects on the Driver

As stated in Section 2.1.1, ride is a subjective quality of a vehicle, combining aspects of both vehicle stability (safety) and driver comfort (feel). The feel of the vehicle to the driver is where the subjectivity comes into play. Besides the vibrations transmitted to the driver through the seat, excitations also reach the driver in the form of audible buzzing and/or visible motion of surrounding components in the cabin. It is difficult to accurately compare one driver's feelings toward noise and vibration in the cab to another driver's. Vibration, sound pressure level, and motion in the cab can all be measured, but their effect on the comfort of the driver is not a simple correlation.

In this study, the subjective ride quality information is already available for the current suspension. This information has also been related to vibration levels at specific points around the driver and to vibrations at the seat itself. By measuring at the same locations, this study generates comparable information on ride quality for the prototype suspension.

Although the ride of a vehicle is a subjective quality, the human body's tolerance to vibrations is measurable, even though there is no accepted standard procedure [1]. Despite the differences in measurement conditions, many researchers find similar results. Figure 2-3 shows the maximum level of vertical vibration tolerable, according to separate tests.

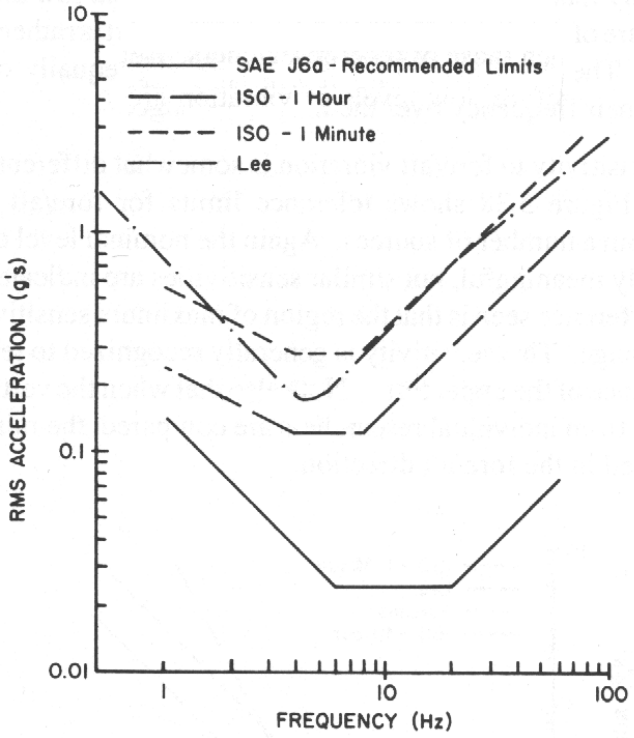

Figure 2-3 Vertical Vibration Limits on the Human Body (adapted from Fig. 5.36 [1]).

Similarly, the maximum level of fore/aft vibration tolerable is shown in Figure 2-4. It is important to point out that, although the tests were conducted separately, the results show a common range of frequencies where the human body has the lowest tolerance to vibration. The range of frequencies is 4-8 Hz for vertical vibration and 1-2 Hz for transverse (i.e. fore and aft or side to side) vibration [1]. Recall the modes important to this study. The primary suspension mode occurs from 1-2 Hz, and the frame beaming is 5-8 Hz. With human tolerance to vibration a minimum in the same ranges, it is no mistake that these two modes dominate the concern of the vehicle manufacturer.

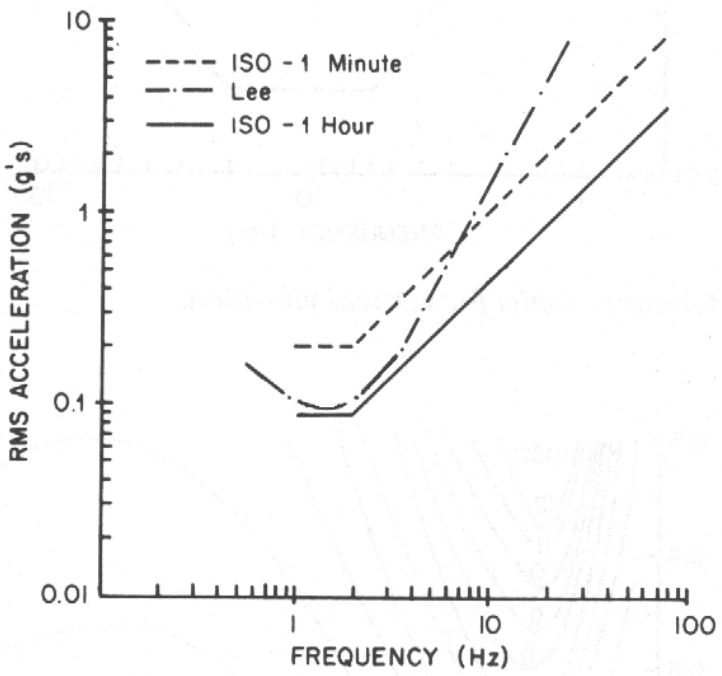

Figure 2-4 Fore/Aft Vibration Limits on the Human Body (adapted from Fig 5.38 [1]).

Now that a detailed definition of vehicle ride has been presented, the background of this study can continue into descriptions of the test vehicles' suspension geometries. Sections 2.2 and 2.3 illustrate several design and performance characteristics of the currently manufactured "Z-bar" suspension and the prototype trailing-arm suspension, respectively.

2.2 "Z-bar" Primary Suspension

The drive axle suspension currently manufactured for the Class 8 road tractor is a "Z-bar" style air suspension. Figures 2-5 through 2-7 show this suspension from several different angles. In Figure 2-5, the forward mounting bracket is visible. Both the leaf

spring and track bar mount to this bracket. The leaf spring is shaped like a "Z", giving the suspension its name. To form the "Z", the leaf spring extends longitudinally over the axle, drops below it immediately thereafter, and continues along the longitudinal axis of the vehicle to where the airspring attaches (as shown in Figure 2-7, and on a similar suspension in Figure 2-8).

The forward mounting bracket, leaf spring, track bar, and other cast parts contribute to the significant weight and cost of this suspension. These are the main reasons for the development for a new suspension.

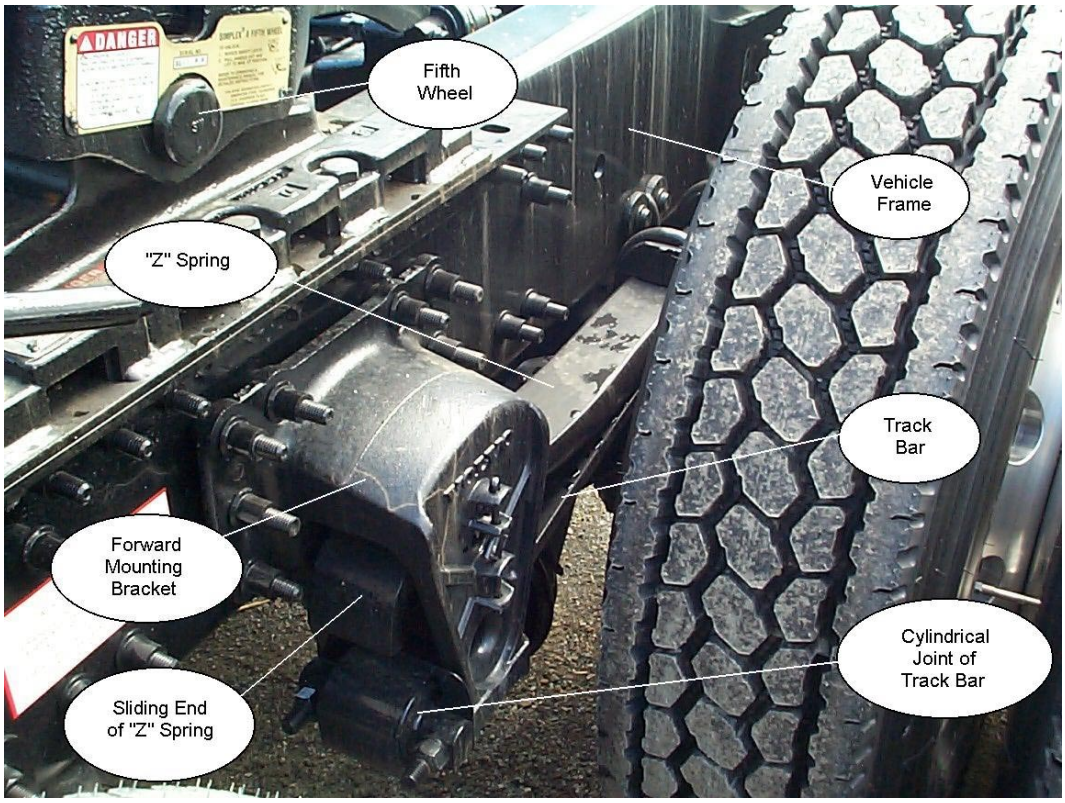

Figure 2-5 Production "Z-bar" Drive Axle Suspension – Front View.

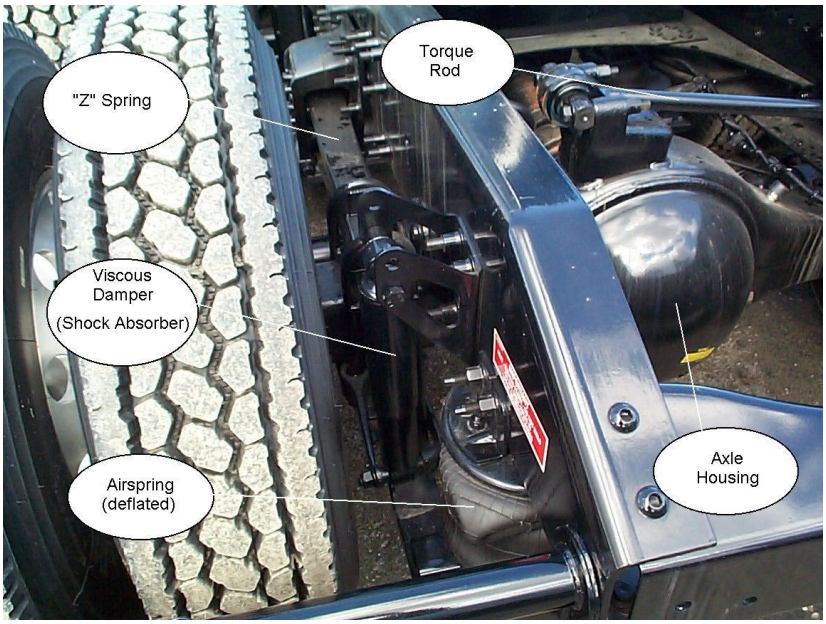

Figure 2-6 Production "Z-bar" Drive Axle Suspension – Rear View.

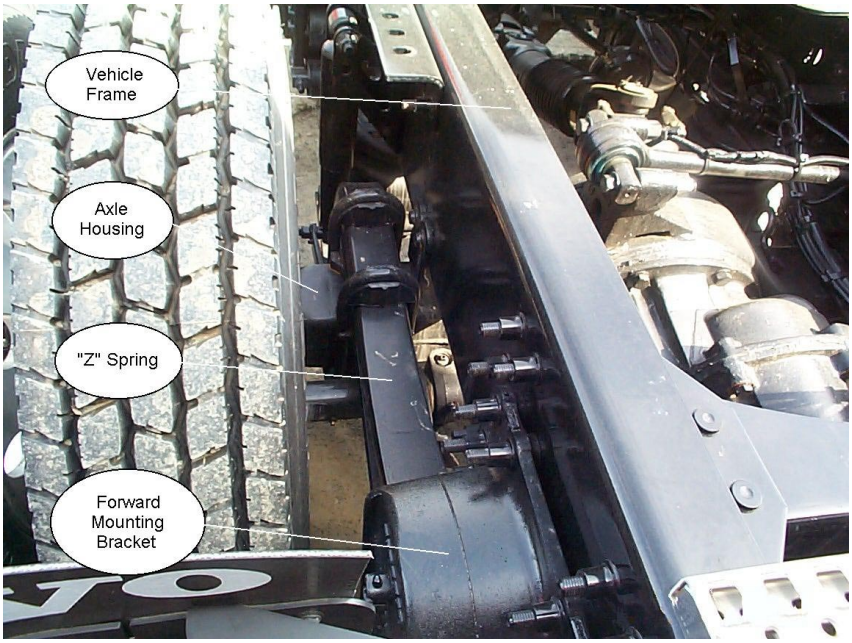

Figure 2-7 Production "Z-bar" Drive Axle Suspension – Top View.

Many other manufacturers use "Z-bar" type suspensions for the drive axles of their road tractors. For example, Figures 2-8 and 2-9 show two different drive axle suspensions that both use "Z" springs. The Ridewell 226R is somewhat similar to the

production suspension to be tested, but the front mounting of the 226R eliminates the need for a track bar. Reyco's 102AR is even more similar to the production unit in that it uses a track bar to locate the axle, allowing the "Z" spring to slide along its forward mount.

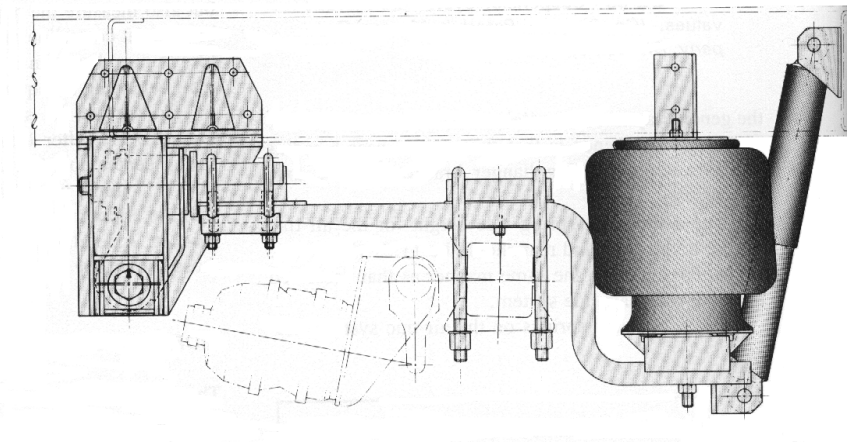

Figure 2-8 Ridewell Air-Ride 226R "Z-bar" type Drive Axle Suspension (adapted from Fig 2-93 [3]).

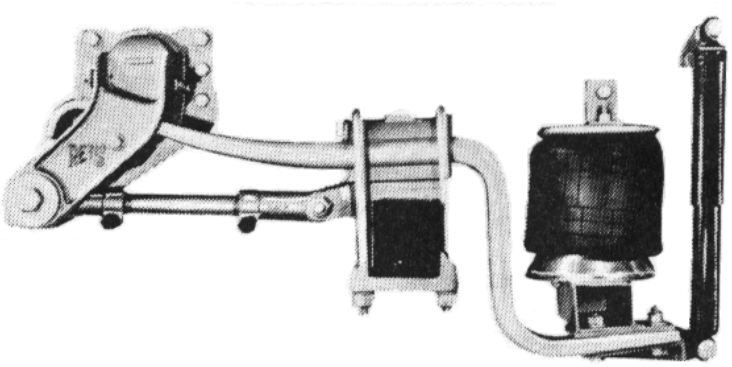

Figure 2-9 Reyco® Transpro® Model 102AR "Z-bar" type Drive Axle Suspension (adapted from Fig 2-11 [3]).

An alternative to the "Z-bar" suspension just described is another class of suspensions that will be referred to as a "trailing-arm" suspension, for the purposes of this study. The major difference between the trailing-arm suspension and the "Z-bar"

suspension is the shape of the leaf spring and the design changes that accompany it. Section 2.3 describes the prototype trailing-arm suspension that was tested in this study.

2.3 Trailing-Arm Primary Suspension

For the prototype suspension on the Class 8 road tractor, a trailing-arm style air suspension is used at the drive axle. Figures 2-10 and 2-11 show the suspension from the front and rear.

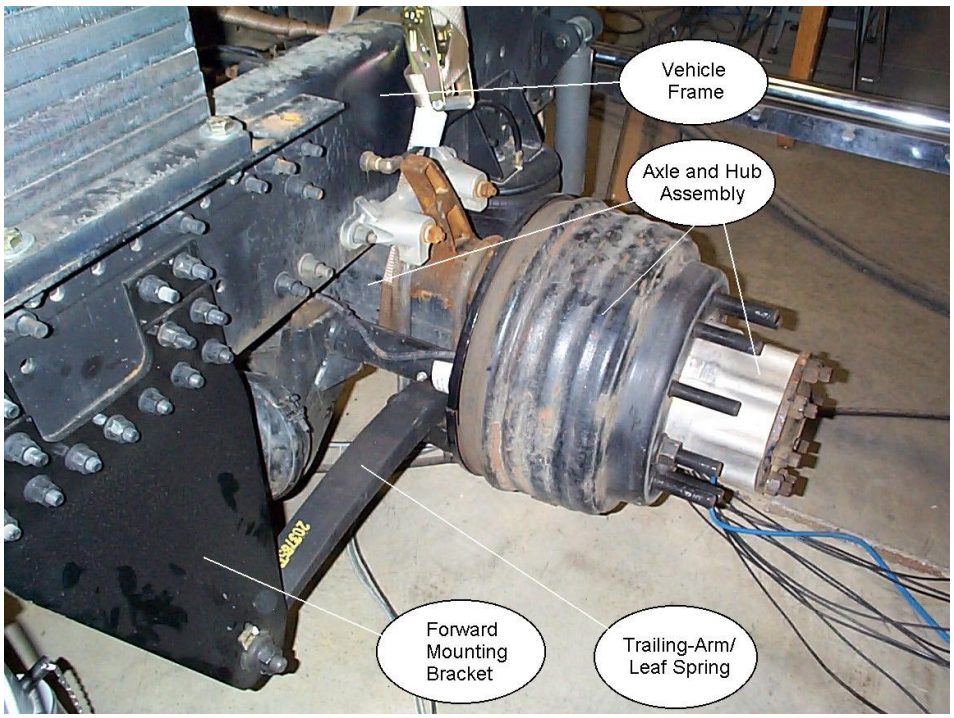

Figure 2-10 Prototype Trailing-Arm Drive Axle Suspension – Front View.

Unlike the "Z" shaped leaf spring, the leaf spring on the prototype suspension is only slightly bowed and it mounts below the axle. The forward mount of the leaf spring uses a cylindrical joint, which resists suspension roll as well as longitudinal and vertical displacement of the spring at that joint while maintaining rotational compliance under suspension deflection. The nature of this joint precludes the use of a track bar, further

eliminating weight from this design. Also, the front spring hanger is made up of two metal plates (visible in Figure 2-10) instead of the heavy cast piece on the production suspension (refer back to Figure 2-5) in an attempt to shed more weight.

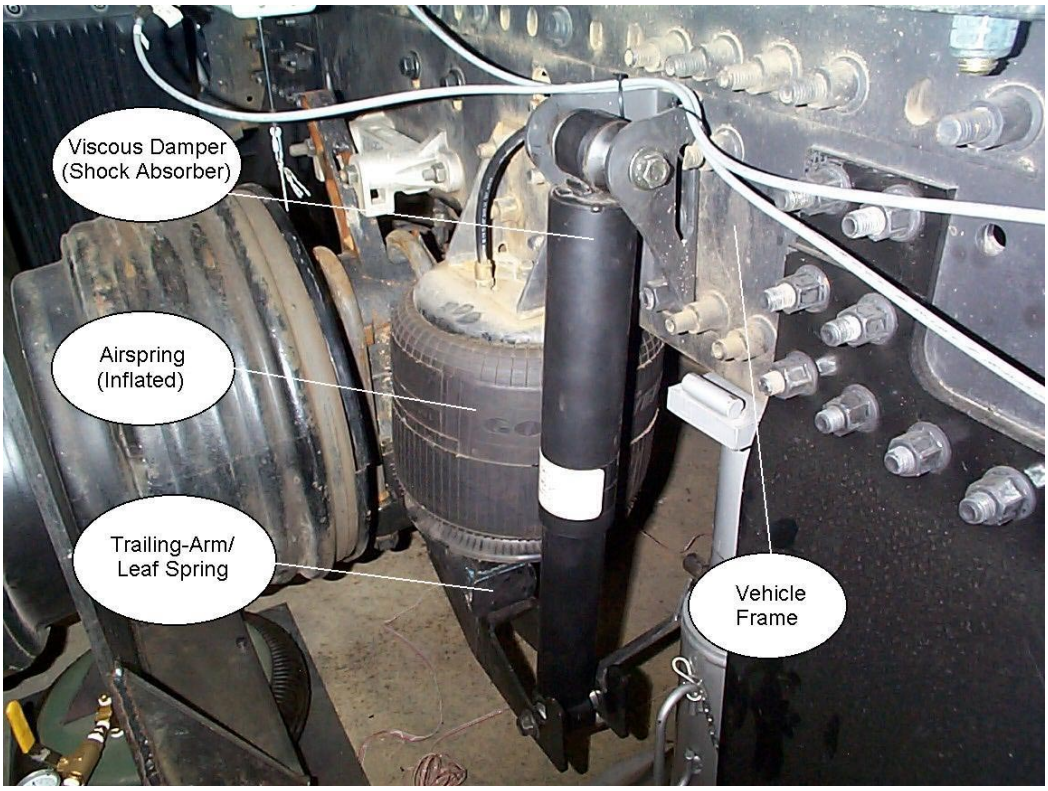

Figure 2-11 Prototype Trailing-Arm Drive Axle Suspension – Rear View.

The industry's use of this type of trailing-arm suspension on a drive axle is much less common when compared to the "Z-bar" style. One manufacturer, Reyco, uses a very similar design, with the exception of the damper mounting (refer to Figure 2-12). The Reyco suspension, however, is used on a trailer axle, not a drive (live) axle on a tractor where longitudinal traction forces exist. Neway, another truck suspension manufacturer, does use a trailing-arm suspension for the drive axles in its Model ARD 125-6 (Figure 2-13). The difference lies in the trailing-arm itself. In the Neway model, the trailing arm does not function as a spring, but as a rigid suspension member.

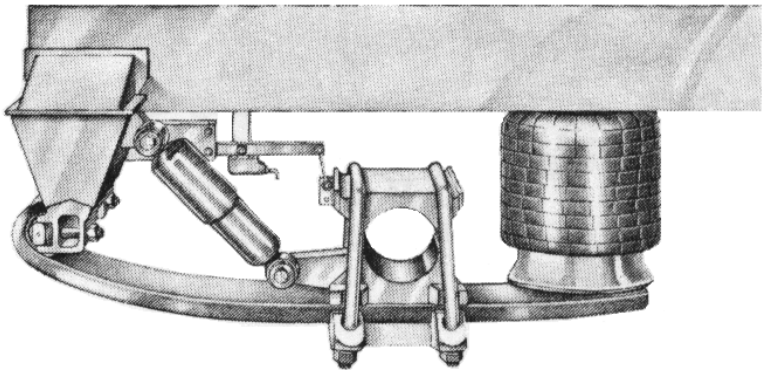

Figure 2-12 Reyco® Transpro® Model 81 Trailing-Arm type Trailer Suspension (adapted from Fig 2-11 [3]).

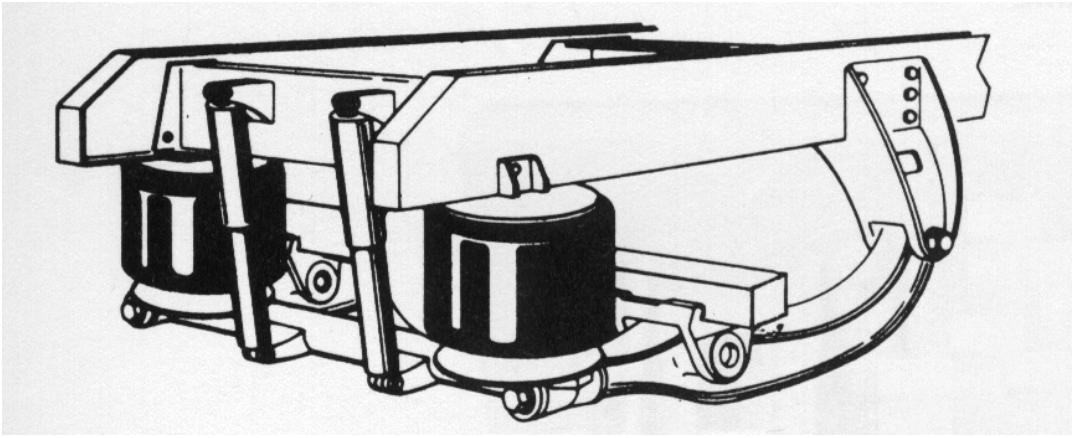

Figure 2-13 Neway Model ARD 125-6 Trailing-Arm type Drive Axle Suspension (adapted from Fig 2-65 [3]).

Both the currently produced "Z-bar" suspension and the prototype trailing-arm suspension have been discussed, and a thorough definition of vehicle ride was presented in Section 2.1. To continue the background of this study, Section 2.4 provides a general description of the tests performed in this study and reinforces the importance of those tests to the manufacturer.

2.4 Description of Tests Conducted

The following two sections discuss the tests that are commonly performed as an analysis of the kinematics and dynamics of primary suspensions for a vehicle.

2.4.1 Kinematics Tests

The kinematics of a vehicle's suspension is linked with the static load capacity of the vehicle, stability in driving, and ride quality, as a function of the primary suspension's stiffness. In this study, the kinematics tests performed include tests of vehicle vertical stiffness, roll stiffness, roll center height, and roll steer.

The undamped natural frequency of the primary suspension is dictated by its vertical stiffness. As emphasized in Section 2.1.2, the relationship between ride quality and the undamped natural frequency of the primary suspension is quite important. Also affected by the vertical stiffness is the cargo capacity of the vehicle. Increasing the vertical stiffness of the primary suspension raises the cargo capacity of the vehicle, but provides a harsher ride.

Roll stiffness is directly related to the stability (safety) of a vehicle. In a turn, a vehicle's tendency to roll over is reduced as roll stiffness is increased. Heavy trucks are designed with high roll stiffness to combat the high center of gravity and significant loads inherent in the vehicles. Accomplishing this while minimizing weight and preventing added vibration from being transmitted to the cab is where the compromise lies.

A vehicle's roll center height is an imaginary point about which the unsprung mass rotates when the vehicle rolls. Applying a lateral force at this point would cause no roll in the vehicle. As a vehicle enters a turn, the roll center height controls how much of

the lateral load goes through the suspension linkage [4]. A higher roll center increases the roll stiffness but lifts the sprung mass when lateral load is applied.

Roll steer is the tendency of the axle to turn (when looking at the axle from above) in response to roll. Since the vehicle is turning along a path not originally intended by the driver, this property of the suspension is not advantageous. However, roll steer is inherent in the design of the suspension geometry and can only be minimized.

2.4.2 Dynamic Tests

Dynamic testing excites the resonant modes of a vehicle in a controlled environment. This testing allows any potential areas of concern to be studied without the added variables of on-road testing. To excite the vehicle, several different types of signals are applied to the drive axle. These include a chirp signal, a "hard bump" signal, and pure tone signals.

A chirp signal is an input signal that excites a range of frequencies, usually by ramping from a low frequency to a high frequency in a specific time period. The chirp signal, however, cannot be applied with constant amplitude throughout the range of frequencies. As the frequency increases, the amplitude must be reduced (a first order filter is used) to prevent exciting the modes with too much energy. The resonant frequencies (modes) of the primary suspension, the frame beaming (in bending), and the exhaust stack(s) are all excited by this signal when testing in the range of ride vibrations (below 25 Hz). Viewing the response to the signal (in the frequency spectrum) allows the identification of the frequency at which each mode occurs.

In this study, a "hard bump" signal is used to observe the transients of the system. This signal is a step input, which causes the axle to jump from rest to a predetermined height almost instantaneously. Impacting the axle in this way sets up oscillations in the axle, frame, and body that can be measured as they decay. The effects of damping are easily seen with this test.

Unlike the chirp signal, a pure tone input signal excites only one frequency. The resonant frequencies (modes) identified with the chirp input are studied individually to remove any transient effects that may be present with the chirp or hard bump signals. Since the response to the pure tone signal is very clean, comparison between other frequencies and other test scenarios is simplified.

After defining vehicle ride, the different vehicle suspensions to be tested, and the tests themselves, one final component of the background to this study remains. Section 2.5 is a literature review of published research in areas similar to and overlapping with the study described in this thesis.

2.5 Literature Review

To further support this study, a detailed literature search was conducted in the area of vehicle suspensions and testing. Three major databases with significant technical engineering content, Compendex, First Search, and INSPEC, were used for the literature search. Although all three of these databases returned a reasonable number of "hits" for each keyword or keyword string, the Compendex database returned the highest number of unique hits. Figure 2-14 shows the flow chart for the Compendex search, complete with keywords and number of hits.

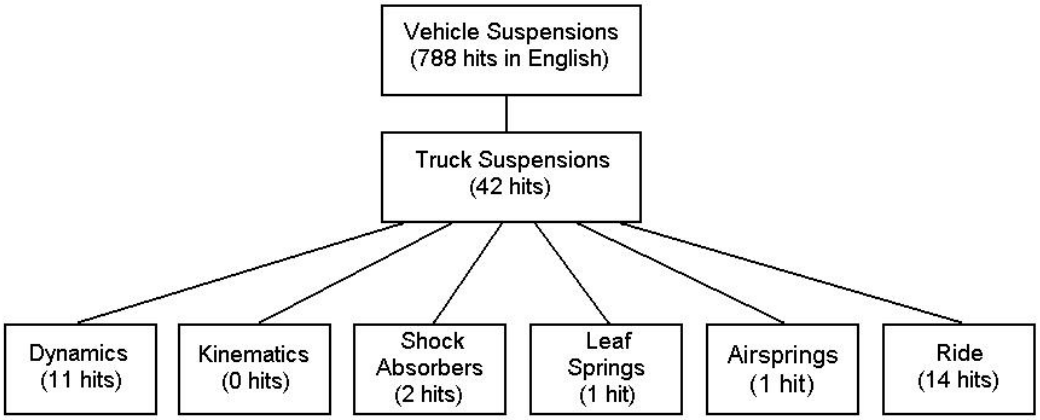

Figure 2-14 Literature Search Flowchart for Compendex Database.

As the number of results in each search decrease with each level of additional keywords, the hits become more relevant to this study specifically. The following sections briefly describe the articles found using the six keywords at the deepest level of the literature search.

2.5.1 Keyword: "Dynamics"

Of the 11 hits for dynamics, 3 were not even articles but anonymous general descriptions of proceeding from the International Truck and Bus Meeting and Exposition. Most of the other 8 articles discussed some type of heavy vehicle computer modeling. For example, Letherwood and Gunter [5] researched the three-dimensional modeling and analysis of a heavy military transport vehicle. In this study, the model was validated using video recordings of the vehicle traversing various types of terrain. In another study, Yang et al. [6] adapted an articulated vehicle model to the limits of a driver's control in the yaw plane. Road damage performance of an individual heavy vehicle was correlated to a simulated fleet of vehicles and then compared to road damage indices in a study by Cole and Cebon [7]. Also, Borges et al. [8] investigated the flexible body

modes in an articulated vehicle using finite elements. The study by Field et al. [9] was interested in one of the same areas as the study described in this thesis. By combining analytical and experimental efforts, Field et al. attempted to characterize and improve the ride quality of a tractor-trailer combination. Lee et al. [10] were also interested in improving the ride quality of heavy trucks. They used the Taguchi Method and computer simulation to optimize spring stiffness and viscous damping in the shock absorbers.

The other 2 articles found under “dynamics” covered areas other than computer modeling. As an alternative to the conventional 3-leaf steel springs used in tractor suspensions, Knouff and Hurtubise [11] discussed a fiberglass composite leaf spring and several advantages inherent in its design. Although the keywords are a match, the study by Suda and Anderson [12] is concerned with the dynamics of lightweight railcar trucks in high-speed trains, so it bears little relevance to the study described in this thesis.

2.5.2 Keyword: “Kinematics”

Unlike the keyword “dynamics”, “kinematics” returned no hits. As was shown in the previous section, many published studies related to modeling of vehicle dynamics exist, but our literature search resulted in zero hits for "kinematics" analysis. This is most likely because university laboratories or other organizations that promote publications of research results do not commonly conduct such studies. We are, however, aware of kinematics studies that are often conducted on a proprietary basis for original equipment manufacturers or their suspension suppliers.

2.5.3 Keyword: "Shock Absorbers"

Only 2 hits matched shock absorbers under truck suspensions. One of the articles, Lee et al. [10], was already discussed in Section 2.5.1. The other article is on a study by Kutsche et al. [13] concerning optimized ride control of heavy vehicle using intelligent suspension control. The shock absorbers were controlled either electronically or pneumatically to vary damping characteristics with changing operating conditions. Although active suspension control using shock absorbers is an area of significant new research, this keyword search does not show it.

2.5.4 Keywords: "Leaf Springs" and "Airsprings"

These two keywords are combined in one section because the same single hit is returned for each keyword. In this article, Mraz [14] identified the different compromises made in designing a suspension for a heavy vehicle. Mraz goes on to describe the different springs used to isolate the driver and cargo from road induced vibrations. Although Knouff and Hurtubise [11] investigated composite leaf springs, as described in Section 2.5.1, the study was not found in the "leaf springs" keyword search.

2.5.5 Keyword: "Ride"

As expected, several of the articles found under keyword "ride" have already been discussed. These include Letherwood et al. [5], Field at al. [9], Lee et al. [10], Kutsche et al. [13], and Mraz [14]. Also, 2 of the hits were general descriptions of proceedings at the International Truck and Bus Meeting and Exposition, like in Section 2.5.1.

Most of the remaining 7 hits are articles involving computer modeling and its application to vehicle ride. For example, Tong et al [15] subjected a 2 degree of freedom (DOF) vehicle model to random road excitation to study its effect on ride quality as well as stress and fatigue on the vehicle structure. One year later, Tong et al [16] performed a computer controlled suspension design study for the vehicle cab and passenger seat suspensions. The vehicle model was increased to 8 DOF and then was coupled to a 6 DOF model of the driver and seat in an attempt to optimize ride quality. In another study that evaluated ride quality, Wang et al. [17] subjected a 9 DOF model of the tractor-trailer combination to an irregular road surface. The results were then compared to ISO 2631, human tolerance to vibration at the driver's seat.

Several other methods of research were discussed in some of the articles found with keyword "ride". Realizing that most studies had been concerned with vehicle loading and vibration in the vertical direction, Forsen [18] concentrated on longitudinal wheel forces in heavy vehicles to see how it influenced vehicle ride. Instead of modeling the vehicle, Blue et al. [19] presented a numerical method for optimizing vehicle performance in pavement damage, ride comfort, stopping distance, and handling. As a comparison to an optimized passive suspension, Oueslati et al. [20] investigated the performance of an active suspension model for an articulated vehicle.

In the final article, a study by Hinzburg et al. [21] attempted to identify the main trends in the suspension design process to optimize stability and handling of a heavy vehicle through experimentation. As discussed in Section 2.1.1, vehicle ride is a compromise between handling and comfort. Unlike any of the other research described in this literature review, Hinzburg et al. chose to concentrate solely on vehicle handling.

2.6 Chapter Summary

This chapter presented background information relevant to this study that may have been necessary for the understanding of the remainder of this document. The next chapter discusses the vehicle, actuation system, and instrumentation setups for both the kinematics and dynamic tests.

Chapter 3

Test Setup

The primary purpose of Chapter 3 is to describe the test setup in sufficient detail that one could recreate it, if desired. Included in this chapter are descriptions of the test vehicles, as well as the setup for both kinematics and dynamic tests.

3.1 Test Vehicles

All of the kinematics and dynamic tests were performed on two vehicles, both of which were complete and operational Class 8 road tractors. One vehicle was equipped with the currently produced "Z-bar" suspension, while the other was equipped with the prototype trailing-arm suspension. Prior to testing, a few temporary modifications were made to each of the vehicles. These modifications are discussed in Section 3.1.3, after the vehicle descriptions.

3.1.1 "Z-bar" Suspension

Although the 2000 Volvo (shown in Figure 3-1) is the newer of the two vehicles, it is fitted with the production "Z-bar" suspension, called Volvo Optimized Air Suspension-1 (VOAS-1). For the remainder of the document, VOAS-1 will be used to refer to the production "Z-bar" suspension. Figure 3-2 shows VOAS-1 on the 2000 Volvo test vehicle, which arrived at our test facility directly from Volvo's production facility. Other than the changes discussed in Section 3.1.3, no other modifications were made to this test vehicle.

Figure 3-1 2000 Volvo VN 770.

Figure 3-2 VOAS-1 Suspension on Test Vehicle.

3.1.2 Trailing-Arm Suspension

Unlike the truck with VOAS-1, the 1999 Volvo (Figure 3-3) had been modified to accept Volvo Optimized Air Suspension-2 (VOAS-2), the prototype trailing-arm suspension shown in Figure 3-4, before arriving at our laboratory. VOAS-2 will be used to designate the prototype trailing-arm suspension from this point forward.

Figure 3-3 1999 Volvo VN 770.

Several changes were made to the VOAS-2 vehicle since initial testing began. For the kinematics tests, the vehicle was fitted with two different versions of VOAS-2 at the same time. The front drive axle was equipped with a 1-¾ in. thick leaf spring and the rear drive axle used a 2 in. thick leaf spring. The vehicle was assembled this way to allow kinematics testing of both possible designs (especially roll stiffness) without removing the vehicle from the test facility. Before beginning dynamic testing, the vehicle was modified again so that both front and rear drive axles were equipped with 2”

springs, due to the unacceptable (too low) roll stiffness of the 1-¾ in. suspension. No other modifications were made on the vehicle with VOAS-2 before it reached our laboratory.

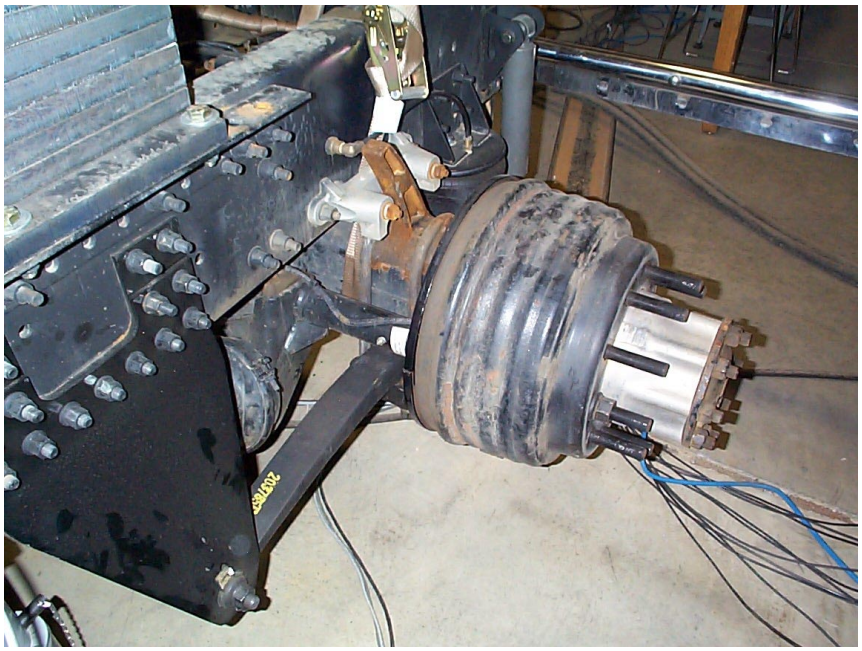

Figure 3-4 VOAS-2 Suspension on Test Vehicle.

The only difference between the VOAS-1 and VOAS-2 vehicles, other than their suspensions, was their exhaust stack configurations. The VOAS-1 truck had a single exhaust, while the VOAS-2 truck had a dual exhaust configuration. This difference is important because the resonance of the exhaust(s) has a significant effect on vibrations in the cab. The extent of this relationship is discussed further in the discussion of dynamic results in Chapter 5.

3.1.3 Modifications to Vehicles Prior to Testing

Several temporary changes had to be made to both vehicles before either kinematics or dynamic testing could begin. These changes are discussed briefly here, and

in much greater detail in Appendices A and B for the kinematics and dynamic tests, respectively.

In order to have greater control over the stiffness of the suspension and the ride height of the vehicle, the load-leveling system and accompanying plumbing had to be modified. The plumbing for the air suspension was rerouted so that the front and the rear drive axles were each on an independent air supply. By removing the connection between the vehicle's air supply and the drive axles, as well as the connection between axles, the ride height of each drive axle could be modified without affecting the rest of the vehicle.

Both vehicles arrived at our laboratory equipped with a fifth wheel. Since both kinematics and dynamic testing schemes require attachment to the vehicle frame at the location of the fifth wheel, the fifth wheel had to be removed. In its place, a 1 in. thick plate (called the fifth wheel plate) was mounted to the frame so that it could accept the attachments for kinematics and dynamic testing. The fifth wheel plate is visible in several of the figures in Sections 3.2 and 3.3.

Various other changes were made to the vehicles, depending on the tests that were conducted, as will be discussed in Sections 3.2 and 3.3.

3.2 Kinematics Test Setup

The next three subsections contain information concerning additional modifications to the vehicle for kinematics testing as well as actuating the suspension and acquiring data.

3.2.1 Vehicle Modifications – Kinematics Testing Specific

Kinematics testing requires grounding the vehicle frame. This allows the suspension to react against the ground as it is deflected. To ground the vehicle frame, a section of I-beam, called the crossbeam, was bolted to the fifth wheel plate, which had already been attached to the vehicle frame. This created a load path to an I-beam structure bolted to the concrete floor of the facility. A close-up of the cross beam in place is shown in Figure 3-5. The fifth wheel plate is also visible in Figure 3-5, as well as some of the grounded I-beam structure. A full view of the kinematics structure is shown in Figure 3-6.

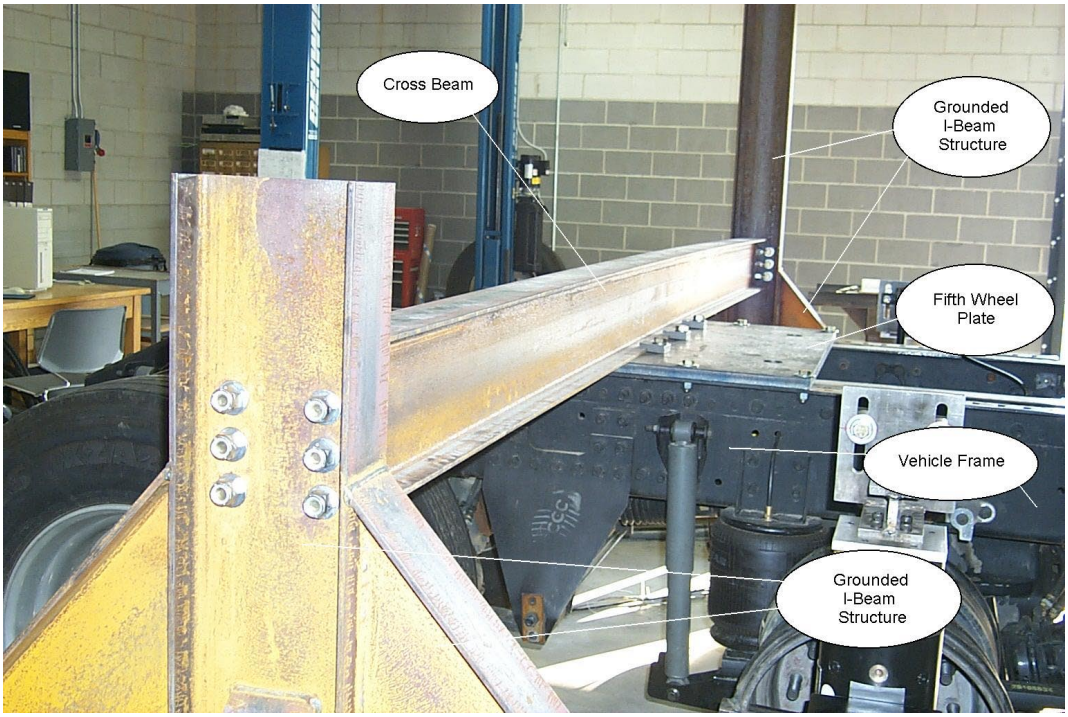

Figure 3-5 Cross Beam Attached to Vehicle Frame.

Once the frame was grounded, the wheels and tires were removed only from the drive axle to be tested, as is shown in Figures 3-5 and 3-6. The axle is moved in a quasi-

static fashion by two hydraulic jacks, as will be discussed in more detail in the next subsection.

Figure 3-6 Structure for Grounding Vehicle Frame During Kinematics Tests.

3.2.2 Actuation of Suspension

Once the frame was tied to the ground, applying a positive vertical force to either end of the axle deflected the suspension. A modified brake drum, shown in Figure 3-7, was used as an attachment to the end of the axle. One was bolted in place of the wheel, on each axle end, and then connected to the modified hydraulic jack shown in Figure 3-8. Raising the jack lifts the end of the axle and, when the suspension air springs are set at ride height, lowering the jack lowers the axle. When one jack was raised and the other was lowered, as compared to being even at ride height, a roll was induced in the suspension. The installation of the modified brake drum and hydraulic jack on the axle is shown in Figure 3-9.

The white box in Figure 3-9, and the gold cylinder in Figures 3-8 and 3-9, are data acquisition devices and they are discussed in Section 3.2.3.

Figure 3-7 Modified Brake Drum for Kinematics Tests.

Figure 3-8 Hydraulic Jack for Actuation of the Suspension in Kinematics Tests.

Figure 3-9 Actuation System for Kinematics Tests, Attached to Vehicle.

Truck suspensions are commonly constrained to the frame in such a way that when they move vertically or roll, they also exhibit motion along axes other than those intended. For example, when the axle rolls, it also translates laterally and develops a slight yaw angle (this is called roll steer). Placing rollers under the jack allows lateral translation of the axle to prevent a significant bending moment from damaging the actuation system. The complete setup is shown in Figure 3-9 and the rollers, which are made of ½ in. round steel stock, are shown in Figure 3-10. No provision had to be made for the yaw motion of the axle when the suspension rolled because it was so small.

Figure 3-10 Hydraulic Jack Rollers.

3.2.3 Data Acquisition

The kinematics tests measured forces due to a quasi-static displacement. Since no movement of the suspension was taking place while data was being collected, the sampling rate could be very low. During a test, data was collected for 5 seconds at 2 samples per second and then averaged at each position of the suspension. Data was collected with a personal computer running Labview (Version 5.0.1) by way of a National Instruments data acquisition board Model AT-M10-16E-10. Once the data was collected, it was put into a Microsoft Excel (Version 9.0.2720) spreadsheet to be analyzed and plotted.

Vertical force was measured at each axle end with a Futek Model L2900 load cell, shown in Figure 3-11. Each load cell is rated to 20,000 lb to handle the high loads encountered when deflecting the suspension to its limits. As shown in Figures 3-8 and 3-9, the load cell was mounted on top of the hydraulic jack, in series with the load path from the vehicle to the ground.

Figure 3-11 Futek Model L2900 Load Cell with Attachment.

All displacements in the kinematics tests were measured with Unimeasure VP510-10-NJC Linear Voltage Differential Transformers (LVDTs), such as the one shown in Figure 3-12. LVDTs, or "string-pots" as they are sometimes called, are capable of measuring displacement and velocity between two points, across the base and free end of the string. Vertical displacement of each hydraulic jack, and therefore the end of the axle, was measured with an LVDT. Lateral displacement of the center of the axle was also measured with an LVDT. In a test for roll steer, longitudinal displacements of each axle were measured, along with the vertical and lateral displacements just mentioned (five LVDTs). Stands, such as the one shown in Figure 3-13, held an LVDT at the axle centerline for longitudinal and lateral measurements.

Figure 3-12 Unimeasure VP510-10-NJC LVDT.

Figure 3-13 Longitudinal and Lateral Displacement LVDT Stand.

Now that the setup for the kinematics testing has been thoroughly described, the description of test setups can continue to the dynamic testing. Section 3.3 includes an explanation the vehicle modifications, actuation system, and instrumentation necessary for the dynamic tests.

3.3 Dynamic Test Setup

Vehicle modifications for the dynamic tests are covered in this section. Also included are descriptions of how the suspension of the vehicle was actuated and how data was collected during the tests.

3.3.1 Vehicle Modifications for Dynamic Tests

To simulate a trailer load, weight was added to the vehicle frame, where the fifth wheel would normally be located. This additional weight was a stack of 34 metal plates,

350 lbs each, which were bolted to the vehicle frame by way of the fifth wheel plate. Figure 3-14 shows the weight stack on a test vehicle. Since dynamic testing was only performed on one drive axle at a time, the wheels were removed from the other axle and then the axle was strapped to the frame (in this study, only the front drive axle was tested on both VOAS-1 and VOAS-2 vehicles). With these modifications, the weight on the test axle was approximately 15000 lbs (6800 kg).

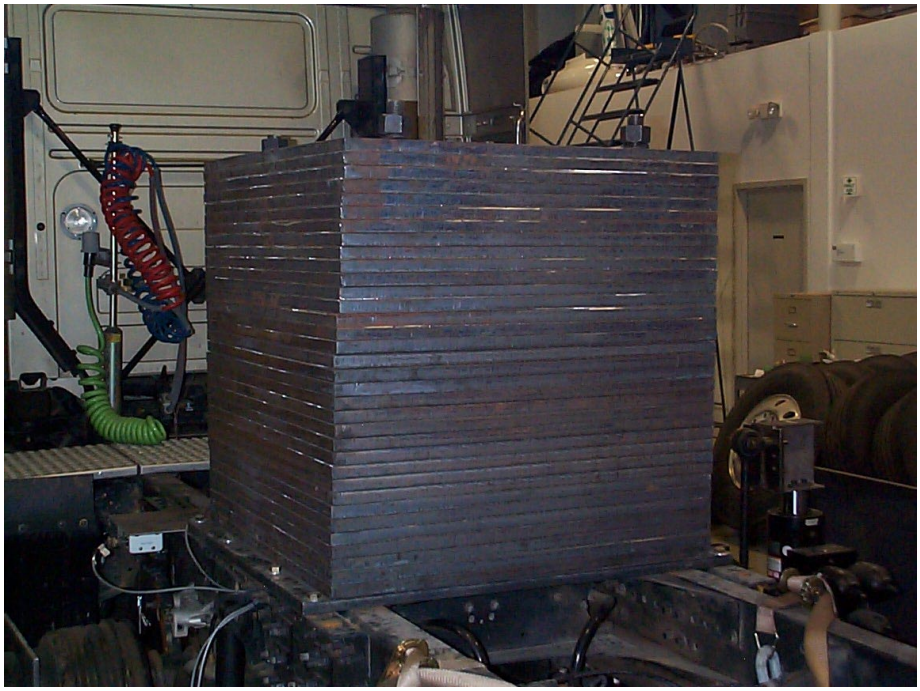

Figure 3-14 Weight Stack on Test Vehicle.

In order to support the static axle load, two airsprings (Goodyear Model 1B14-350) were attached to the axle, one at each end. An "L"-shaped metal fixture was bolted between the brake drum on the axle and the modified brake drum (slightly different than the one discussed in Section 3.2.2) and then the fixture was attached to the top of the auxiliary airspring, as is shown in Figure 3.16. By regulating the auxiliary airsprings to

80 psi, each actuator supported approximately 2500 lbs (at rest) and was not overloaded during testing.

The dynamic tests were conducted in both damped and undamped configurations. The undamped tests provide a cleaner measure of the resonant frequency of the primary suspension, whereas the damped tests provide a more realistic measure of the vehicle's dynamic response to different inputs.

3.3.2 Actuation of Suspension

Unlike the kinematics tests, a computer controlled the actuation of the suspension during dynamic testing. For each test, the input –which included a chirp, bump, or pure tone signal– was created in Simulink (Version 5.3.0.10183) and then downloaded into dSpace Control Desk (Version 1.2 P2). dSpace provided the user interface for controlling the tests and recording the data. The dSpace output was used as an external input to the MTS 458.20 Hydraulic Controller, shown in Figure 3-15. The controller regulated motion of the hydraulic actuators (MTS Model 248.03) mounted to each axle end. The setup for actuation of the suspension during dynamic testing, including the hydraulic actuator and attachments, is shown in Figure 3-16.

Figure 3-15 MTS 458.20 Hydraulic Controller.

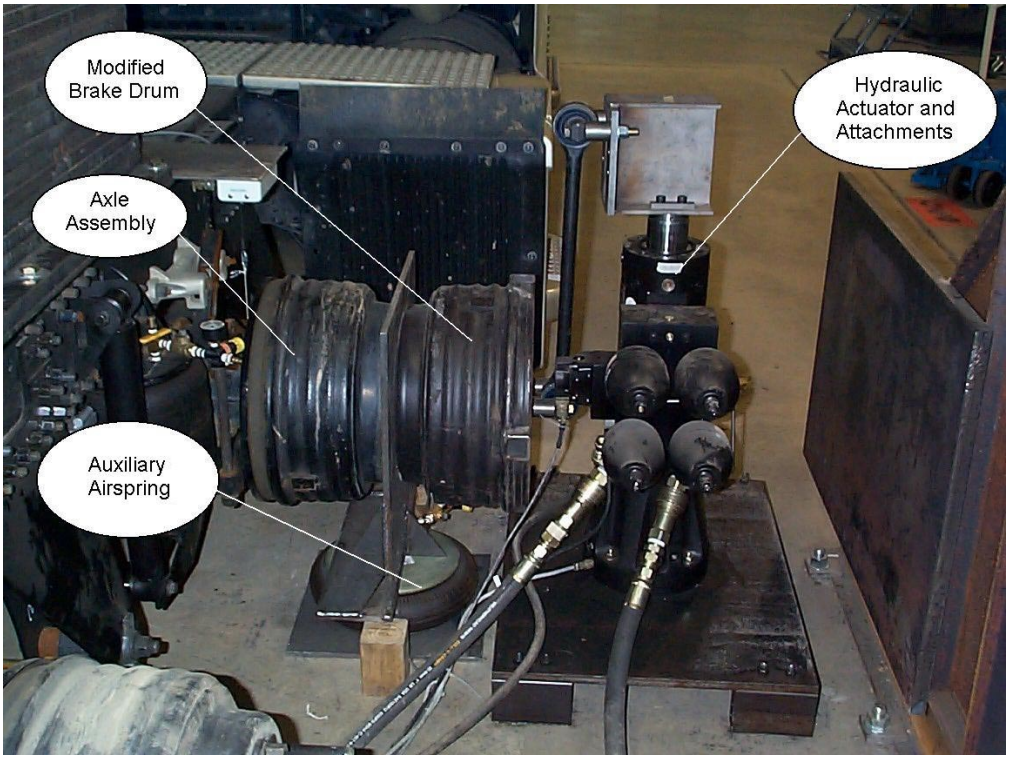

Figure 3-16 Dynamic Actuation Setup with Auxiliary Airspring.

3.3.3 Data Acquisition

As mentioned in the previous subsection, data collection and recording of all measurements was performed with dSpace. A dSpace AutoBox DS 2201 data acquisition unit, converted to use 110 VAC, recorded data from all the measurement devices on a desktop computer. To be well above the Nyquist frequency, a sampling frequency of 200 Hz was chosen (the highest test frequency in any of the input signals was 16.5 Hz). Also, the built-in anti-aliasing filters of the AutoBox prevented data acquisition errors brought about by signal aliasing. The measurements performed in dynamic testing included acceleration, relative velocity, displacement, and load.

Acceleration was measured with PCB Model 288B02 (ICP) accelerometers, such as the one shown in Figure 3-17. These accelerometers were acceptable for use in the range of frequencies tested in this study (0.5 to 16.5 Hz). To power the accelerometers and boost the resolution of their output, a PCB ICP 16 channel signal conditioner like the one in Figure 3-18 was used. The accelerometers plug into the signal conditioner and the signal conditioner has BNC outputs that go to the AutoBox.

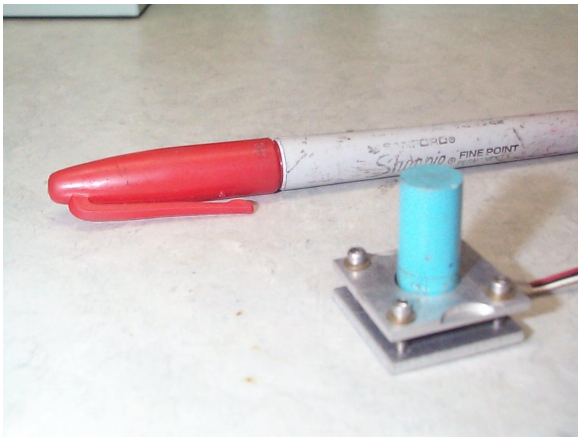

Figure 3-17 PCB Model 288B02 Accelerometer.

Figure 3-18 PCB ICP 16-Channel Signal Conditioner.

On the test vehicle, acceleration was recorded at several points, including three places on the frame, at the aft of the cab, and in two directions at the B-Post. Two of the

frame accelerometers were mounted on the bottom of the frame rail, just above the axle centerline, on each side of the axle. One is shown in Figure 3-19. The other frame accelerometer was mounted just below the rear cab mount, in the center of the frame cross-member as shown in Figure 3-20. Also shown in Figure 3-20 is the accelerometer mounted on the cab, just visible behind the edge of the cab bottom, but the accelerometer positioned at an angle, where the frame had not been cleaned, was a spare. To tie into a solid structure in the cab, the two accelerometers located there were mounted to the seatbelt anchor. Figure 3-21 shows the accelerometers mounted in the passenger compartment of the cab. These two accelerometers measured vertical and fore/aft vibrations that reach the driver.

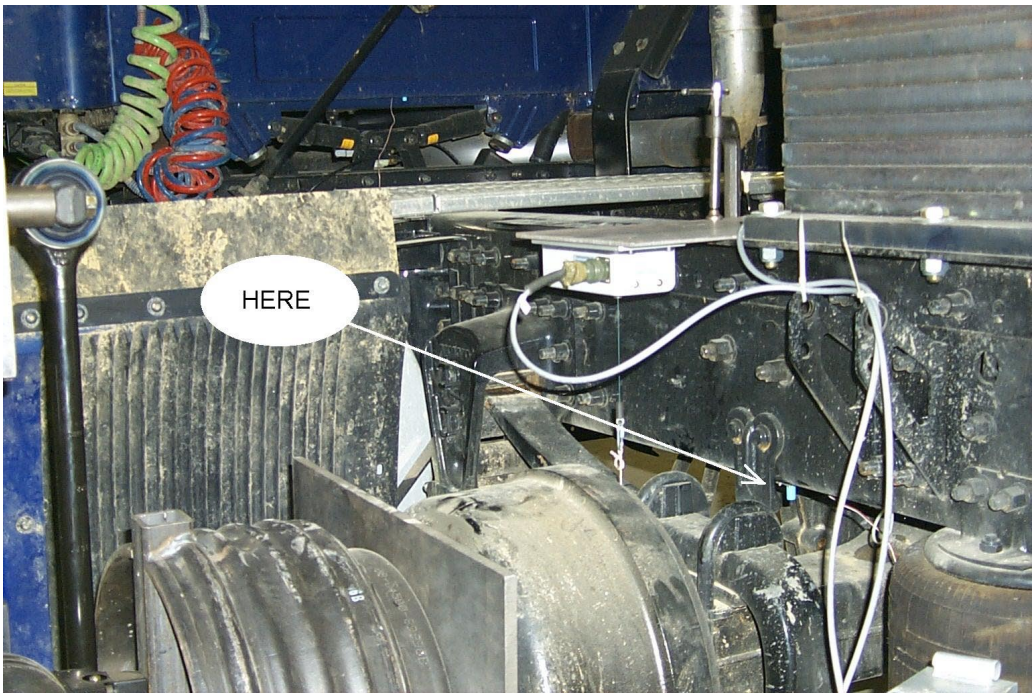

Figure 3-19 Accelerometer Mounted on Frame Rail.

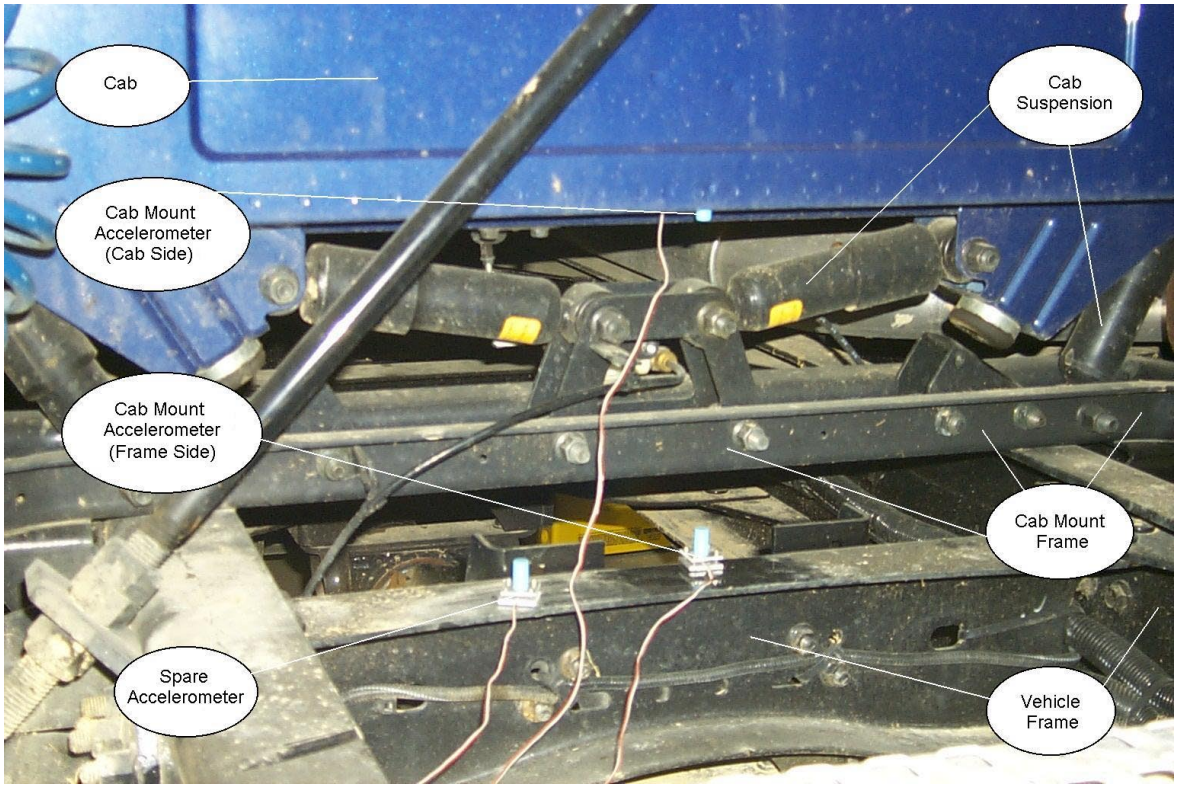

Figure 3-20 Accelerometers Mounted at Cab Suspension.

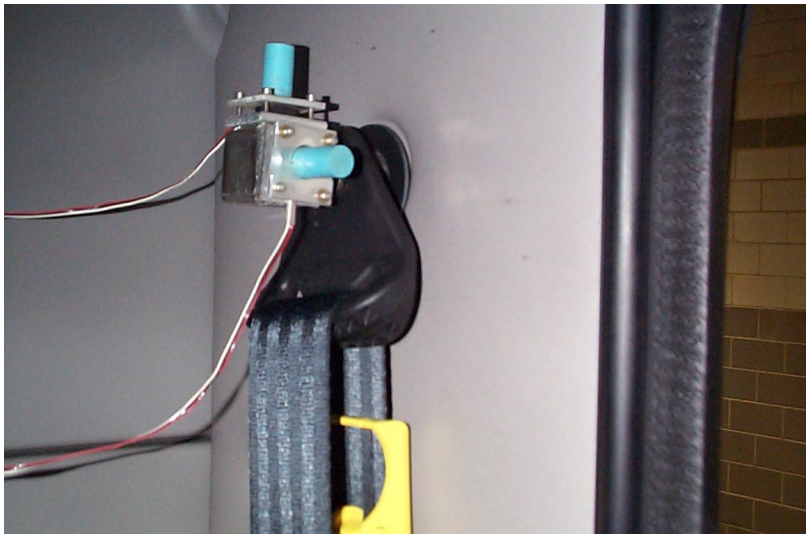

Figure 3-21 Accelerometers Mounted inside Cab.

Relative velocity was measured with the same Unimeasure LVDTs described in Section 3.2.3. The body of the device was mounted to the vehicle frame and the string

was attached to the axle. When motion between the axle and frame occurred, this LVDT would measure it (but as a velocity, not as a displacement). One of the LVDTs is visible in Figure 3-22.

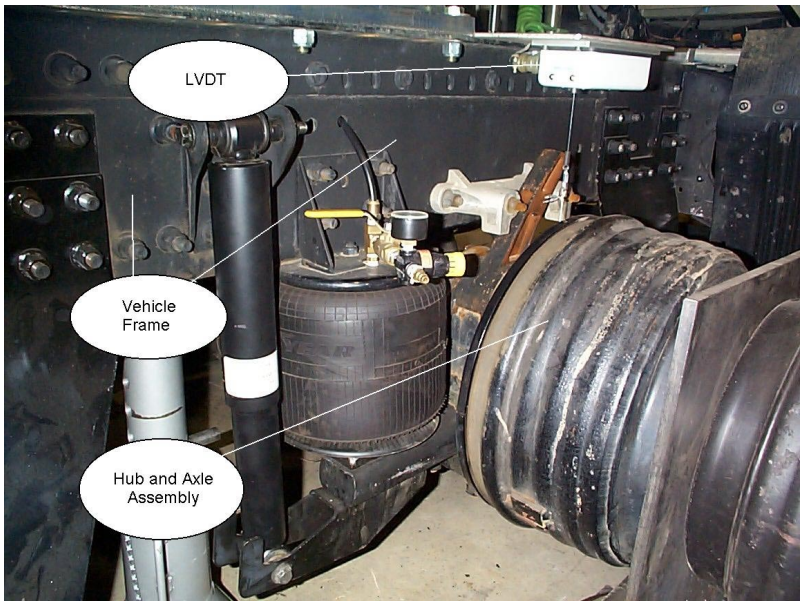

Figure 3-22 LVDT for Measuring Relative Velocity.

Other measurements recorded during the dynamic tests include the actuator displacement and force, both directly available from the hydraulic controller. Since each of the hydraulic actuators are rigidly connected to the axle, the actuator displacement and force measurements indicate the same measurements that would be made if the measurements were taken at each end of the axle.

3.4 Chapter Summary

This chapter gave a detailed description of the setups for kinematics and dynamic testing including modifications to the test vehicles, actuation systems, and data acquisition. The next chapter presents the results of the kinematics testing.

Chapter 4

Kinematics Test Results

Chapter 4 details the results of the kinematics tests. A description of the measurements made during the tests, the test procedures, and methods for data reduction are all included in this chapter. Next, the kinematics test results are presented and analyzed in detail.

4.1 Description of Measurements

The measurements made during each of the three kinematics tests are described in this section. At each position of the suspension during a test, measurements were collected in Labview for 5 seconds at 2 samples per second for each channel. Then, a value for each channel was found by averaging the 10 samples.

The only measurements collected during a test for vertical stiffness were vertical load and vertical displacement at both ends of the axle. For vertical load, a load cell was placed between the axle end and the ground, at the top of the hydraulic actuator. Vertical displacement was measured across the same two points with a Linear Voltage Differential Transformer (LVDT).

Determining roll stiffness requires taking measurements of vertical load, vertical displacement, and lateral displacement of the axle center. During a test for roll stiffness, vertical load and displacement were measured the same way as they were during a test for vertical stiffness. The lateral displacement of the axle center was measured with another LVDT. This LVDT was mounted to a stand so that the measurement was taken at the same vertical height as the axle centerline. Mounting the LVDT at this height

ensured the lateral displacement measurement was not corrupted by a vertical displacement component.

For a test of roll steer, longitudinal displacement of the axle ends was measured, along with vertical displacement. Measuring longitudinal displacement was achieved with two LVDTs, mounted on stands, just as if lateral displacement of the axle centerline were being measured. The exception is that each of the two LVDTs was mounted to an axle end, parallel to the vehicle frame (to measure displacement in that direction). Since the axle ends move vertically during a test for roll steer, the change in height of the axle ends had to be considered in the calculations.

4.2 Test Procedure

This section outlines the procedure followed while performing each of the kinematics tests. For a detailed description of each test, as well as preparation of the vehicle prior to testing, refer to Appendix A.

4.2.1 Vertical Stiffness

With the suspension at ride height, the air pressure of the suspension was set. Next, the axle was lowered to 2 in below ride height. The first measurement was taken at this position. In increments of ¼ in, both sides of the axle were raised and another measurement was taken. This continued until the axle was 2 in above ride height, giving a total of 17 measurement points.

4.2.2 Roll Stiffness

Just as with the test for vertical stiffness, the air pressure was set when the axle was at ride height. The passenger side of the axle was raised 2 in and the driver side was lowered 2 in (full positive roll, clockwise when viewed from the front of the vehicle). Once this position was reached, the first measurement was recorded. Then, the passenger side was lowered ¼ in, the driver side was raised ¼ in, and another measurement was taken. This continued until the axle had reached full negative roll (passenger side 2 in below ride height and driver side 2 in above ride height). Next, the roll was reversed while recording measurements in ¼ in increments. When the axle returned to full positive roll, the test was not yet complete. The last step in the test involved bringing the axle from the full positive roll to the horizontal (no roll) position (while continuing to record the force and displacement at every ¼ in), which resulted in a total of 41 data points.

4.2.3 Roll Steer

The test for roll steer followed the same procedure as for roll stiffness, except that the axle was rolled in increments of 1 in instead of ¼ in. This reduced the total number of measurements to 11.

4.3 Data Reduction

Equations for the reduction of the data, and how they are used, are included in this section. For all three kinematics tests, the origin of the coordinate system was defined at the midpoint of the axle centerline. A positive *X* vector points from origin to the cab, a

positive *Y* vector points from the origin toward the driver side axle end, and a positive *Z* vector points straight up. Side *A* is the passenger side of the vehicle and side *B* refers to the driver side.

4.3.1 Vertical Stiffness

Vertical displacement from ride height, ΔZ, was found by averaging the height of both axle ends, Z_A and Z_B, after subtracting the ride height, Z_{AO} and Z_{BO}, i.e.:

$$\Delta Z = \frac{(Z_A - Z_{AO}) + (Z_B - Z_{BO})}{2}, \tag{4-1}$$

To visualize the relationship between the axle housing and these variables, refer to Figure 4-1.

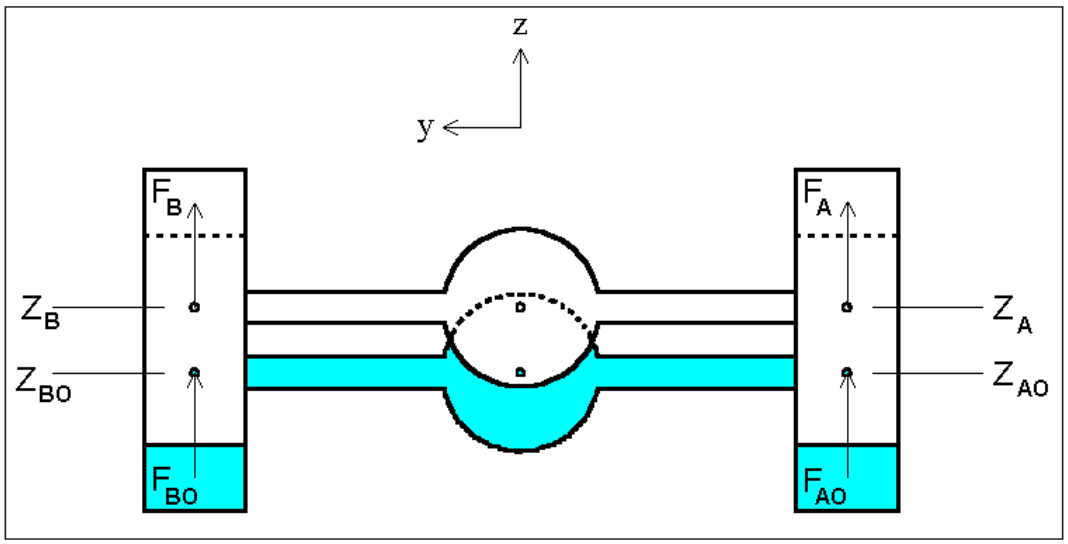

Figure 4-1 Axle Housing Schematic for Vertical Stiffness Test (Rear View of Axle Housing).

The vertical load was also referenced from ride height. The load at each axle end at ride height, F_{AO} and F_{BO}, was subtracted from the total load, F_A+F_B, at each

measurement position to give the difference in load, F, which is defined mathematically as:

$$F = (F_A - F_{AO}) + (F_B - F_{BO}) \ , \tag{4-2}$$

Plotting the difference in load, F, as a function of the displacement, ΔZ, gives a curve of which the slope is:

$$K_V = \frac{F}{\Delta Z} , \tag{4-3}$$

where K_V is the vertical stiffness of the suspension.

4.3.2 Roll Stiffness

The roll angle, Θ_R, of the axle was found using:

$$\Theta_R = \frac{|Z_A - Z_{AO}| + |Z_B - Z_{BO}|}{d_{ROLL}} \ , \tag{4-4}$$

The Z displacements are the same as for vertical stiffness. For a schematic that relates these equations and variables to the axle housing, refer to Figure 4-2.

The lateral distance between the measurement locations is termed d_{ROLL}. The lateral displacement of the axle housing, ΔY, was calculated according to:

$$\Delta Y = Y_O - Y \ , \tag{4-5}$$

where Y_O is the lateral displacement of the axle housing with zero roll and Y is the measured lateral displacement with any degree of roll. Next, the roll center height of the suspension, H_{RC} , was calculated as:

$$H_{RC} = \frac{\Delta Y}{\Theta_R} + z \ , \tag{4-6}$$

where z is the distance between the axle centerline and the ground. To determine the change in torque, ΔT, across the axle housing, we used:

$$\Delta T = (F_B - F_{BO}) \cdot \left(\frac{d_{ROLL}}{2} - \Delta Y \right) - (F_A - F_{AO}) \cdot \left(\frac{d_{ROLL}}{2} + \Delta Y \right), \tag{4-7}$$

where the F loads are the same as in the test for vertical stiffness. Plotting the change in torque as a function of roll angle gives a curve with the slope of:

$$K_R = \frac{\Delta T}{\Theta_R}, \tag{4-8}$$

where K_R is the roll stiffness of the suspension.

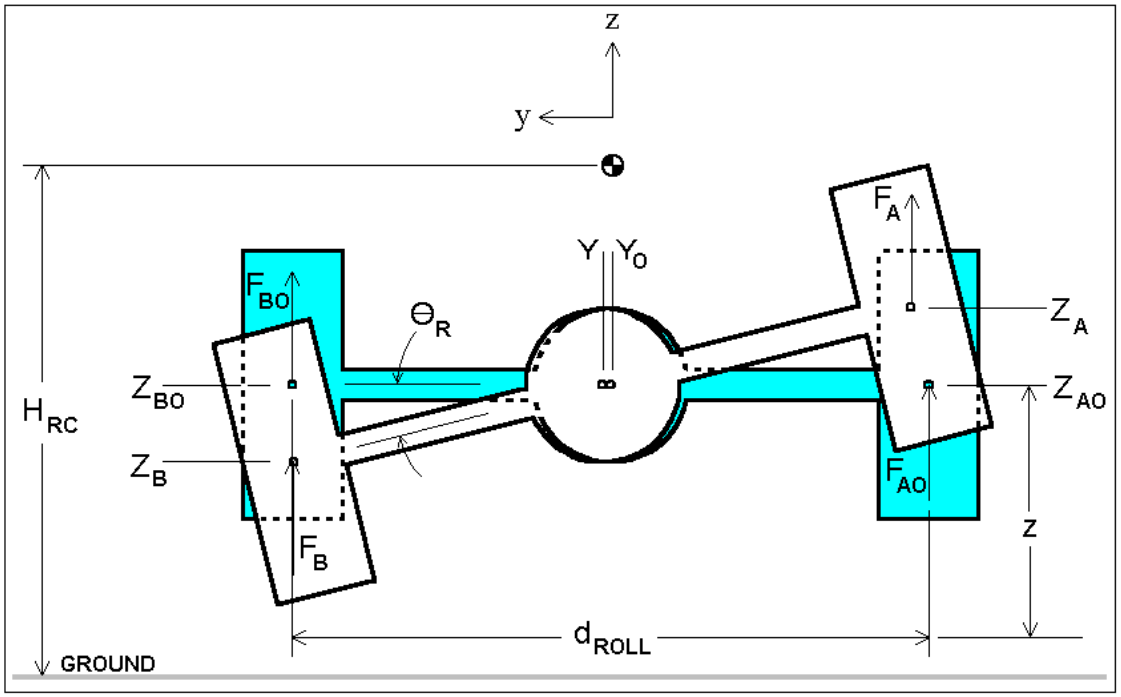

Figure 4-2 Axle Housing Schematic for Roll Stiffness Test (Rear View of Axle Housing).

4.3.3 Roll Steer

Figure 4-3 depicts the relationship between the axle housing and the following variables of the roll steer test. For this test, the roll angle of the suspension was found in the same manner as the roll stiffness test, and the yaw angle was computed as:

$$\Theta_Y = \frac{|X_A - X_{AO}| + |X_B - X_{BO}|}{d_{YAW}}, \tag{4-9}$$

where X refers to the longitudinal displacement of each axle end and d_{YAW} is the distance between the two locations where the X measurements were made. The roll steer of the suspension, defined by:

$$Roll\ Steer = \frac{\Theta_Y}{\Theta_R}, \tag{4-10}$$

is the ratio between the yaw angle (caused by the roll angle) and the roll angle, Θ_R.

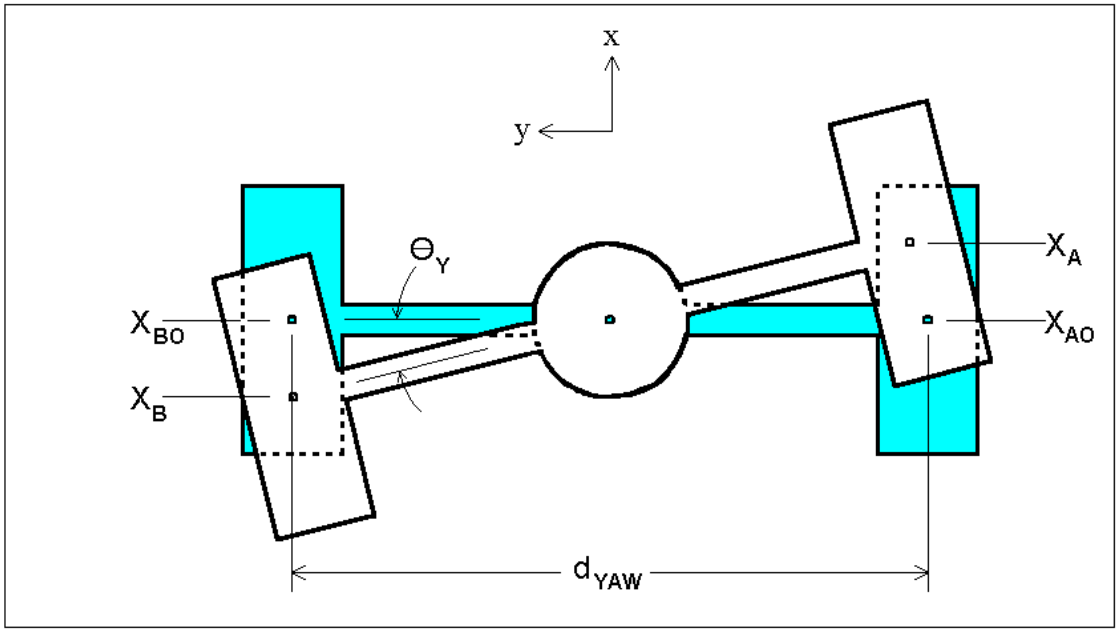

Figure 4-3 Axle Housing Schematic for Roll Steer Test (Top View of Axle Housing).

4.4 Results

Results for the kinematics tests are included in this section. It is important to note that the VOAS-2 test vehicle's front and rear drive axles were equipped with two different trailing-arms. On the front drive axle, a 1-¾ in thick trailing-arm was used, while the trailing-arm on the rear drive axle was 2 in thick. Both of these designs were under consideration and the manufacturer was interested in the test results of both versions.

4.4.1 Vertical Stiffness

The curve defined by the difference in load at the axle versus the displacement of the axle, both referenced from ride height, is the vertical stiffness of the suspension. For VOAS-1, the vertical stiffness is shown in Figure 4-4. Similarly, Figure 4-5 shows the vertical stiffness of both drive axles on the VOAS-2 equipped test vehicle. For a numeric value of the stiffness, the slope of the curve was determined in the linear range of the suspension with a trend line. Figures 4-6 and 4-7 show this for VOAS-1 and VOAS-2, respectively. On each figure, positive displacement means the axle was in jounce (compression) and a negative displacement means the axle was in rebound (extension). If the difference in load is greater than zero, it means that the load was higher at that point than at ride height.

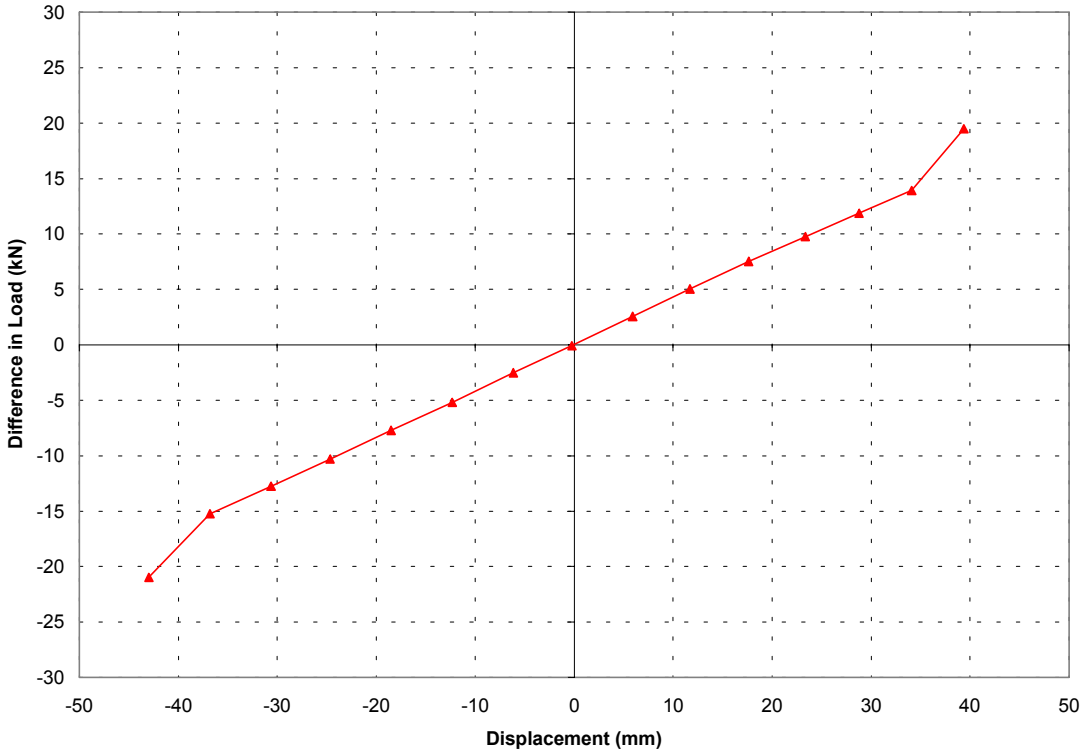

Figure 4-4 Vertical Stiffness of VOAS-1 Suspension (Front Drive Axle, Full Range, 55psi).

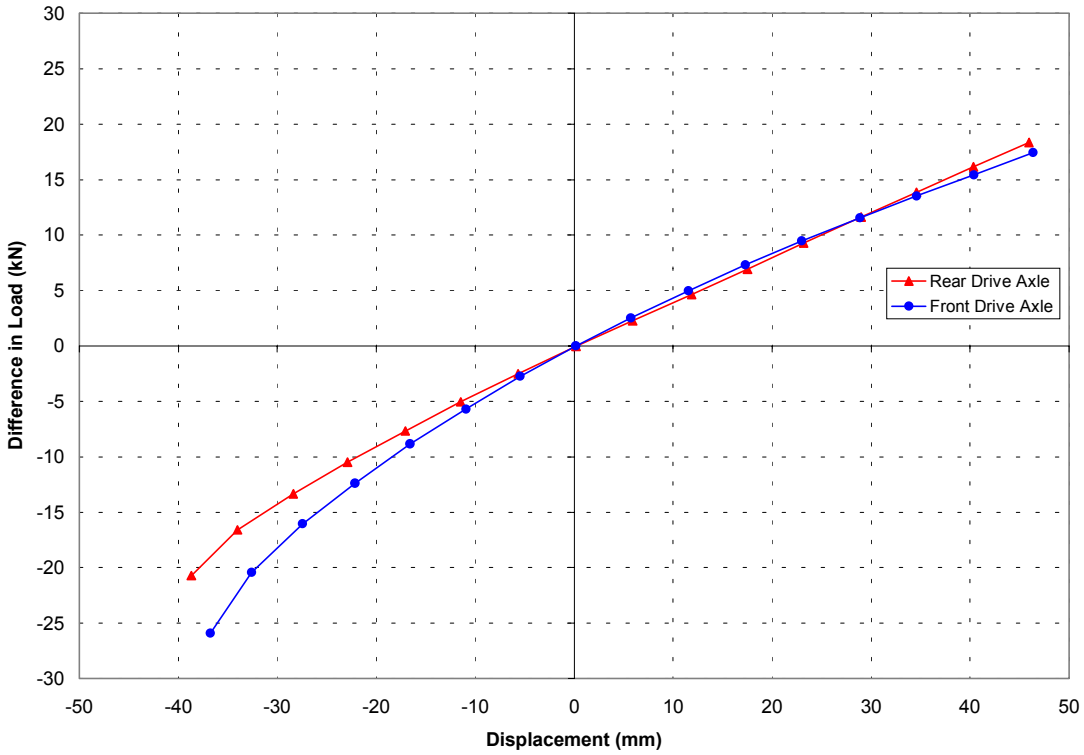

Figure 4-5 Vertical Stiffness of VOAS-2 Suspension (Both Drive Axles, Full Range, 85psi).

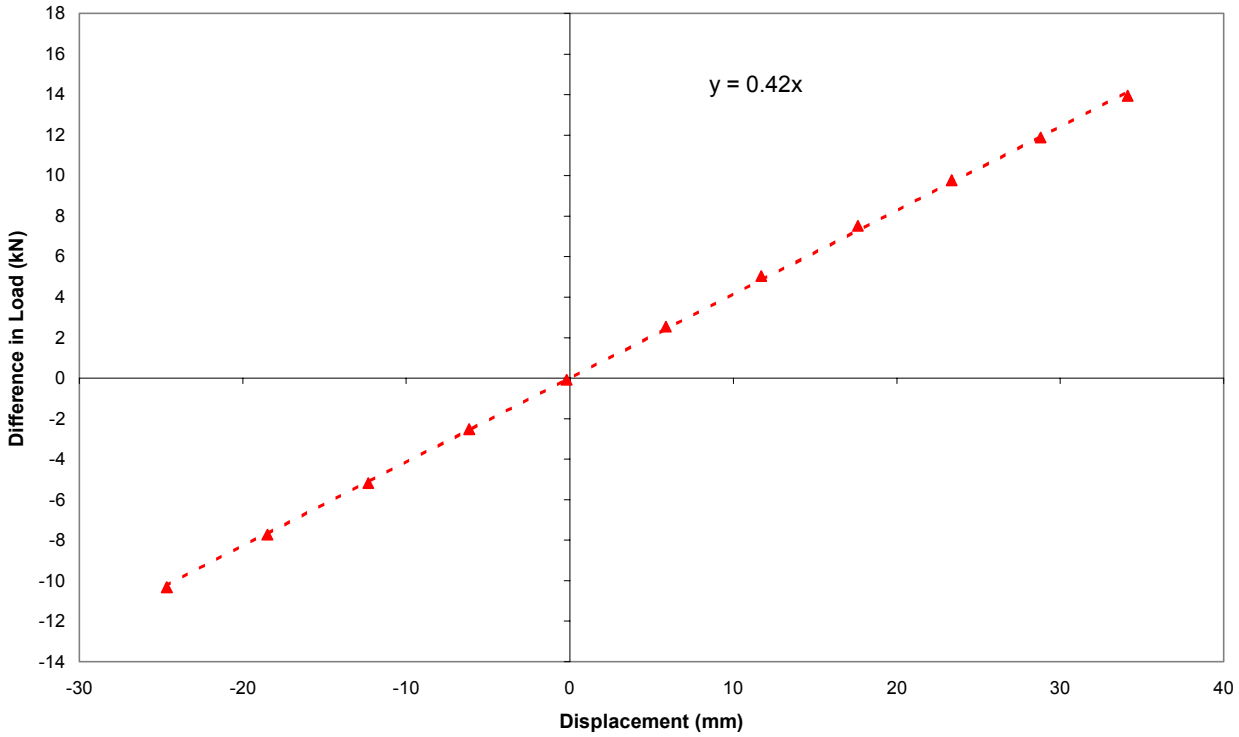

Figure 4-6 Vertical Stiffness of VOAS-1 Suspension
(Front Drive Axle, Linear Range, 55psi).

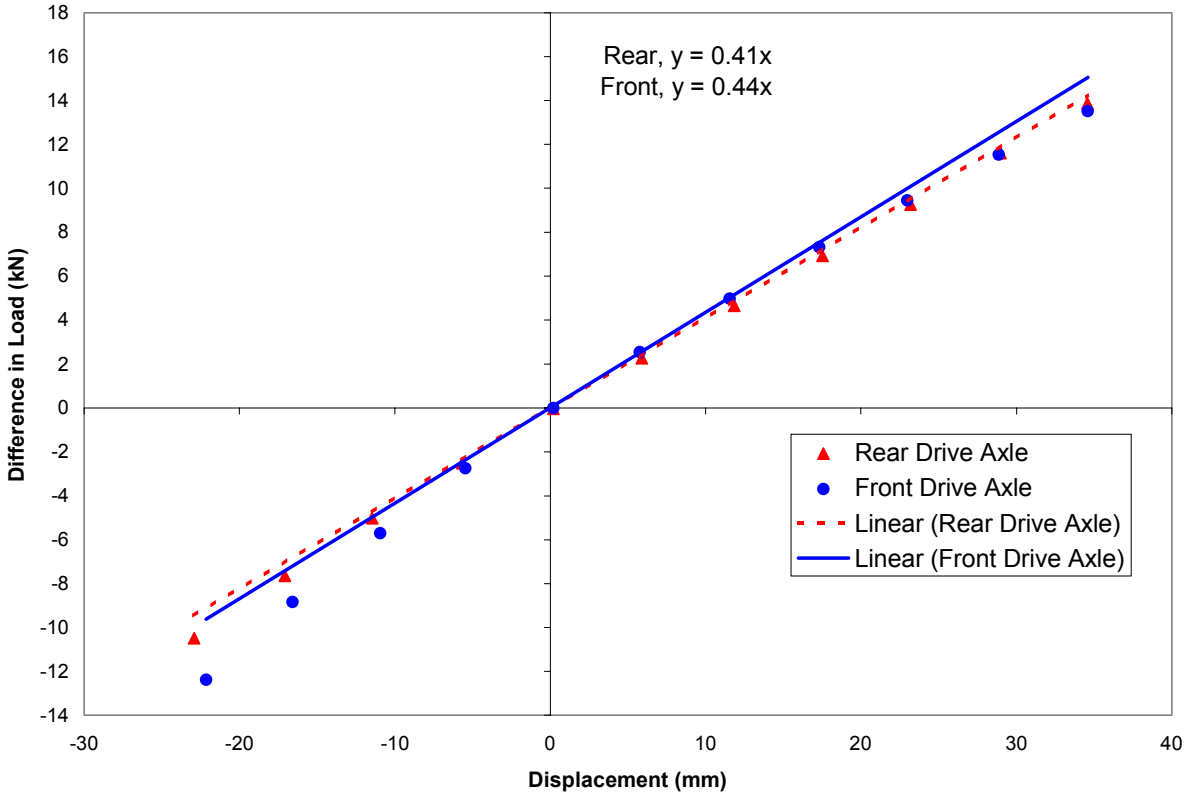

Figure 4-7 Vertical Stiffness of VOAS-2 Suspension
(Both Drive Axles, Linear Range, 85psi).

4.4.2 Roll Stiffness

When plotting the change in torque across the axle housing (referenced from zero roll) versus the roll angle, the slope of the curve is the roll stiffness of the suspension. The roll stiffness of VOAS-1 is shown in Figure 4-8, while Figure 4-9 show the roll stiffness for VOAS-2. Both of these figures include numeric values of the roll stiffness found by fitting a trend line through the data. A positive roll angle occurs when the passenger side of the axle is above ride height and the driver side is below ride height (the axle is rotated clockwise when viewed from the front of the vehicle). The change in torque is also referenced from ride height. When a positive roll is induced, the change in torque from ride height is also positive, except when considering hysteretic effects (discussed further in Section 4.5.2).

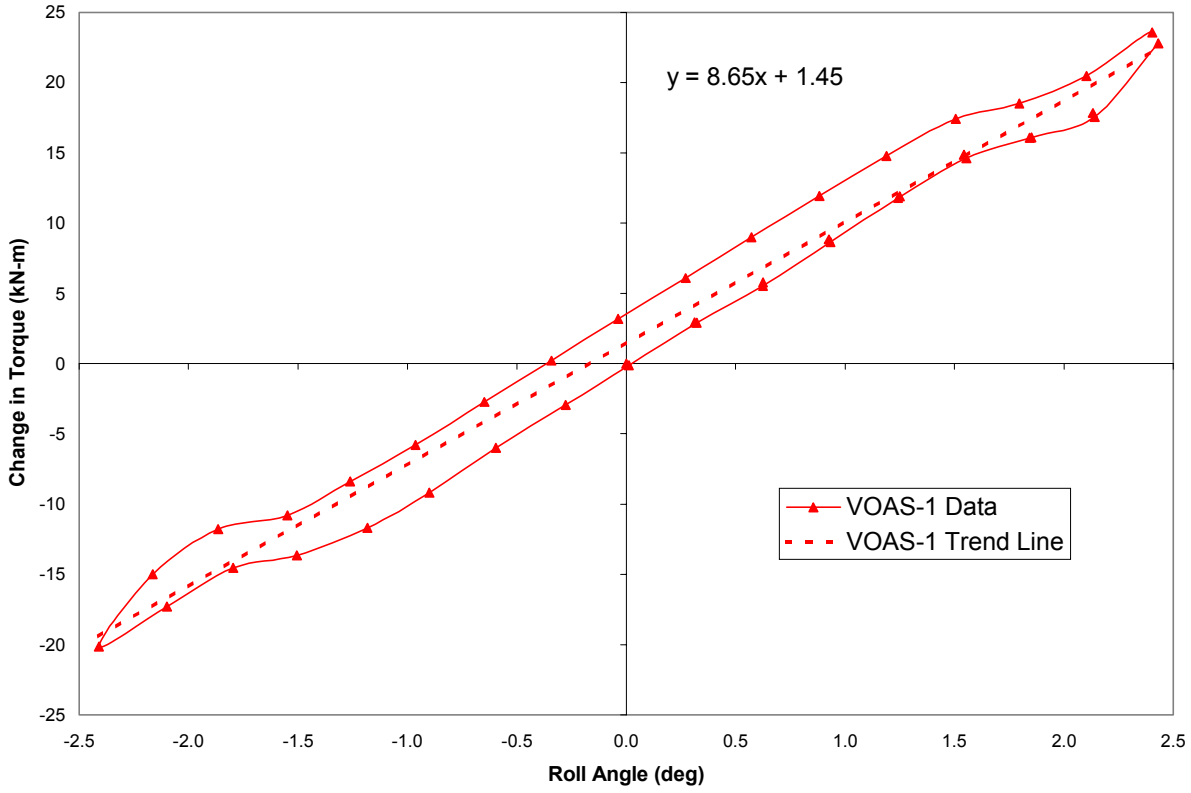

Figure 4-8 Roll Stiffness of VOAS-1 Suspension (Front Drive Axle, 55psi).

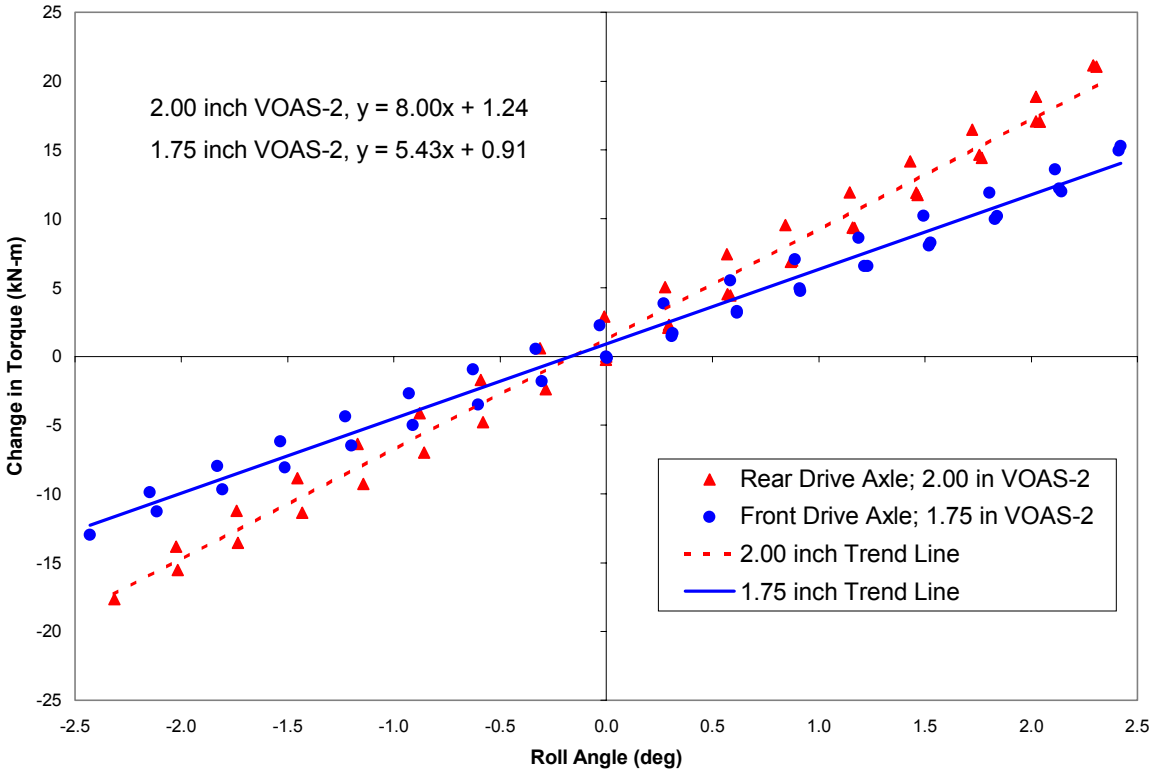

Figure 4-9 Roll Stiffness of VOAS-2 Suspension (Both Drive Axles, 85psi).

The roll center height of each test vehicle, which is calculated according to Equation 4-6, is shown in Table 4-1.

Table 4-1 Roll Center Height for VOAS-1 and VOAS-2 Suspensions.

	Roll Center Height (mm)
VOAS-1 Front Drive Axle	853.2
VOAS-2 Front Drive Axle	868.6
VOAS-2 Rear Drive Axle	845.5

4.4.3 Roll Steer

The test for roll steer was only performed on the VOAS-2 equipped test vehicle. Yaw angle is the angle of the axle when viewed from above. A positive yaw angle is clockwise; meaning the driver side of the axle is further forward than the passenger side. Figure 4-10 shows the results of the test for both VOAS-2 drive axles.

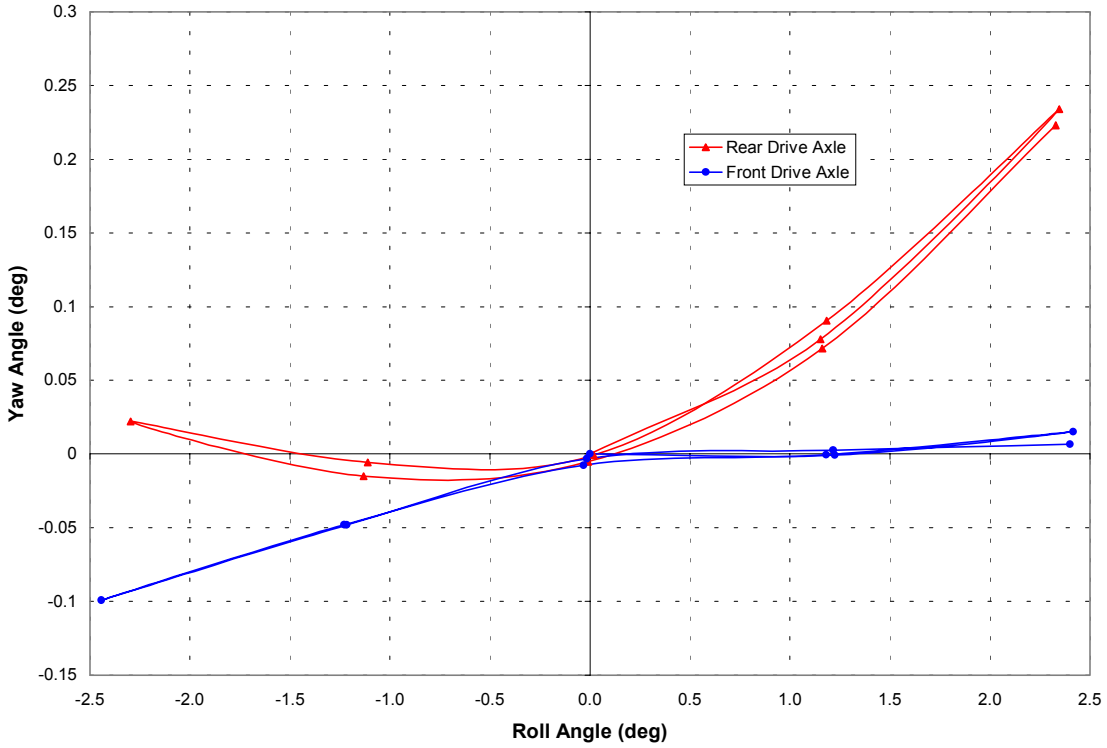

Figure 4-10 Roll Steer of VOAS-2 Suspension
(Both Drive Axles, 85psi)

4.5 Discussion of Results

In the following three subsections, the necessary support is included for the results presented in the previous section. VOAS-2 results are compared to those of VOAS-1, with the intent of proving whether or not the new suspension meets the goal of matching the kinematics performance of the current suspension.

4.5.1 Vertical Stiffness

The vertical stiffness of each VOAS-2 drive axle was very similar to the vertical stiffness of VOAS-1, as is especially visible in Figures 4-6 and 4-7. VOAS-1 had a vertical stiffness of 420 N/mm, while the VOAS-2 front and rear drive axles had a stiffness of 440 N/mm and 410 N/mm, respectively. The difference between VOAS-1 and VOAS-2 front was less than 5% and less than a 3% difference occurred when VOAS-1 was compared to the rear drive axle of VOAS-2.

Differences arose when VOAS-1 and VOAS-2 were compared at displacements greater than +/- 20mm (outside of the linear regions of the data). Refer to Figure 4-4, the full range of VOAS-1. At approximately +/- 35mm, the slope of the curve (the stiffness) more than doubled. Both VOAS-2 drive axles exhibited a similar "stiffening effect", but its onset was much more gradual. Figure 4-5 shows this effect on both VOAS-2 drive axles, especially with rebound greater than (-)10 mm. This stiffening effect was expected (and desirable) as the suspension neared its limits of travel. Several factors can contribute to the stiffening of the suspension as it reaches its limits. The shape of the "bell" that the air spring rides upon significantly affects the behavior of the suspension's stiffness, as does the shape and mounting of the trailing-arm. Differences between the trailing-arms of VOAS-1 and VOAS-2 were the most likely cause of this slight inconsistency in behavior.

4.5.2 Roll Stiffness

Before discussing the similarities and differences of VOAS-1 and VOAS-2 in roll, several aspects of Figures 4-8 and 4-9 need to be addressed. In both figures, a hysteretic

effect is visible. This effect is a "loop" in the data as the suspension was moved from positive roll, to negative roll, and back. Coulomb friction between the trailing-arm and its mounts is the most likely cause of this hysteresis, which was expected in the results for both suspensions. Another aspect requiring further discussion is seen in Figure 4-8 only, as it was unique to the design of VOAS-1. At roll angles greater than +/- 1.5 deg, the slope of the curve decreases slightly before returning to "normal". This flattening of the curve is attributed to the lash inherent at the sliding end of the trailing-arm against its support. As with the hysteretic effect, lash was an expected phenomenon, but only for VOAS-1.

When comparing the roll stiffness of VOAS-1 and both VOAS-2 drive axles, the results were not as similar as those of the vertical stiffness test. As indicated by the trend line in Figure 4-8, roll stiffness for VOAS-1 was 8.65 kN-m/deg, yet the front drive axle of VOAS-2 was 5.43 kN-m/deg (see Figure 4-9). This is almost a 40% difference in roll stiffness. If the VOAS-2 front drive axle is intended to see the same loading as the VOAS-1 axle, the vehicle could experience a 60% larger roll angle.

The VOAS-2 rear drive axle, which was equipped with a 2 in trailing-arm (versus the 1-¾ in one on the front drive axle), had the much higher roll stiffness of 8.00 kN-m/deg. With a percent difference of less than 8%, the VOAS-2 drive axle had a roll stiffness much closer to VOAS-1 than the front drive axle version.

The roll center height was slightly different for each drive axle, as Table 4-1 shows. The VOAS-2 front drive axle had a roll center 15mm higher than VOAS-1 (868.6 mm compared to 853.2 mm), while the VOAS-2 rear drive axle had a roll center height of only 845.5 mm (8 mm lower than VOAS-1). A higher roll center increases the roll

stiffness of the vehicle through the geometry of the suspension, but this is not represented well in Figures 4-8 and 4-9. The results indicate the trailing-arm torsional stiffness dominates the roll stiffness of the suspension, when compared to the roll center height. Figure 4-9 supports this claim. The only difference between VOAS-2 front and rear drive axles, that affects roll stiffness, was the trailing-arm torsional stiffness, which was caused by different thicknesses of the trailing-arm. Increasing the thickness of the trailing-arm by ¼ in, a 12.5% change, increases the suspension's roll stiffness by over 30%.

4.5.3 Roll Steer

Ideally, a suspension would exhibit no roll steer, as it causes steering of the vehicle not originally intended by the driver. Some roll steer is inevitable in a given design, and so it can only be minimized. Understeer caused by roll steer is more desirable than oversteer. Understeer occurs when the axle turns away from the direction of the turn, requiring more steering effort and/or less vehicle speed to keep the vehicle on its intended path. If understeer is not corrected, the vehicle will "push" and will take the turn too wide. Oversteer is the opposite case. The axle turns in the direction of the turn, possibly causing the rear of the vehicle to spin out, if traction is overcome, or the vehicle to roll, if traction is maintained.

To give the results some clarity, imagine that a vehicle is making a left turn. The body of the vehicle rolls to the outside of the turn, loading the passenger side of the axle and unloading the driver side. When the axle is in this position, its roll angle is positive, clockwise when viewed from the front of the vehicle. Understeer (more desirable) would

occur if the axle turned away from the (left) turn. A rotation of the axle in this direction is a positive yaw angle, clockwise when viewed from above the vehicle. In a right turn, the opposite occurs; roll and yaw angles are both negative in the case of understeer. So in the results, an axle with measurements in the first and third quadrants (when roll angle is positive, so is yaw angle, and vice versa) of a roll steer plot will exhibit understeer.

Both VOAS-2 drive axles had measurable roll steer, as is shown in Figure 4-10. For the front drive axle, yaw angle was less than 0.1 deg for all roll angles. If the axle were 2.5 m wide, this would correspond to a longitudinal displacement of 2 mm at the outermost edge of the tire. The rear drive axle showed more roll steer, almost a 0.25 deg yaw angle at full positive roll. Using the same axle dimensions as in the previous example, this yaw angle would cause a maximum longitudinal displacement of 5.5 mm. The results of both drive axles indicate understeer tendencies, except when the yaw angle of the rear drive axle becomes positive at high negative roll angles. If this condition occurred, the maximum yaw angle would be 0.025 deg and the outermost edge of the tire would only be displaced 0.5 mm.

4.6 Chapter Summary

This chapter described the measurements, the procedures, the methods of data reduction, and ultimately the results of the kinematics testing performed in this study. The next chapter follows a similar format and presents the results of the dynamic testing.

Chapter 5

Dynamic Test Results

The results of the dynamic tests are covered in Chapter 5. This includes a description of the measurements made during the tests, the test procedures, the test configurations, and the data reduction. Results of all the dynamic tests are presented next, followed by a section that discusses the significant results.

5.1 Description of Measurements

For the three input signals, chirp, hard bump, and pure tone, measurements were collected the same way. Data acquisition was performed with a dSpace AutoBox that was connected to a personal computer. All measurements, acceleration, relative velocity, displacement, and force, were sampled at 200 Hz for the duration of the input signal. Since the maximum analysis frequency was 16.5 Hz, sampling at 200 Hz alleviated any concerns of aliasing in the results.

Acceleration was measured at six locations on the vehicle. An accelerometer was mounted on the underside of each of the frame-rails, just above the axle centerline (in the results, only one of these two accelerometers is included because the measurements are so similar). At the cab mount, one accelerometer was mounted on the frame side of the mount, and another was mounted on the cab side. The final two accelerometers were mounted in the cab, at the seat belt anchor on the B-post. One of those two accelerometers was mounted horizontally to measure fore-and-aft acceleration; the other five accelerometers were mounted vertically.

To measure relative velocity across the suspension, two Linear Voltage Differential Transformers (LVDTs) were used, one for each side of the axle. The base of the LVDT was secured to one of the frame-rails and the string was extended to the axle. Just as with the accelerometer mounted here, the results were only reported for one of the LVDTs (the same side as the reported accelerometer) to avoid redundancy.

Displacements of each axle end, as well as the forces at those locations, were the same as the displacement and force at each hydraulic actuator. The hydraulic controller measured these two quantities and they were recorded directly into the AutoBox from there.

5.2 Test Procedure

This section gives an overview of the procedure followed during the dynamic tests. Although the order of the dynamic tests is not significant, if all three input signals are to be tested, performing them in the order in which they are described in this section is recommended. Before performing each of the tests, the ride height of the suspension must be set. To do this, the air pressure of the suspension air springs is adjusted until the distance between the axle housing and the frame rail (the ride height) is correct. Appendix B can be consulted for a more detailed description of the dynamic testing.

The chirp signal input (Figure 5-1, shown in its entirety) is loaded first, and gain was slowly increased until visible motion of the vehicle occurred. Next, the window was set to capture the entire signal (64 seconds). When a complete signal was visible in the window, the gain was increased to 1.0. Once the signal starts over, data was collected for the length of the signal and the capture was saved.

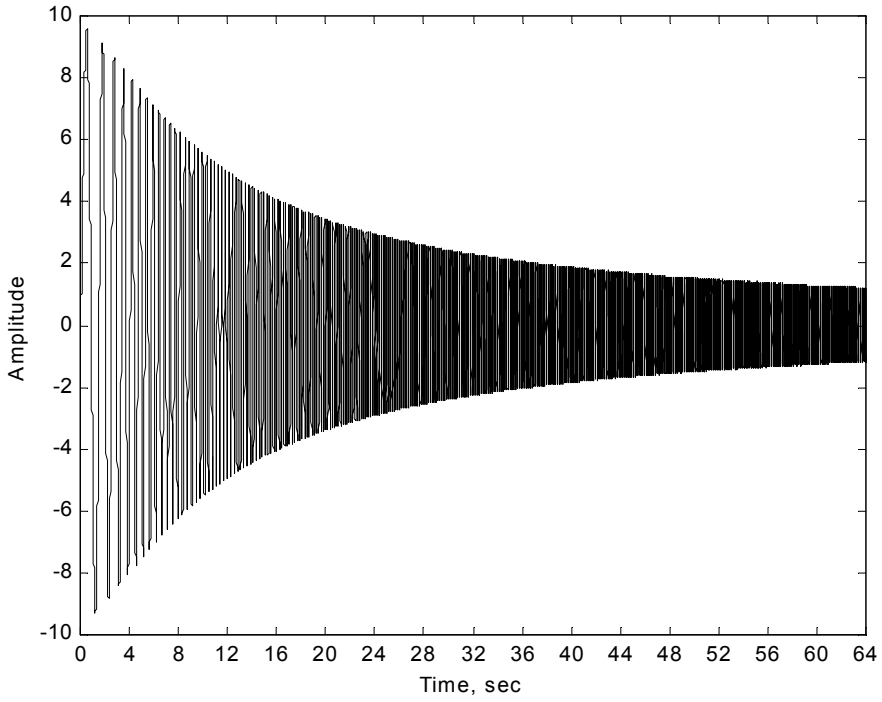

Figure 5-1 Chirp Input Signal.

The hard bump input was loaded next, after confirming that the ride height was correct. The gain was slowly increased until motion of the vehicle was visible and then the window was set to capture 60 seconds of data. When this was complete, the gain was increased to 0.5 and data collection was started the next time the amplitude was zero. Figure 5-2 shows the hard bump signal, although only the first impact (the 0 to 5 amplitude jump occurring at just under 10 seconds) was used in the results.

Pure tone inputs were tested last. The input signal was loaded and the gain was increased slightly. A 10 second window was set to capture the data and the first input frequency was run at its corresponding gain. The data was recorded and the next input frequency was tested (possibly with a different gain). This continued until all pure tone frequencies had been tested and all of their captures had been recorded. As an example, a 1.2 Hz pure tone input signal is shown in Figure 5-3.

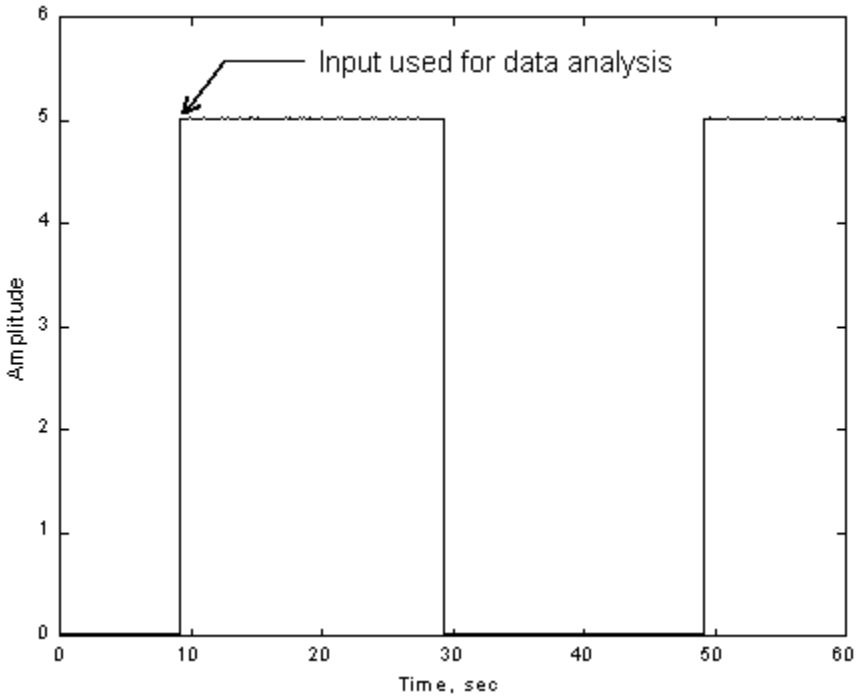

Figure 5-2 Hard Bump Input Signal.

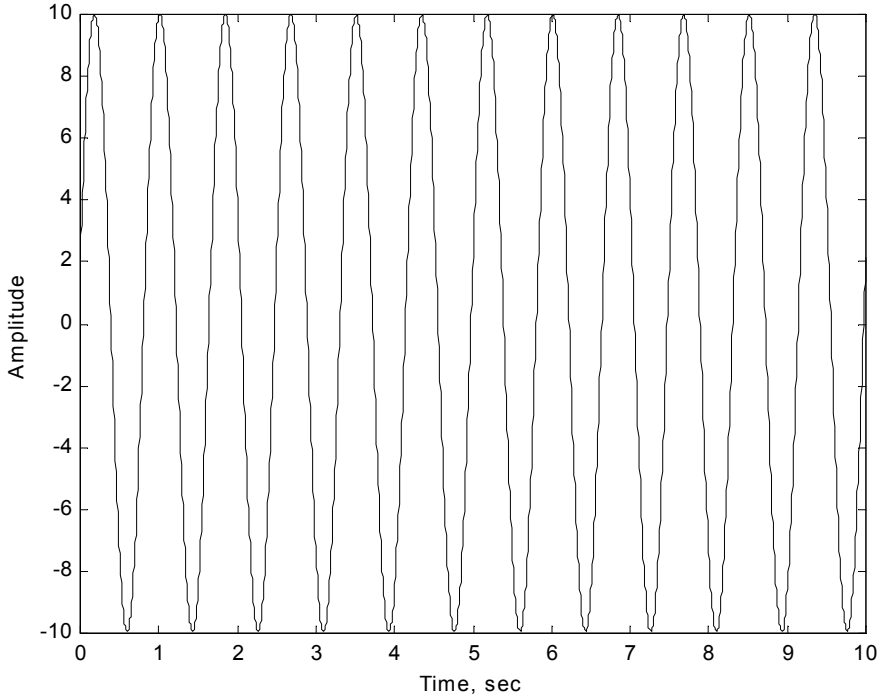

Figure 5-3 Pure Tone (1.2 Hz) Input Signal.

5.3 Test Configurations

Three suspension configurations were tested in the dynamic testing schedule. For the first configuration, the vehicle equipped with VOAS-1 was tested without dampers. This configuration provided the baseline with which to compare the undamped VOAS-2 test vehicle, the second configuration. Direct comparison of these two configurations shows any differences in undamped dynamic performance between the two suspensions. The final configuration tested was the VOAS-2 equipped test vehicle with dampers, in order to more accurately represent the suspension configuration on a production vehicle.

5.4 Data Reduction

The following three sections describe the reduction of the raw data collected during the chirp, hard bump, and pure tone input signals. Although there are no differences in the collection of the data between the three input signals, analysis of each one was distinctive.

5.4.1 Chirp Signal

The main purpose of the chirp signal was the excitation of all major modes of vibration of the vehicle occurring between 0.5 and 16.5 Hz. By looking at the frequency response of the vehicle to this input, the dominant modes could be identified and then compared between test configurations.

To develop the frequency response, the time domain measurements were imported into Matlab®. Next, the data was truncated so that only the measurements made during the 64 second span of the input signal were included, although more than 64

seconds worth of data was collected to ensure that the complete signal was captured. Assuming that t is the time vector of the data and i is the index of some value in that vector, the time increment, Δt, can be calculated as:

$$\Delta t = t(i+1) - t(i) \ , \tag{5-1}$$

The inverse of Δt also represents the sampling frequency, f_{samp}. The total time, or period, of the signal is denoted T, and the total number of samples, N, can be calculated as:

$$N = \frac{T}{\Delta t} \ , \tag{5-2}$$

The frequency increment, Δf, used when plotting the frequency domain, was determined using:

$$\Delta f = \frac{1}{T} \ , \tag{5-3}$$

After specifying the number of FFT (Fast Fourier Transform) points, the time domain data, and the order of fit, a Matlab® command called *pburg* was used to determine the power spectrum of the data and fit a curve to it. The number of FFT points was equated to N, and a 150^{th} order fit was used because it provided the highest amplitude and frequency accuracy without being excessive. "Cleanliness" of the results (in the sense of reducing the noise levels in the plots) after the estimation was the main reason for choosing *pburg*. This cleanliness greatly simplified the comparison of the data for different vehicles. The results of the chirp signal input are presented in Section 5.5.1.

5.4.2 Hard Bump Input

Unlike the chirp input data, the data collected during the hard bump input was only analyzed in the time domain. This was because the hard bump input results were used to show damping, the decreasing amplitude of a measurement as a function of time. The LVDTs that were mounted across each vehicle primary suspension measured relative velocity between the axle and the frame. Since the damper was mounted between the axle and frame as well, data collected with the LVDTs during a hard bump input was perfectly suited for this application.

After loading the data into Matlab®, relative velocity was plotted versus time without modification. The maximum positive and negative amplitudes were recorded and the maximum peak-to-peak amplitude was just the difference of those two values. Damping ratio, ζ, was a little more complicated to calculate. First, the logarithmic decrement, δ, must be determined, according to:

$$\delta = \frac{1}{j} \ln\left(\frac{x_1}{x_{j+1}} \right), \tag{5-4}$$

where x_1 is the amplitude of the first peak, j is an integer, and x_{j+1} is the amplitude at the $(j+1)^{th}$ peak [22]. For example, the amplitude at the third peak is denoted as x_3, and in that case, j is 2. Now that δ is known, the percent damping, ζ, can be calculated as:

$$\zeta = \frac{\delta}{\sqrt{(2\pi)^2 + \delta^2}} X\ 100, \tag{5-5}$$

Results for the hard bump input testing are in Section 5.5.2. This includes plots of relative velocity versus time and a table containing maximum peak-to-peak amplitude and damping ratio for each test configuration.

5.4.3 Pure Tone Input

The pure tone input signal was used to determine vibration transmissibility between several different components in each of the three test configurations. Unlike the chirp input, a pure tone input only excites a single frequency. A frequency response can still be generated, but it must be assembled manually by comparing measurements at the same location for all of the pure tone frequencies. For the specific case of this study, the time domain plots at each pure tone frequency were generated directly from the data. Then, the peak-to-peak amplitudes were recorded and tabulated for each frequency and test configuration.

In its simplest form, transmissibility is the ratio of an output to an input. Transmissibility greater than 1 means there is an amplification occurring between the two measurement points and similarly, a value less than 1 means there is a reduction occurring. By taking the peak-to-peak amplitude ratio of any two measurements, for each of the pure tones, transmissibility can be determined for that system of input and output as a function of frequency. The transmissibility results of the pure tone input testing can be found in Section 5.5.3.

5.5 Results

Sections 5.5.1-5.5.3 give the results of the dynamic signal inputs for each of the three vehicle configurations. The chirp signal results are presented first, followed by the results for the hard bump and pure tone inputs. A discussion of the results is presented in Section 5.6.

5.5.1 Chirp Input

Figure 5-4 shows the chirp input, as axle displacement versus time, on the vehicle with the undamped VOAS-1 configuration. For this specific plot, only one of the test configurations is included because the other two are quite similar to it. Figures 5-5 through 5-7 are plots of the force at the axle end versus time, for each of the three configurations.

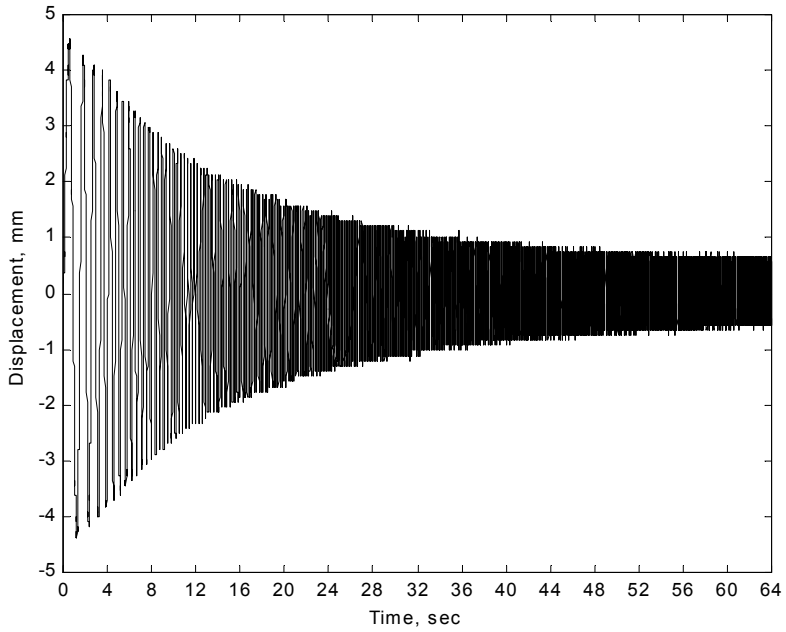

Figure 5-4 VOAS-1 Undamped, Chirp Input as Axle Displacement vs. Time.

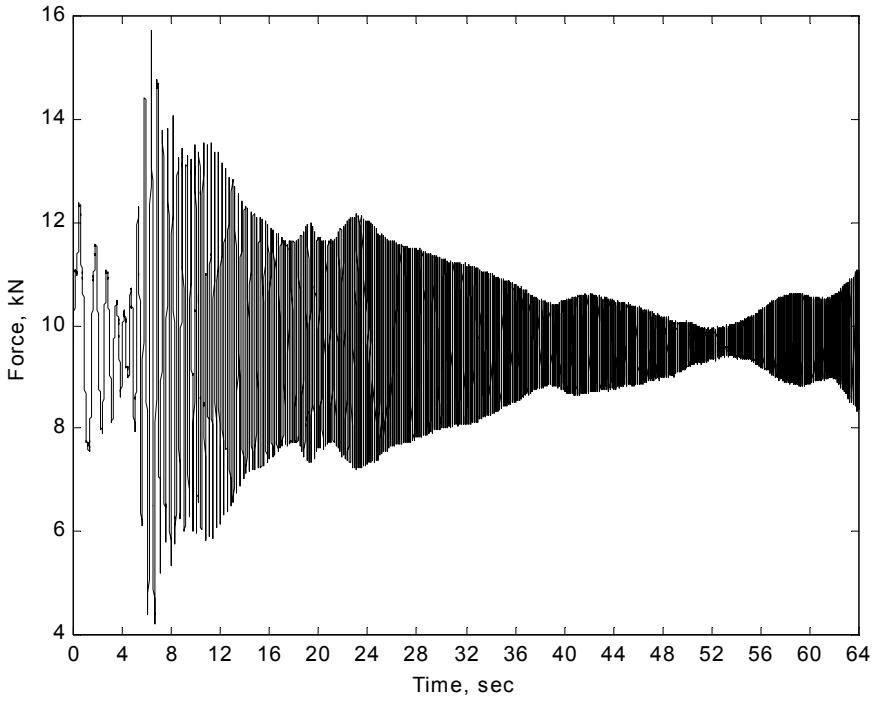

Figure 5-5 VOAS-1 Undamped, Chirp Input
Measurement: Force at Axle vs. Time.

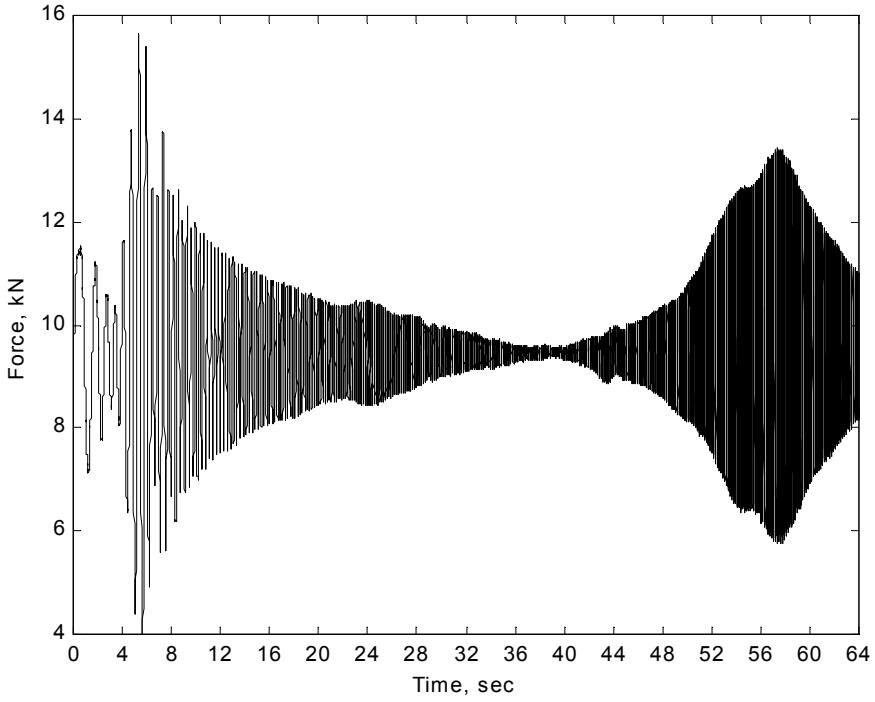

Figure 5-6 VOAS-2 Undamped, Chirp Input
Measurement: Force at Axle vs. Time.

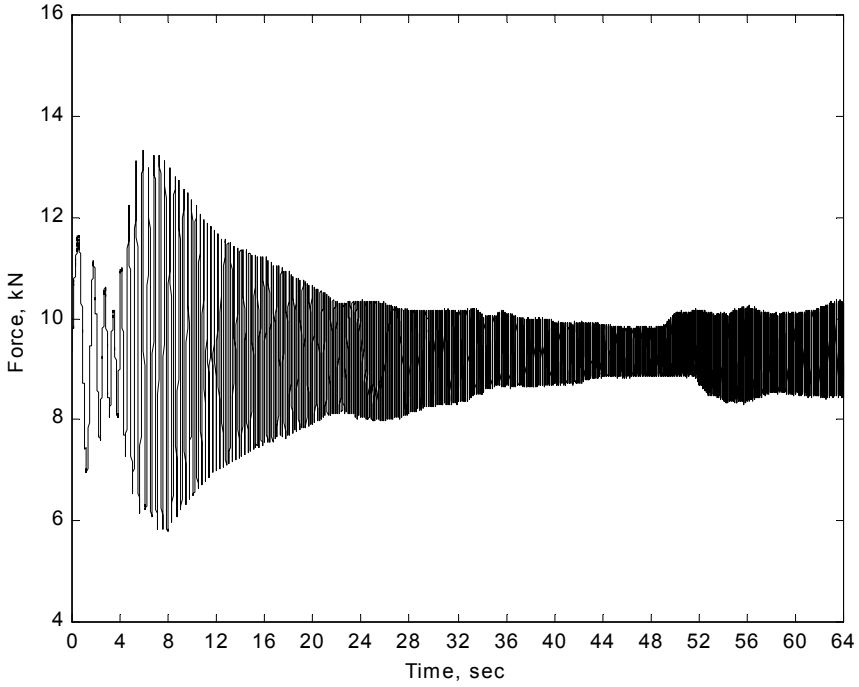

Figure 5-7 VOAS-2 Damped, Chirp Input
Measurement: Force at Axle vs. Time.

The remaining results from the chirp input are plotted in the frequency domain. With the exception of Figures 5-8 to 5-11, which are the power spectrums of the relative velocity measurements across the suspension, the remaining plots are the power spectrum of acceleration measurements at the various locations mentioned earlier. Further, the chirp input results are presented in groups of three, corresponding to the three different vehicle configurations that were tested.

Figures 5-12 to 5-15 relate to the power spectrum of the measurements made at the frame, just above the axle. Similarly, Figures 5-16 to 5-19 show the measurements at the frame side of the cab mount, and Figures 5-20 to 5-23 show the cab side of the cab mount. The power spectrum of measurements at the B-Post in the cab are presented in Figures 5-24 to 5-27 for the vertical direction, and Figures 5-28 to 5-31 for the fore-and-aft direction.

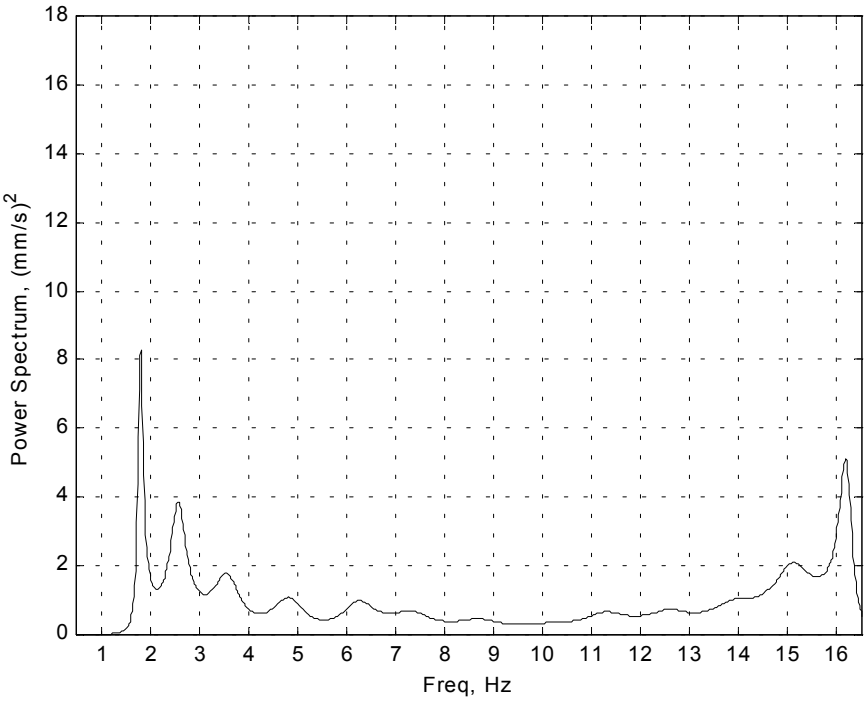

Figure 5-8 VOAS-1 Undamped Response to Chirp Input Measurement: Relative Velocity Between Axle and Frame.

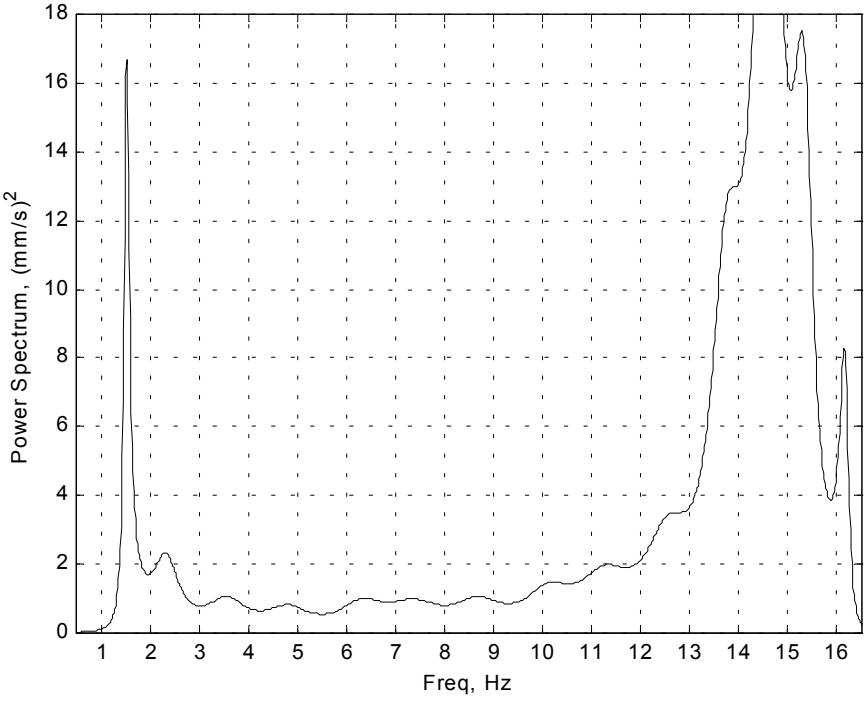

Figure 5-9 VOAS-2 Undamped Response to Chirp Input Measurement: Relative Velocity Between Axle and Frame.

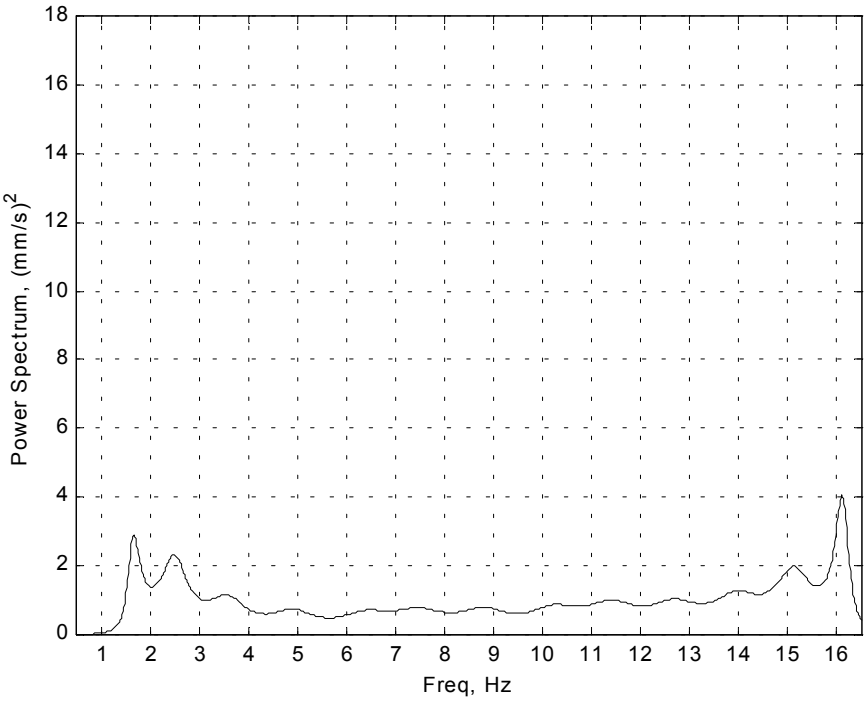

Figure 5-10 VOAS-2 Damped Response to Chirp Input
Measurement: Relative Velocity Between Axle and Frame.

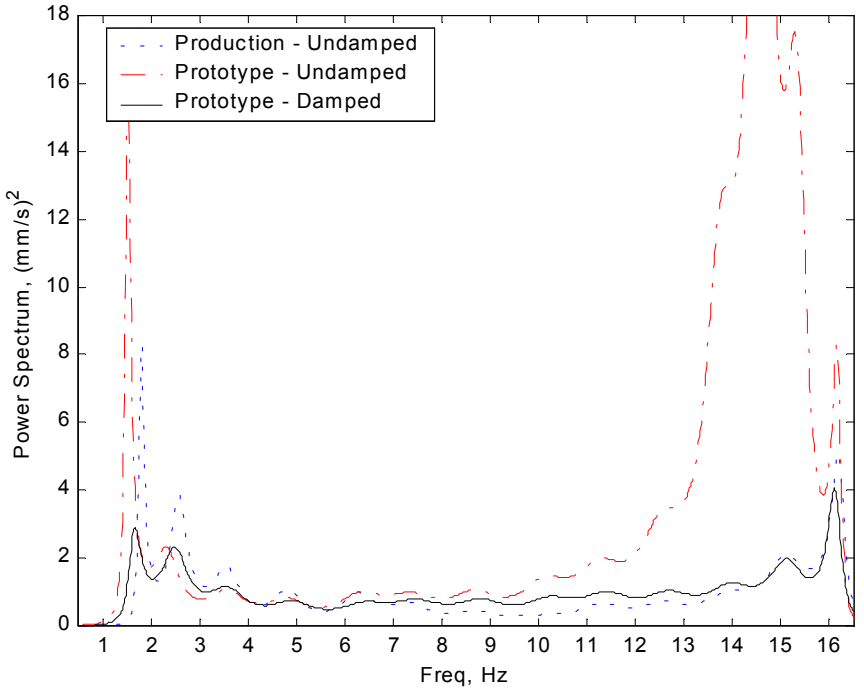

Figure 5-11 Response to Chirp Input for All Test Configurations
Measurement: Relative Velocity Between Axle and Frame.

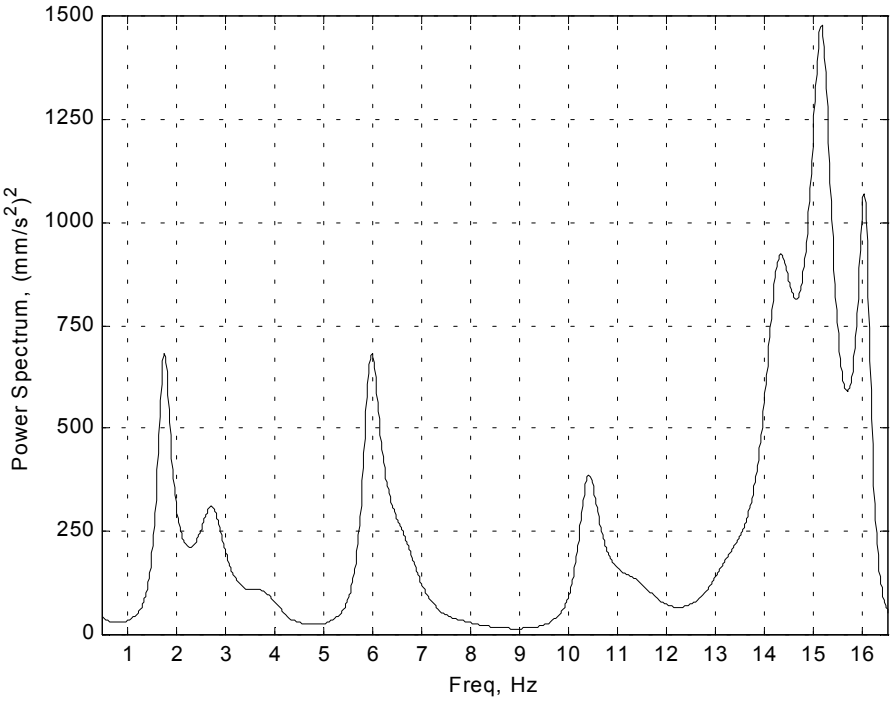

Figure 5-12 VOAS-1 Undamped Response to Chirp Input
Measurement: Acceleration at Frame, Directly Above Axle.

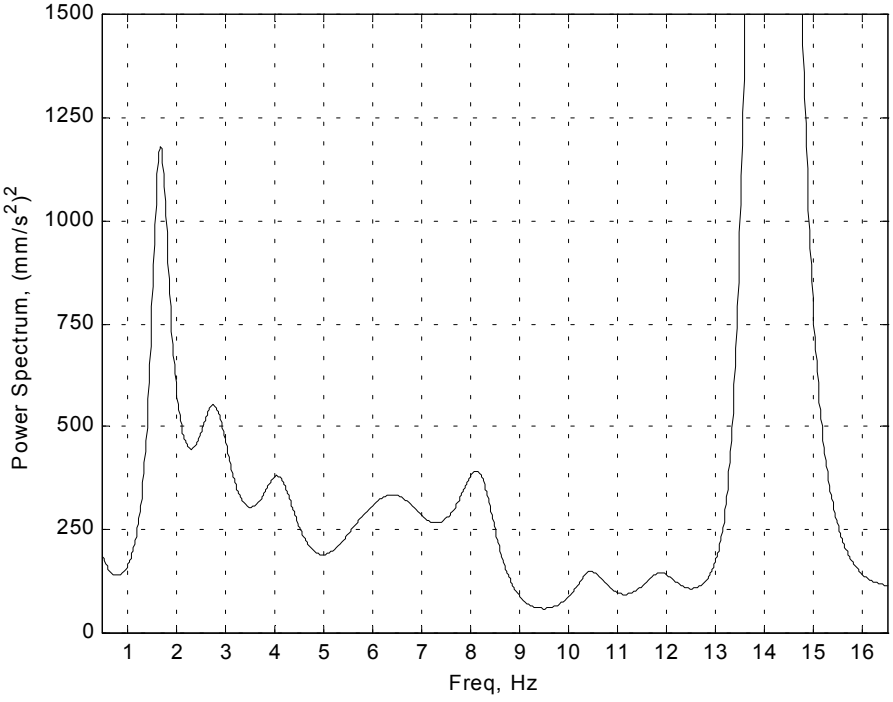

Figure 5-13 VOAS-2 Undamped Response to Chirp Input
Measurement: Acceleration at Frame, Directly Above Axle.

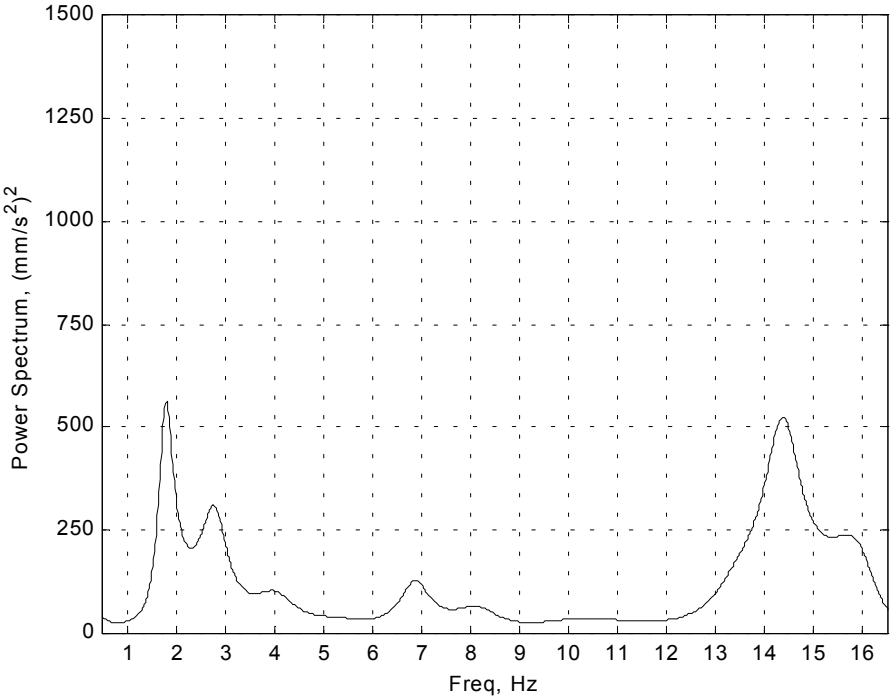

Figure 5-14 VOAS-2 Damped Response to Chirp Input
Measurement: Acceleration at Frame, Directly Above Axle.

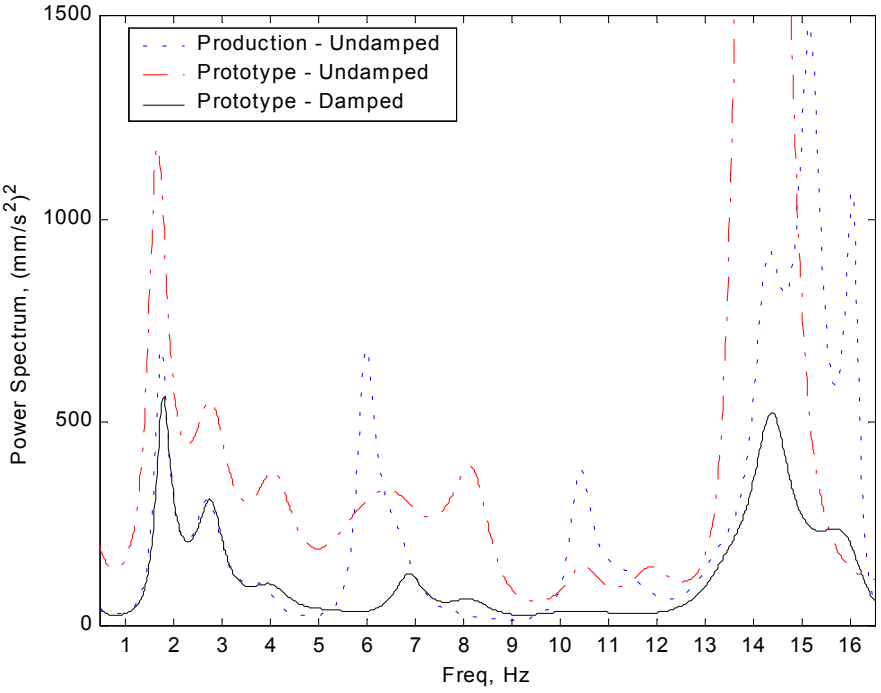

Figure 5-15 Response to Chirp Input for All Test Configurations
Measurement: Acceleration at Frame, Directly Above Axle.

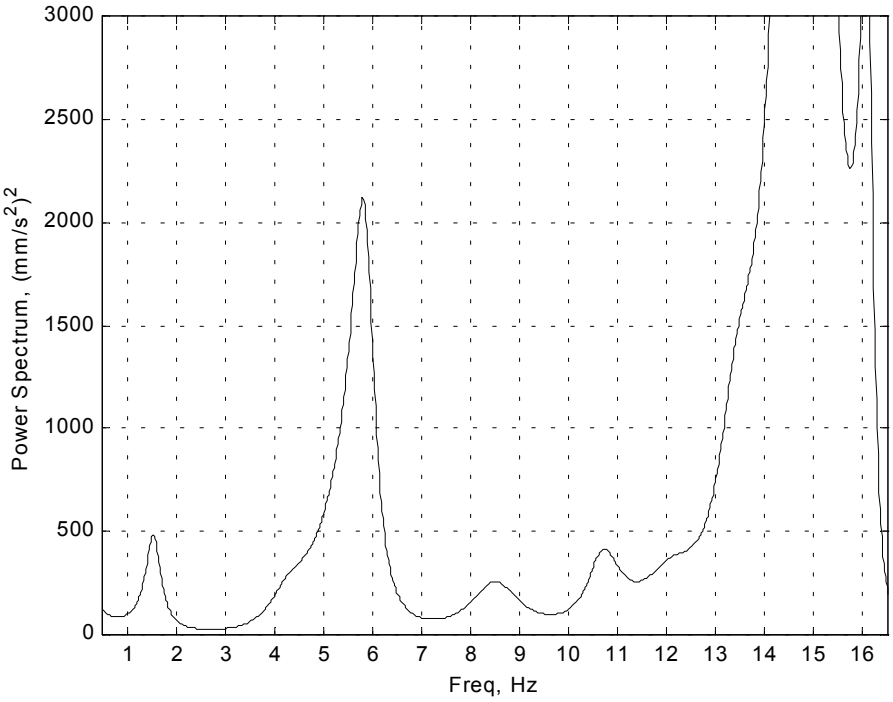

Figure 5-16 VOAS-1 Undamped Response to Chirp Input
Measurement: Acceleration at Cab Mount, Frame Side.

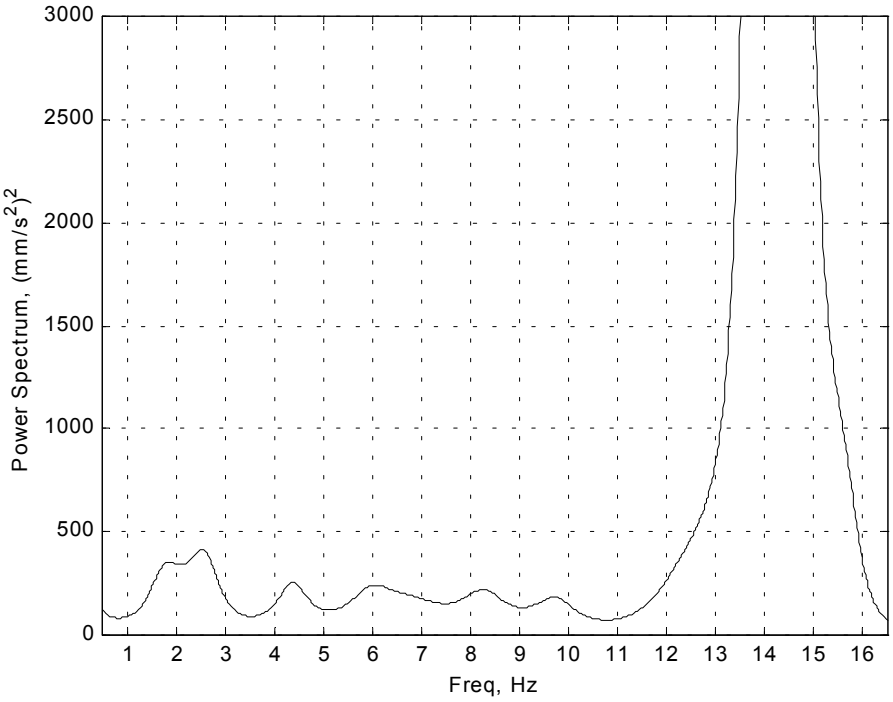

Figure 5-17 VOAS-2 Undamped Response to Chirp Input
Measurement: Acceleration at Cab Mount, Frame Side.

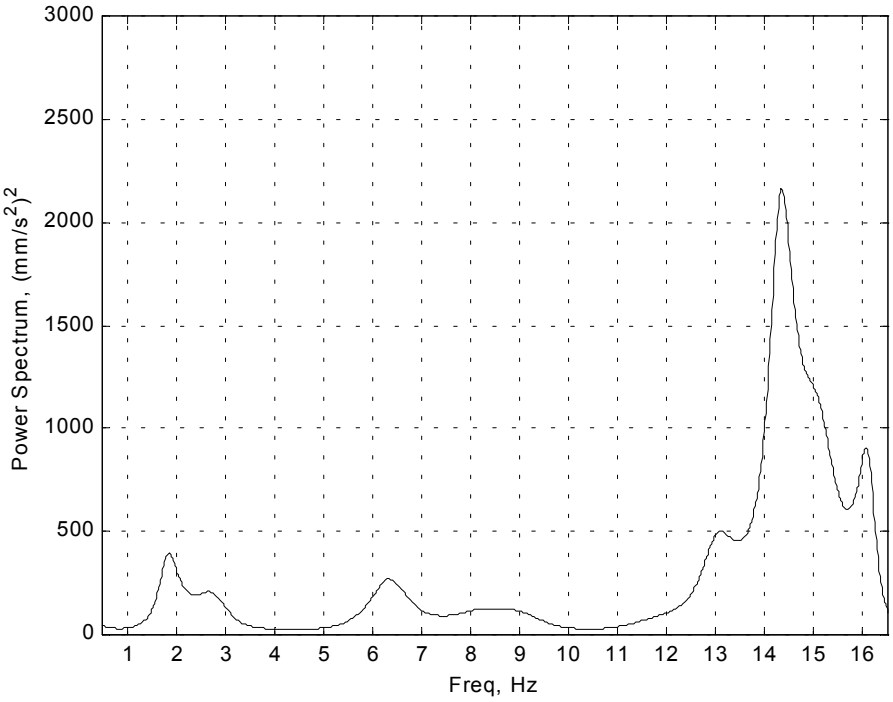

Figure 5-18 VOAS-2 Damped Response to Chirp Input
Measurement: Acceleration at Cab Mount, Frame Side.

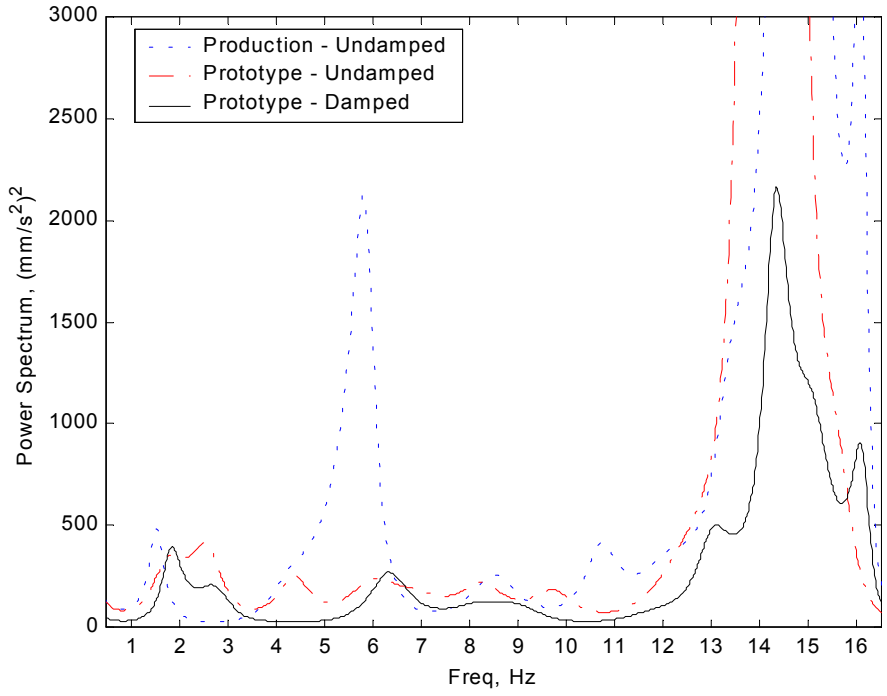

Figure 5-19 Response to Chirp Input for All Test Configurations
Measurement: Acceleration at Cab Mount, Frame Side.

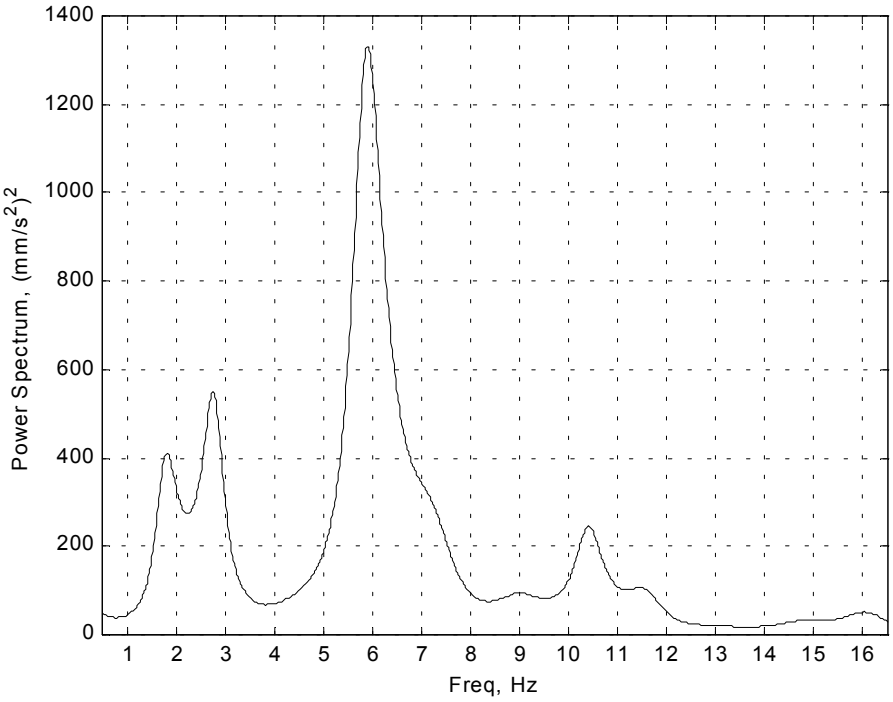

Figure 5-20 VOAS-1 Undamped Response to Chirp Input
Measurement: Acceleration at Cab Mount, Cab Side.

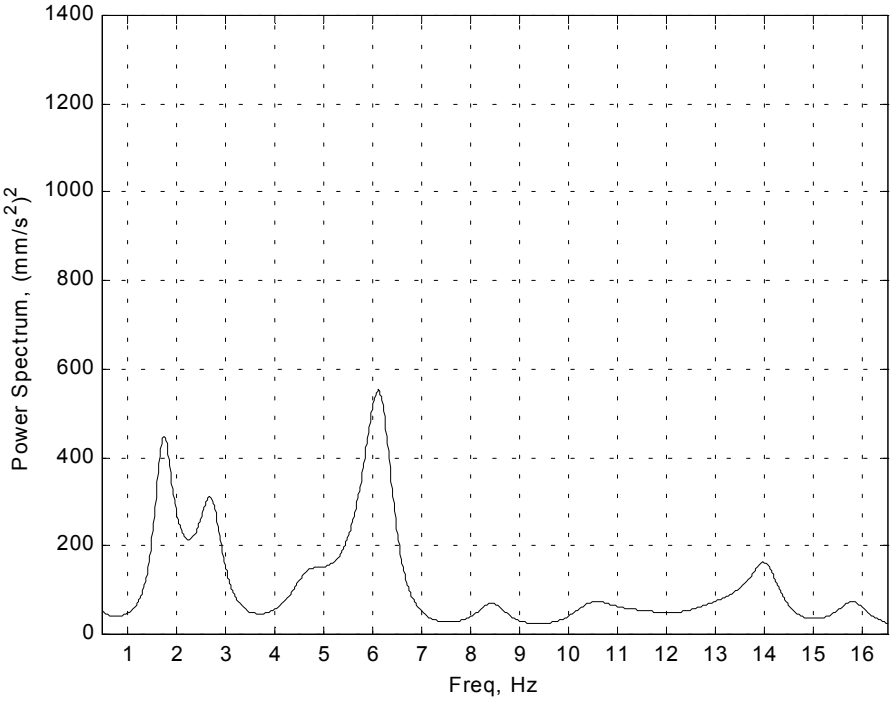

Figure 5-21 VOAS-2 Undamped Response to Chirp Input
Measurement: Acceleration at Cab Mount, Cab Side.

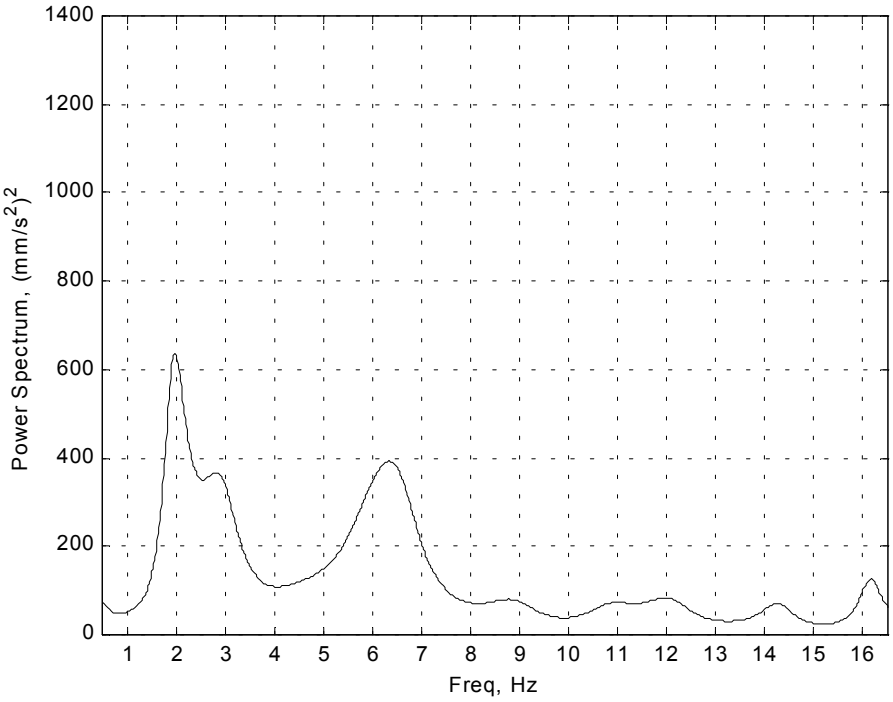

Figure 5-22 VOAS-2 Damped Response to Chirp Input
Measurement: Acceleration at Cab Mount, Cab Side.

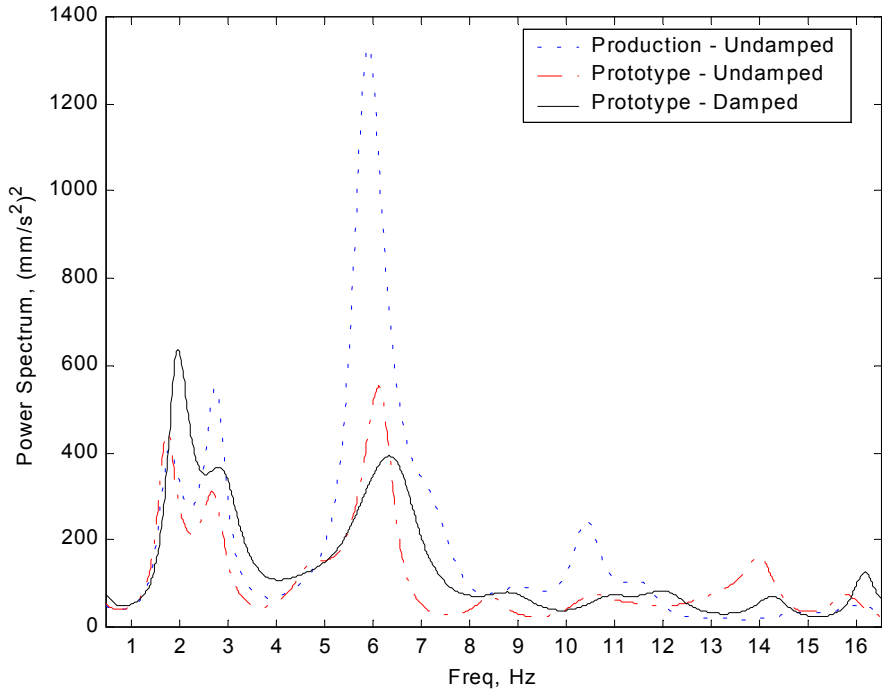

Figure 5-23 Response to Chirp Input for All Test Configurations
Measurement: Acceleration at Cab Mount, Cab Side.

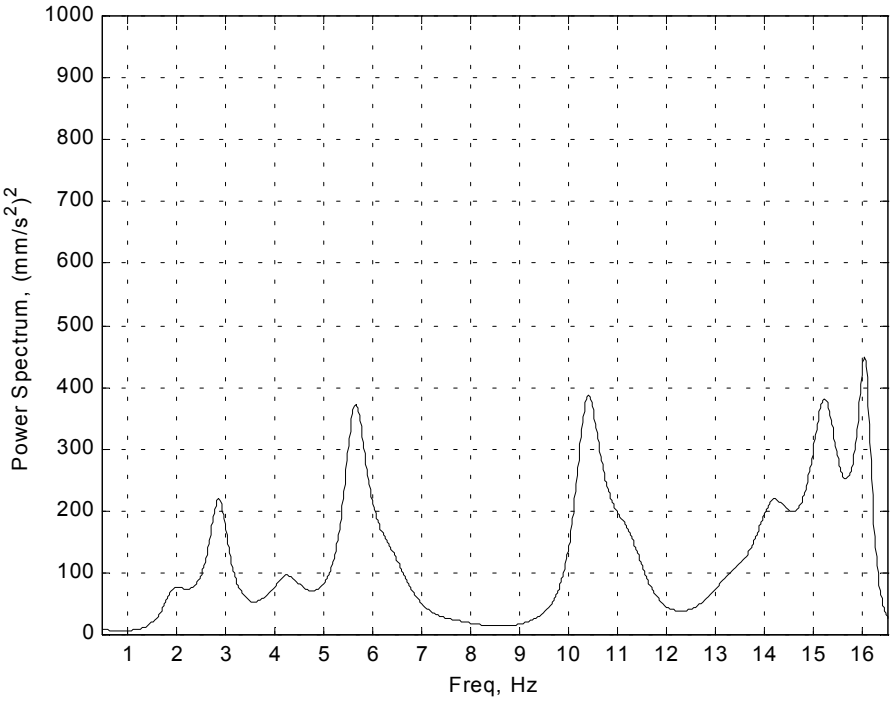

Figure 5-24 VOAS-1 Undamped Response to Chirp Input
Measurement: Acceleration at B-Post, Vertical.

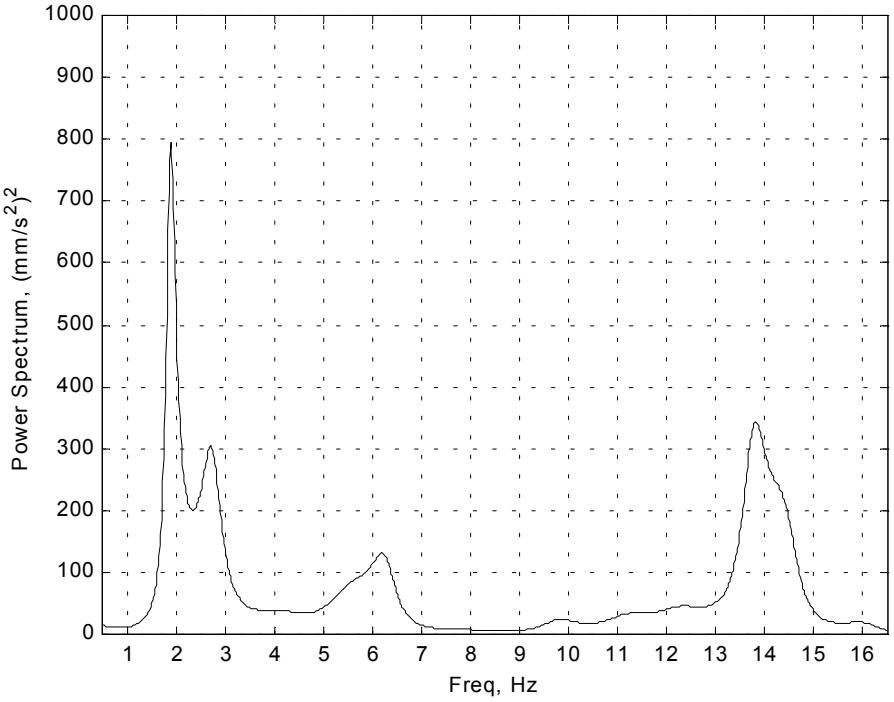

Figure 5-25 VOAS-2 Undamped Response to Chirp Input
Measurement: Acceleration at B-Post, Vertical.

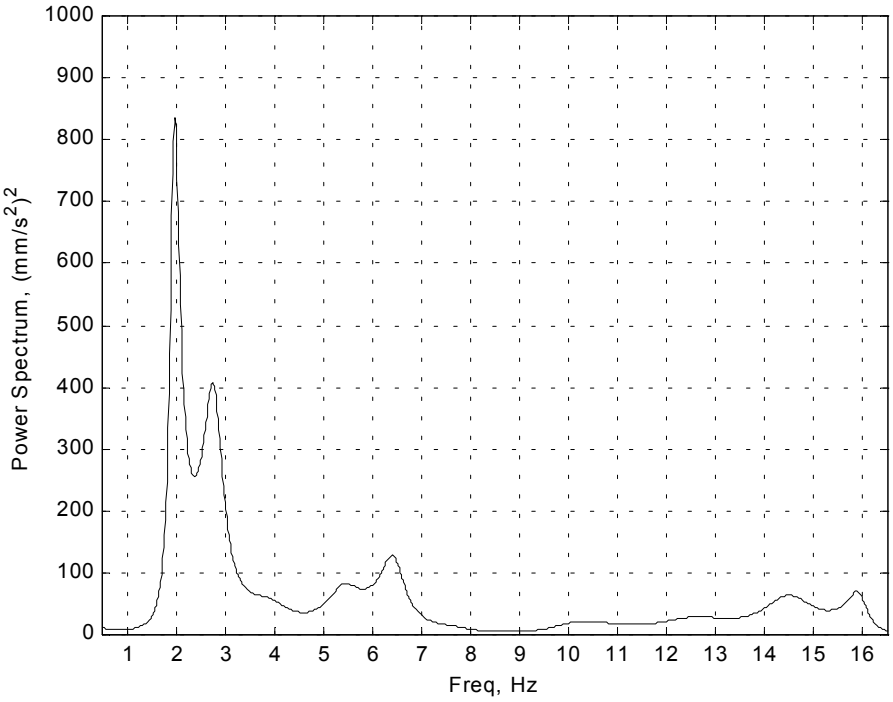

Figure 5-26 VOAS-2 Damped Response to Chirp Input
Measurement: Acceleration at B-Post, Vertical.

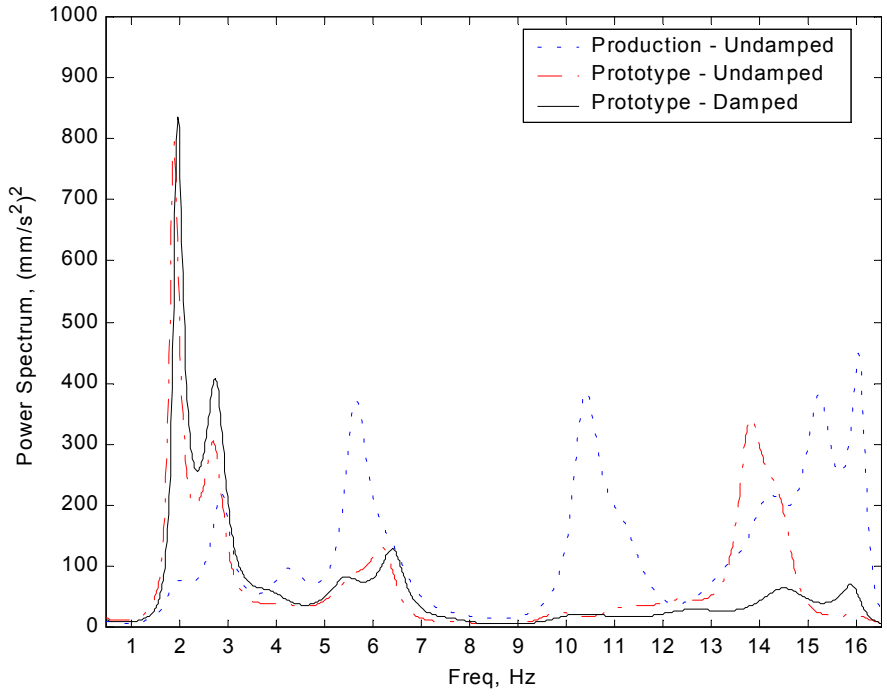

Figure 5-27 Response to Chirp Input for All Test Configurations
Measurement: Acceleration at B-Post, Vertical.

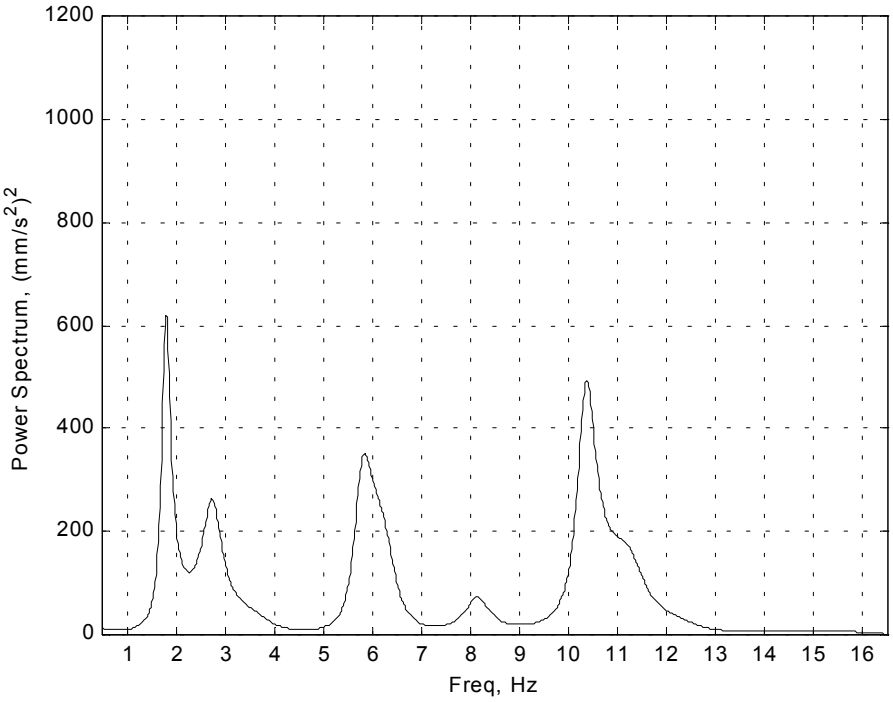

Figure 5-28 VOAS-1 Undamped Response to Chirp Input
Measurement: Acceleration at B-Post, Fore/Aft.

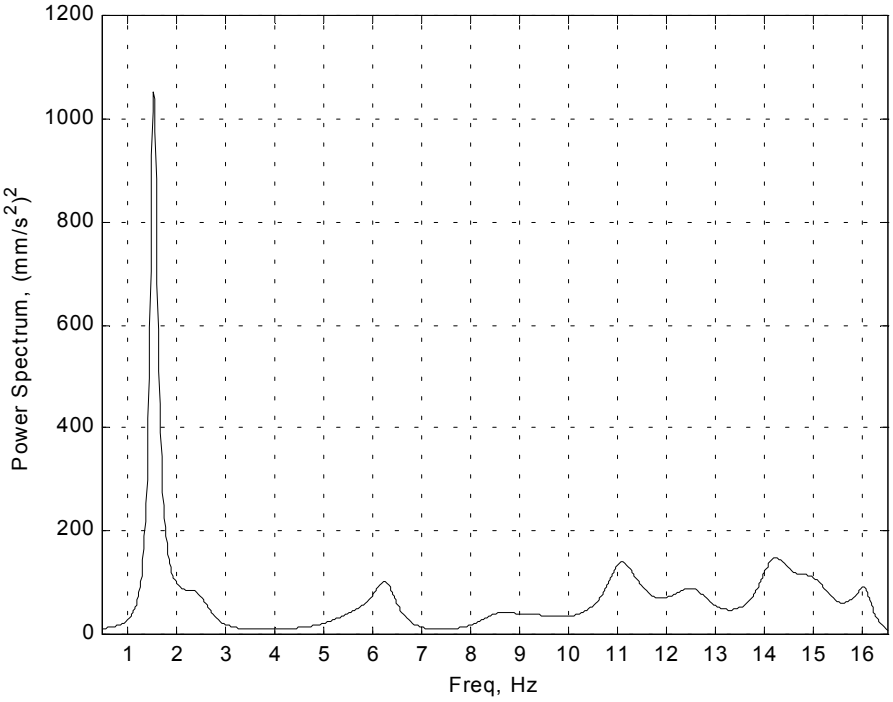

Figure 5-29 VOAS-2 Undamped Response to Chirp Input
Measurement: Acceleration at B-Post, Fore/Aft.

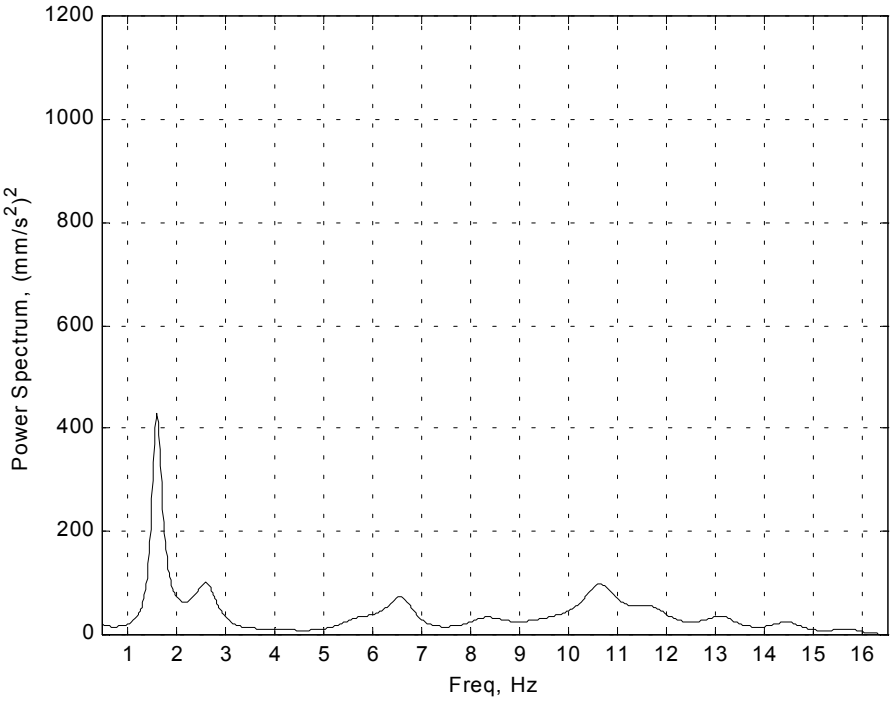

Figure 5-30 VOAS-2 Damped Response to Chirp Input
Measurement: Acceleration at B-Post, Fore/Aft.

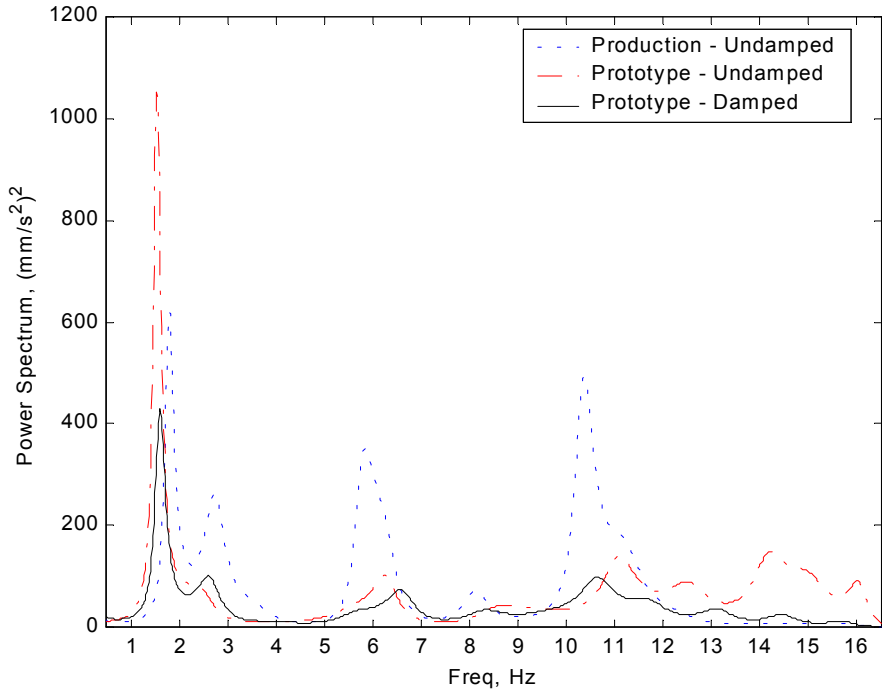

Figure 5-31 Response to Chirp Input for All Test Configurations
Measurement: Acceleration at B-Post, Fore/Aft.

5.5.2 Hard Bump Input

The relative velocity across the suspension is shown for each of the three vehicle configurations in Figures 5-32 to 5-35, respectively. These plots are shown in the time domain to clearly show the decreasing amplitude of the response with respect to time. To further clarify the response, the time axis starts at "–1", in order to capture the full effect of the hard bump input.

The maximum peak-to-peak amplitude, the logarithmic decrement, and the damping ratio for each of the three configurations are shown in Table 5-1.

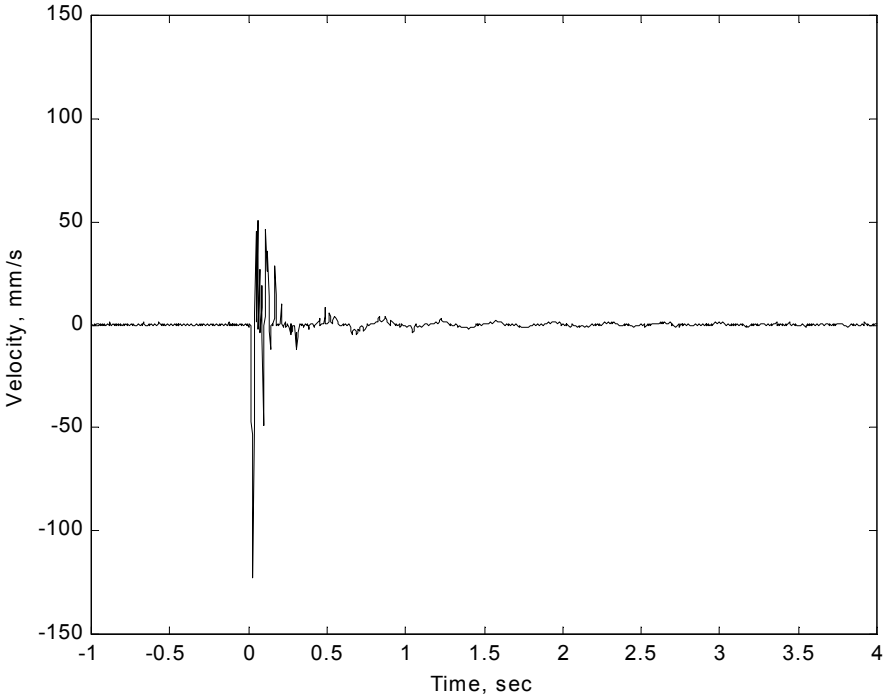

Figure 5-32 VOAS-1 Undamped Response to Hard Bump Input Measurement: Relative Velocity Between Axle and Frame.

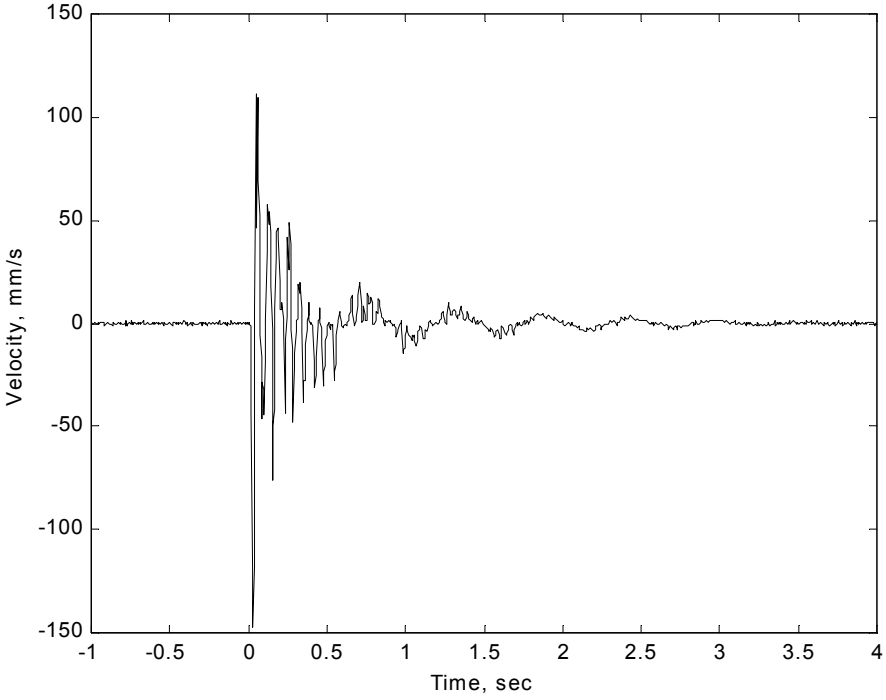

Figure 5-33 VOAS-2 Undamped Response to Hard Bump Input Measurement: Relative Velocity Between Axle and Frame.

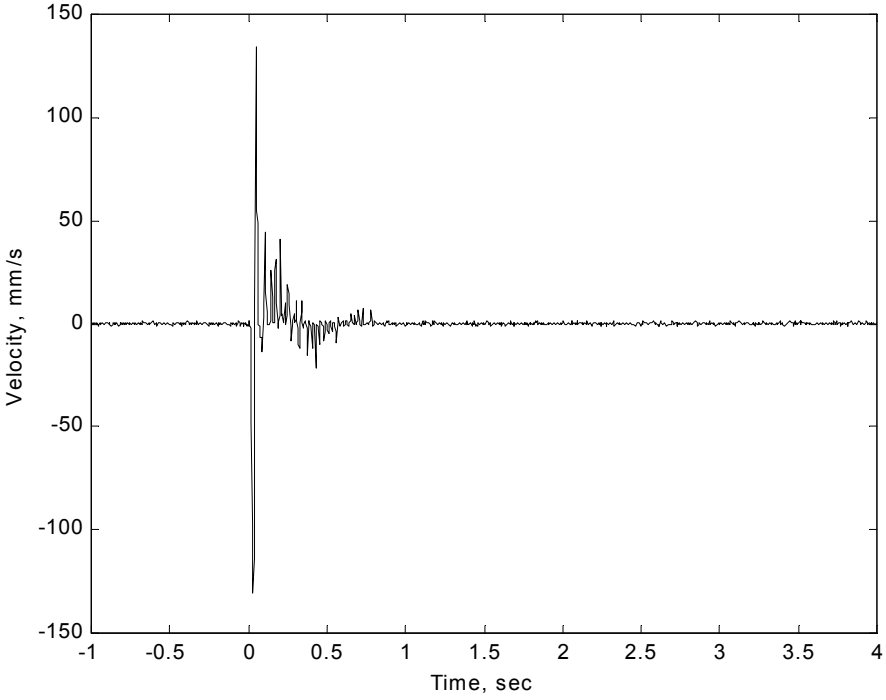

Figure 5-34 VOAS-2 Damped Response to Hard Bump Input Measurement: Relative Velocity Between Axle and Frame.

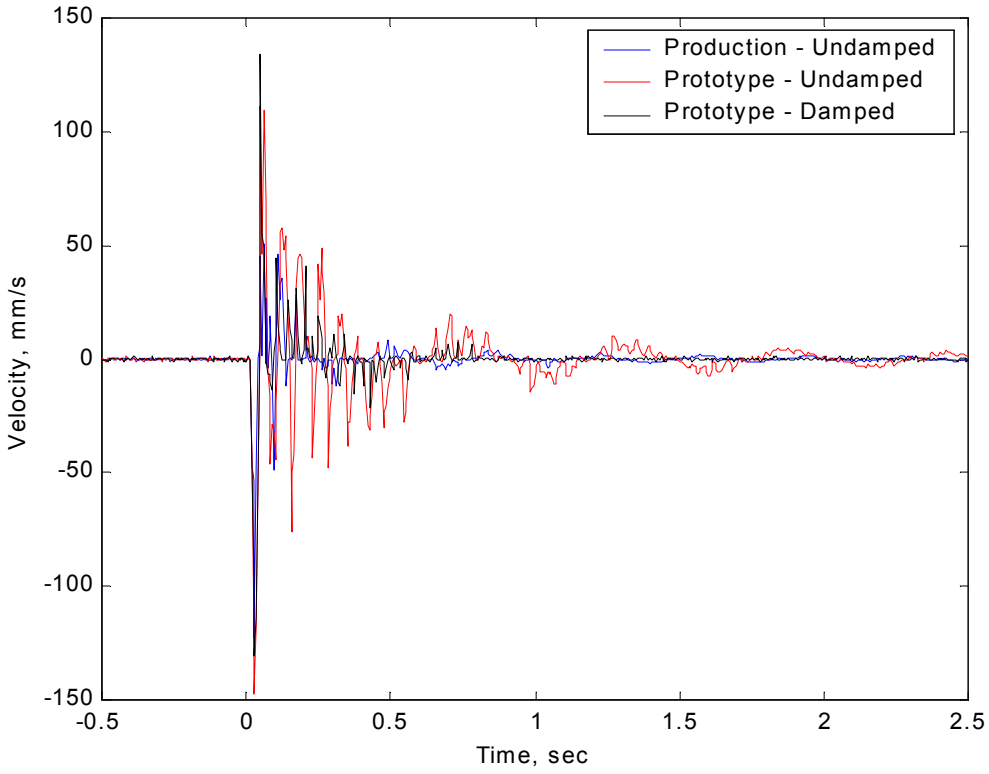

Figure 5-35 Response to Hard Bump Input for All Test Configurations
Measurement: Relative Velocity Between Axle and Frame.

Table 5-1 Hard Bump Input Response – Maximum Amplitude and Damping Ratio.

Suspension Configuration	Max. Peak-to-Peak Amplitude (mm/s)	Log. Decrement (unitless)	Damping Ratio (%)
VOAS-1 Undamped	172.8	1.15	18.0
VOAS-2 Undamped	258.2	0.33	5.2
VOAS-2 Damped	265.2	3.13	44.6

5.5.3 Pure Tone Input

As stated in Section 5.4.3, the results of the pure tone inputs give transmissibility between several of the components on each vehicle. For each of the particular transmissibility comparisons, each figure in this section includes the results of all three test configurations.

The transmissibility between an input at the axle and a measurement at the frame directly above the axle is shown in Figure 5-36. Figure 5-37 is the transmissibility across the cab suspension, as defined by the ratio of the acceleration at the aft of the cab to the acceleration directly below it on the vehicle frame. This transmissibility is intended to capture the cab suspension dynamics. Next, Figure 5.38 shows the transmissibility at two locations on the frame, in order to capture some of the frame dynamics, most prominently the frame beaming.

The transmissibility between vertical and fore-and-aft accelerations at the B-Post, and the truck frame at the aft of the cab (i.e. the input to the cab) are shown in Figures 5-39 and 5-40, respectively. The transmissibility measurements shown in Figures 5-41 and 5-42, which are similar to those described above for other locations, are intended to provide a better understanding of the B-Post dynamics, and therefore the ride comfort, due to the different suspensions.

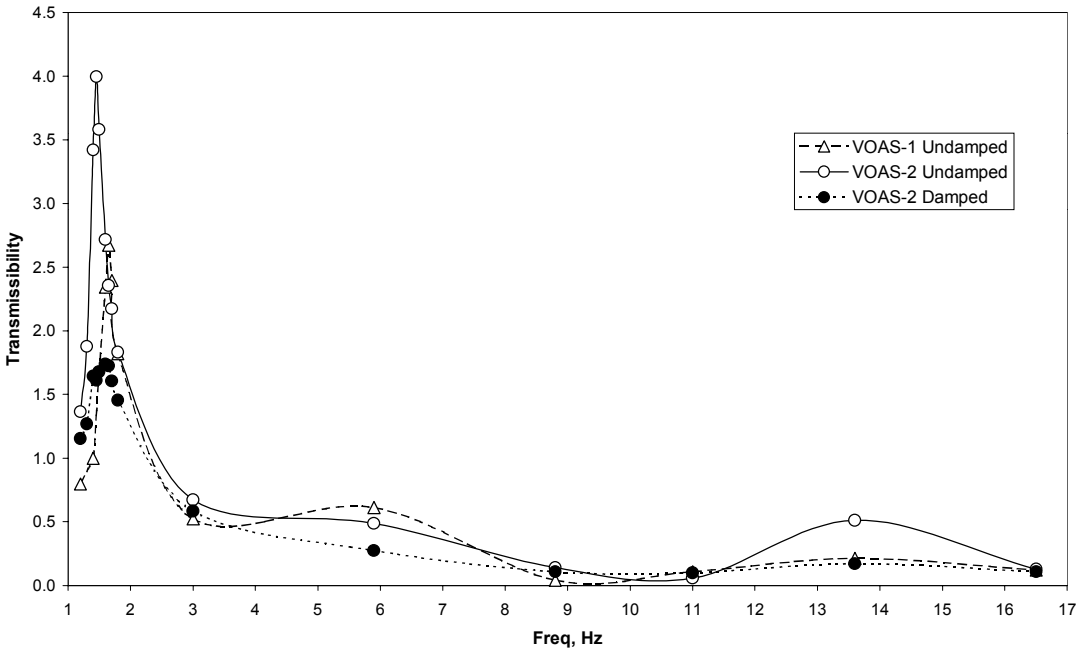

Figure 5-36 Transmissibility with Pure Tone Inputs
Measurement: Frame Directly Above Axle, Input: Axle.

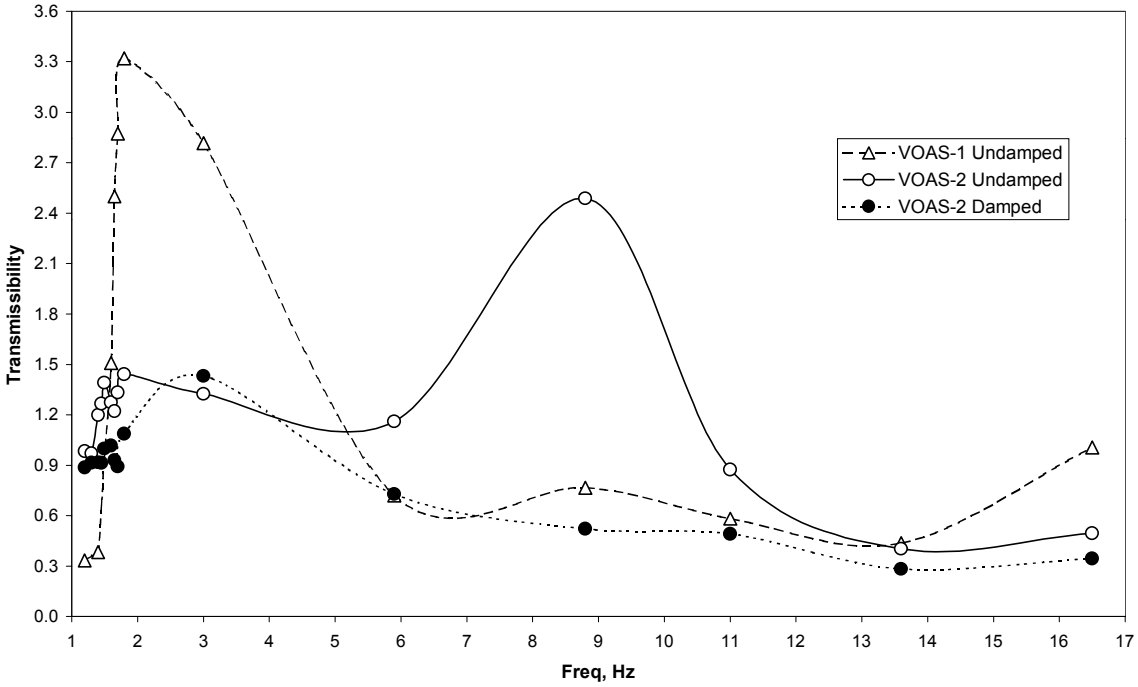

Figure 5-37 Transmissibility with Pure Tone Inputs
Measurement: Cab at Cab, Input: Cab at Frame.

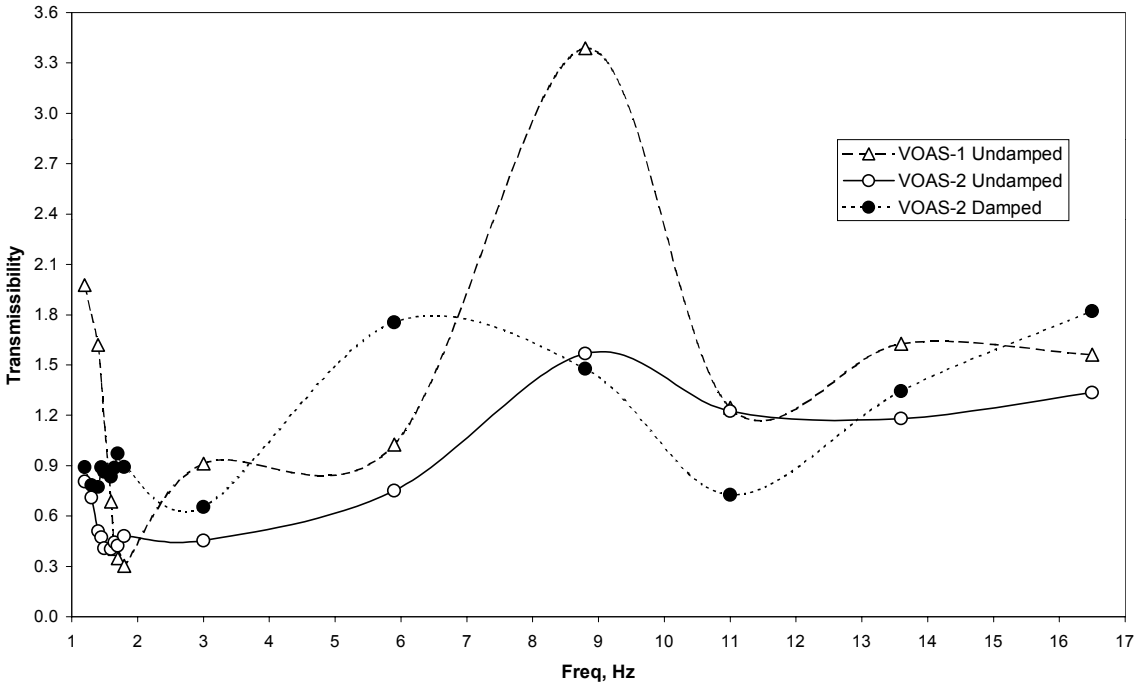

Figure 5-38 Transmissibility with Pure Tone Inputs
Measurement: Cab at Frame, Input: Frame Above Axle.

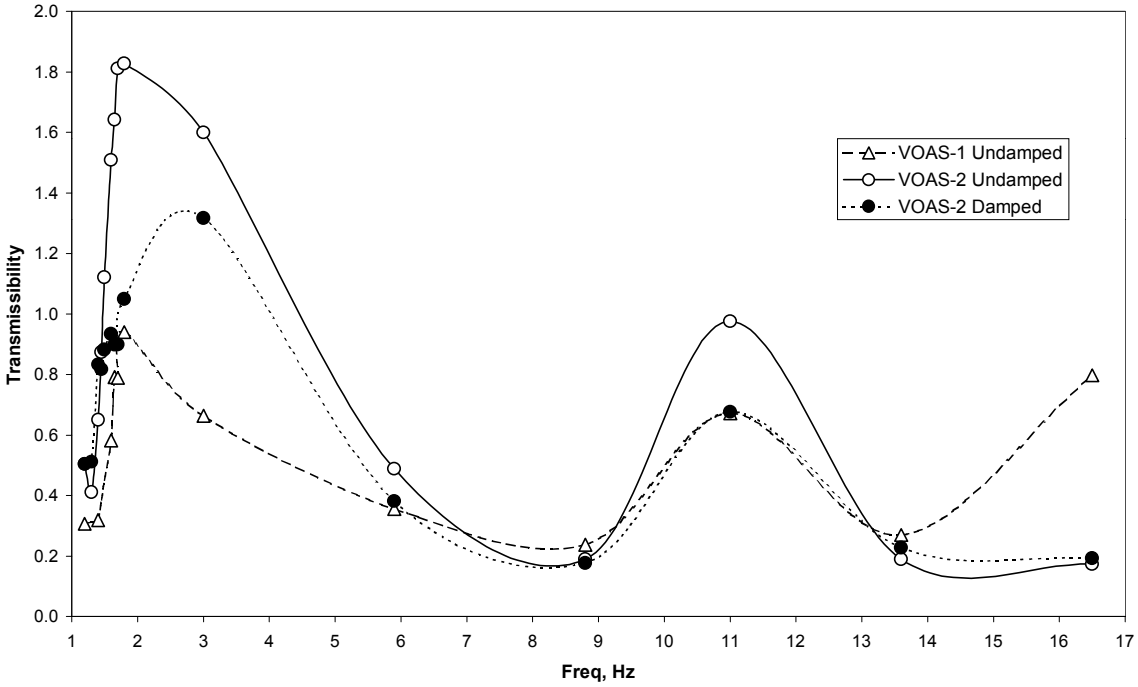

Figure 5-39 Transmissibility with Pure Tone Inputs
Measurement: B-Post Vertical, Input: Cab at Frame.

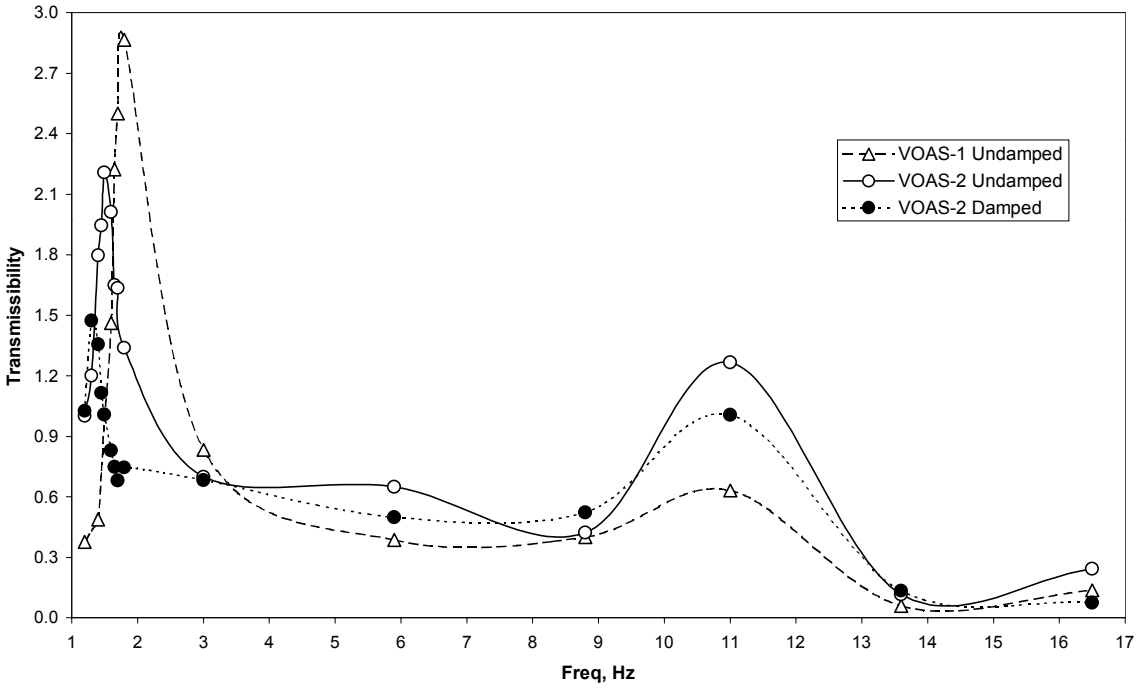

Figure 5-40 Transmissibility with Pure Tone Inputs
Measurement: B-Post Fore/Aft, Input: Cab at Frame.

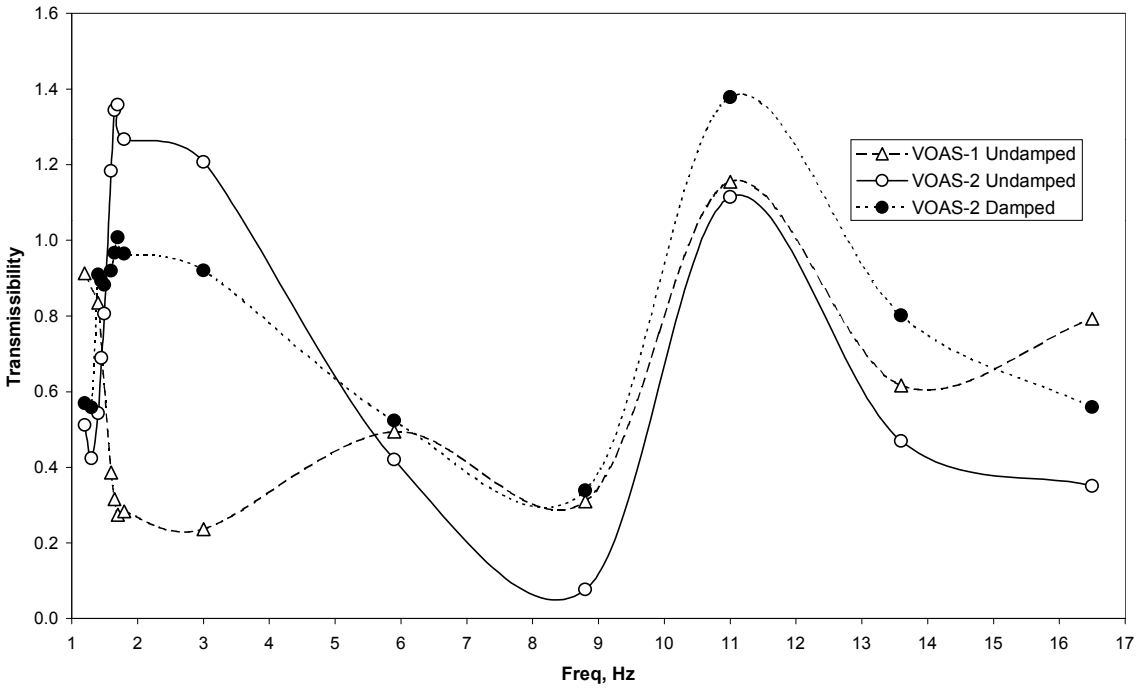

Figure 5-41 Transmissibility with Pure Tone Inputs
Measurement: B-Post Vertical, Input: Cab at Cab.

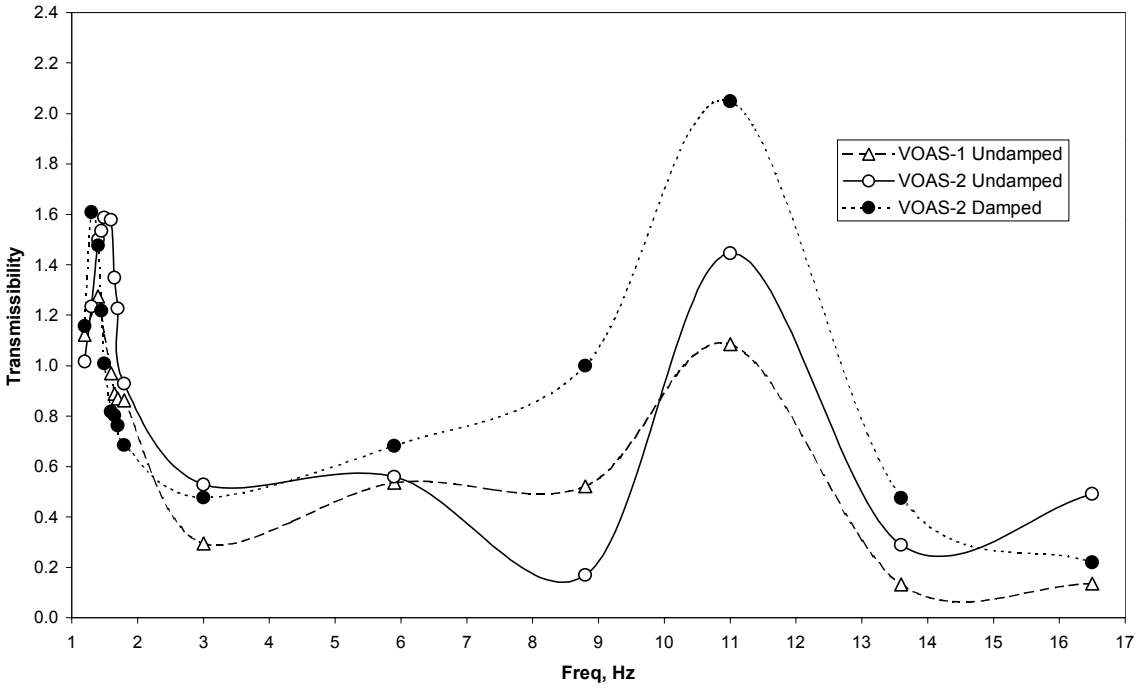

Figure 5-42 Transmissibility with Pure Tone Inputs
Measurement: B-Post Fore/Aft, Input: Cab at Cab.

5.6 Discussion of Results

The following three sections support the results presented in Section 5.5. Describing any significant differences between the results of the three test configurations is the main focus of each of these sections.

5.6.1 Chirp Input

As mentioned in Section 5.5.1, the chirp signal input (axle displacement versus time) was identical for each of the three test configurations. Therefore, any differences in the results were due to the differences between the test configurations themselves. The force at axle versus time plots, in Figures 5-5 to 5-7, were the first signs of some differences in the dynamics of the three configurations. All three figures show peak forces occurring between 6 and 8 sec. into the chirp signal, but the amplitude for damped VOAS-2 was much less than the other two, as shown in Figure 5-7. Since these peaks in force occur while the input signal is passing the primary suspension resonant frequency, damping would be expected to decrease the amplitude. Another difference is visible from 48-64 seconds in Figure 5-8, for VOAS-2 undamped. The increase in peak forces during that time was much more severe than in the other two configurations. Several different sources could contribute to this significant increase in amplitude late in the chirp signal, as will be discussed later.

When the relative velocity between the axle and frame reaches a maximum, it is an excellent indicator that the input signal is passing the primary suspension resonant frequency. Figures 5-8 to 5-11 show the power spectrum of this measurement in the frequency domain. The resonant frequency of the primary suspension for VOAS-1 was

already known to be 1.7 Hz and the sharp peak at that frequency in Figure 5-8 supports. Undamped VOAS-2 was closer to 1.5 Hz (Figure 5-9), and the resonant frequency shifts upward slightly to 1.6 Hz when damped, as Figure 5-10 shows. It is also important to notice the magnitudes of these three peaks. The power spectrum at the resonant frequency of undamped VOAS-2 was twice that of VOAS-1. This is because the design of VOAS-2 has very little frictional damping compared to VOAS-1. This necessitates the use of viscous dampers to reduce the amplitude, as shown in Figure 5-10. The response of a lightly damped system, such as undamped VOAS-2, is much more likely to vibrate at large amplitudes when excited at its resonant frequency than a more heavily damped system. Section 5.6.3 further elaborates on the damping of each test configuration.

Several different modes of vibration are visible in Figures 5-12 to 5-15. These three figures are the power spectrum of the accelerometer mounted on the frame-rail, directly above the axle. The VOAS-1 undamped response, Figure 5-12, shows the resonant frequency of the primary suspension at 1.7 Hz, the cab's resonant frequency at 2.7 Hz, the first beaming mode of the frame at 6 Hz, the first torsional mode at 10.4 Hz, and several other phenomena above 13 Hz. The other phenomena could be contributions from the second frame beaming mode, the resonant frequency of the hydraulic actuators, or another dynamic effect. Additional testing is underway to determine this specifically, and it is discussed in Section 6.2.

With such high amplitude, the resonant frequency of the undamped VOAS-2 primary suspension is clearly visible in Figure 5-13. This figure shows the cab frequency at 2.7 Hz and frame beaming at 6.3 Hz, although it is not as easily distinguished as in Figure 5-12. It is not surprising that the frame beaming shifts slightly higher in frequency

for VOAS-2. The front spring hangers for VOAS-2 were twice the length of those for VOAS-1 and were mounted in such a way that they actually help stiffen the frame. The torsional mode of the frame occurred at the same frequency as VOAS-1 and other factors also dominate the response after 13 Hz. The accelerometer at the frame above the axle in VOAS-2 damped reiterates the response of VOAS-2 undamped with the expected drop in amplitude across the whole frequency range.

Figures 5-16 to 5-19 are the responses of each configuration when measured at the frame side of the cab mount. Of these three figures, the most noteworthy event is the frame beaming peak that dominates the 1-10 Hz frequency band in the undamped VOAS-1 configuration, as shown in Figure 5-16. The significance of the frame beaming is that it propagates all the way to the driver, and in most cases, becomes a major source of ride complaints, as will be discussed later.

The next measurement location was still at the cab mount, but this time the accelerometer was mounted on the cab side of the cab suspension. Figures 5-20 to 5-23 give the power spectrum response at this location. The frame beaming mode in VOAS-1 undamped, Figure 5-20, dwarfs both primary and cab suspension resonances, and torsional bending mode of the frame. In Figures 5-21 and 5-22, undamped and damped VOAS-2, respectively, share the same modes, but frame beaming is not quite so overpowering as in VOAS-1. Also visible in Figures 5-21 and 5-22 is the resonance of the exhaust stacks between 8 and 9 Hz.

Vertical acceleration response at the B-Post is shown in Figures 5-24 to 5-27 for VOAS-1 undamped, VOAS-2 undamped, and VOAS-2 damped, respectively. For VOAS-1, the frame beaming and torsional modes were the most significant contributors

to large amplitude response at the B-Post. The resonant frequency of the cab was also a factor, but the primary suspension's contribution was much less significant. Both damped and undamped VOAS-2 differed from VOAS-1 completely. The resonant frequency of the primary suspension was the dominant mode, followed by the cab suspension. Frame beaming was a distant third and the effect of the frame's torsional mode was barely noticeable.

The final four figures of Section 5.5.1 are also response measurements at the B-Post, but in the fore-and-aft direction. In Figure 5-28, the VOAS-1 response at the primary suspension resonant frequency is the dominant factor, while the cab, frame beaming and torsional modes continue to be significant. The exhaust stack has some effect, too, as evidenced by the small peak just above 8 Hz. Cab suspension, frame beaming, exhaust stack, and torsional frame modes are all distinguishable, but Figures 5-29 and 5-30 show both VOAS-2 configurations are most sensitive to the primary suspension's resonance in the fore-and-aft direction.

5.6.2 Hard Bump Input

Although there were no viscous dampers across the primary suspension in either of the undamped VOAS-1 and VOAS-2 configurations, both configurations have frictional damping inherent in the connections between components in the suspension. In the case of VOAS-1, the "Z" spring is not constrained from fore-and-aft motion at its forward mount (the track rods prevent the axle from moving in this direction). Since the spring is not constrained in the fore-and-aft direction, it is free to slide back and forth as it is loaded and unloaded. The friction of the metal spring sliding on the metal perch

dissipates force, similar to a frictional damper. VOAS-2, on the other hand, has very little inherent damping in the suspension components. The trailing-arm spring is constrained by a bushing that has very low rotational friction and reduces the suspension's ability to dissipate energy without an additional viscous damper. This aspect of VOAS-2 is quite desirable from the standpoint of controlling suspension damping, and for providing better ride and harshness characteristics due to the suspension.

Figures 5-32 to 5-35 show the impact response of each test configuration to the hard bump input. The VOAS-1 undamped response died out between 2.5 and 3 seconds after the impact, as shown in Figure 5-32. In the case of undamped VOAS-2, the settling time of the response was almost 4 seconds after the impact, and the peak-to-peak amplitude was much larger than that of VOAS-1. Adding the viscous damper to VOAS-2 caused the response to die out in less than 1 second.

Table 5-1 lends support to Figures 5-32 to 5-35. VOAS-1 had a maximum peak-to-peak amplitude of 172.8 mm/s, 33% less than the maximum peak-to-peak amplitude of undamped VOAS-2. Although adding a viscous damper reduced the settling time of the suspension, it did slightly increase the maximum peak-to-peak amplitude. Once the logarithmic decrement was found for each configuration, the damping ratio was calculated as a percent. The frictional damping in VOAS-1 contributed to an 18.0 % damping ratio compared to 5.2 % for undamped VOAS-2. With the addition of the viscous damper, the VOAS-2 damping ratio increased by more than 8 times to 44.6 %, nearly 2.5 times undamped VOAS-1. The hard bump results highlight the significance of

viscous damping in controlling the suspension dynamic transients for VOAS-2, as compared to VOAS-1.

5.6.3 Pure Tone Input

As stated in Section 5.5.3, transmissibility is defined as the ratio of two measurements, where one (the numerator) is considered to be the output, and the other (the denominator) is the input. Transmissibility values greater than 1 represent an amplification of the input and values less than 1 represent attenuation. In a single degree of freedom system, the transmissibility converges to a value of 1 at low frequencies. Some of the figures found in Section 5.5.3 show a transmissibility ratio less than 1 at low frequencies. A component on the vehicle with a resonance below 1 Hz could dissipate the input energy enough to reduce the low frequency transmissibility if the component was either small and vibrating violently or very large. If this were the case the component would be called a "tuned vibration absorber" and the mass of both the weight stack and the drive axle not being tested are significant enough that very little resonant vibration would be required to reduce the transmissibility. Other factors, however, may contribute to this phenomenon including structural non-linearity, interactions between multiple low frequency vibration modes, and peculiarities of obtaining transmissibility plots from pure tone test measurements.

Figure 5-36 is the transmissibility between acceleration measured at the frame directly above the axle and acceleration on the axle. As the figure shows, acceleration at the frame was 4 times the acceleration at the axle when undamped VOAS-2 passes through the resonance of the primary suspension. The other two configurations also had

maximum transmissibility at their respective primary suspension resonant frequencies. At frame beaming, which occurred around 6 Hz, there was a rise in the transmissibility of all three configurations, although not as pronounced in damped VOAS-2.

The transmissibility across the cab suspension is shown in Figure 5-37, for all three configurations. VOAS-1 undamped shows the most significant peak coinciding with the natural frequency of the cab itself. Both VOAS-2 configurations showed a rise in transmissibility near the resonant frequency of the cab as well, although not as severe as VOAS-1. The second major peak on this plot occurred with undamped VOAS-2 at 8.8 Hz. This frequency was the resonant frequency of the exhaust stacks and, based on the figure, this had a significant effect on the vibrations transmitted across the cab suspension. Once viscous damping was added to VOAS-2, however, the effect of the exhaust stacks was substantially reduced.

Figure 5-38 is the transmissibility of an input at the frame, directly above the axle, to the frame at the cab mount. Two points on the figure deserve further discussion. The transmissibility of VOAS-2 was a local maximum near the beaming frequency of the frame, 5.9 Hz. Also, the exhaust stack had a significant effect on vibrations reaching the frame in undamped VOAS-1, evident from the increase in transmissibility at approximately 9 Hz.

For measurements at the B-Post in the vertical direction, input at the frame where the cab mounts was amplified in the frequency range associated with the resonant frequencies of the primary and cab suspensions. Amplification also occurred near the torsional mode of the frame in all three test configurations, as shown in Figure 5-39.

The fore-and-aft B-Post measurements were most sensitive to the resonant frequency of the vehicle primary suspension, as Figure 5-40 shows. Just as the vertical B-Post had increased transmissibility at the torsional bending mode of the frame, so did fore-and-aft B-Post measurements.

Figures 5-41 and 5-42 show the transmissibility at the B-Post, in both directions, as referenced from an input at the cab side of the cab mount. The results are quite similar to the B-post measurements referenced to the frame at the cab mount (aft of the cab). Transmissibility increased around the resonant frequencies of the primary and cab suspensions and showed a marked increase at the torsional mode of the frame.

5.7 Chapter Summary

This chapter gave a description of the measurements, test procedures, and methods of data reduction, followed by the results themselves, for the dynamic testing performed in this study. The next, and final, chapter of this thesis provides a summary of the whole study as well as suggestions for future research in the area of vehicle kinematics and dynamic testing.

Chapter 6

Conclusions

This chapter includes a summary of the study presented in this thesis. It also provides several recommendations for possible future work in the kinematics and dynamic testing of heavy vehicles.

6.1 Summary of the Study

A permanent facility was constructed to support the testing of different heavy truck suspensions. This facility includes a structure that acts as a reaction frame for the kinematics testing and as a conveyance for the weight that is added to the vehicle for the dynamic tests. For actuation of the vehicle suspension, manual actuators were used in the kinematics tests, whereas to excite the vehicle during dynamic tests, a MTS hydraulic actuation system was used. A series of transducers for measuring force, displacement, velocity, and acceleration at various locations on the suspension and the test vehicle were installed. A digital controller and data acquisition system was used to provide several inputs to the actuators and to record the test data.

Two test vehicles were acquired and prepared for testing. The first test vehicle was equipped with VOAS-1, the currently manufactured drive axle suspension. The second vehicle was outfitted with two versions of VOAS-2, a new drive axle suspension. The main difference between the two VOAS-2 suspensions was in the thickness of the trailing-arm used in conjunction with the airspring.

Kinematics tests were performed first. For VOAS-1, and both VOAS-2 drive axles, similar vertical stiffnesses were obtained. VOAS-2 front was only 5% stiffer than VOAS-1 and VOAS-2 rear was only 3% less stiff than VOAS-1. The roll stiffness of VOAS-1 and the VOAS-2 suspension with a thicker trailing-arm differed by only 8%, with VOAS-1 having the larger roll stiffness of the two. The VOAS-2 suspension with the thinner trailing-arm, however, had a much smaller roll stiffness, nearly 40% less than VOAS-1. The roll centers for the three different suspensions, were approximately the same. Although roll steer was not tested on VOAS-1, it was still tested on both versions of VOAS-2. Both had desirable performance, showing a little understeer at full roll.

Based on the kinematics test results, several conclusions can be made concerning the performance of VOAS-2 compared to VOAS-1. The VOAS-2 suspension with a thinner trailing-arm provides a roll stiffness that may be unacceptable for trucks with heavier axle loads. The other version of VOAS-2 (i.e. the one with the thicker trailing-arm) exhibited kinematics characteristics that are quite similar to the currently manufactured VOAS-1, and as such, can be considered as a direct replacement for it.

Three different test configurations were compared using the dynamic testing schedule. These were: VOAS-1 undamped, VOAS-2 undamped, and VOAS-2 damped. All three configurations were on the front drive axle of either test vehicle. Before performing any of the dynamic testing, however, both front and rear drive axles of the VOAS-2 vehicle were outfitted with the thicker trailing-arm configuration. The dynamic testing consisted of three input signals commonly used to excite a body during dynamic analysis: a chirp signal input, a hard bump signal input, and a range of pure tone inputs.

Results from the chirp signal input showed the resonant frequencies of VOAS-1 undamped, VOAS-2 undamped, and VOAS-2 damped to be 1.7 Hz, 1.5 Hz, and 1.6 Hz, respectively. Several other important modes of vibrations were identified with the chirp signal, including the cab resonant frequency, the first beaming mode of the frame, the resonance of the exhaust stack, and the first torsional mode of the frame. Both VOAS-2 configurations showed these modes occurring at the same frequencies, with the exception of the frame beaming and the exhaust stack. Differences between the mounting of VOAS-2 to the frame accounted for a 0.3 Hz increase in the frame beaming frequency. Also, the VOAS-2 vehicle was equipped with two exhaust stacks versus the single exhaust stack on the VOAS-1 vehicle.

Major differences between the two different suspensions were apparent when comparing the vibrations at the B-Post in the cab. In VOAS-1, the frame's beaming and torsional modes dominate the response to vertical acceleration at that location, but in VOAS-2, the resonance of the primary suspension is followed by the resonance of the cab suspension as the major factor. However, fore-and-aft vibration at the B-post is most sensitive to the primary suspension resonant frequency on all three configurations.

The hard bump input gave a good indication of the suspension response to transient inputs, as well as the extent of damping in each of the configurations. High frictional damping was inherent in the design of VOAS-1 and led to a damping ratio of 18 %. On the other hand, the undamped VOAS-2 did not have the same sliding contact as VOAS-1 and damping ratio was reduced to 5 %. This means that VOAS-2 tends to rely more heavily on viscous dampers to control the suspension dynamics due to transient

inputs. The addition of viscous dampers brought the damping ratio of the VOAS-2 up to 44.6 %.

The transmissibility ratios between several vehicle components were determined with the pure tone input. Across the primary suspension, transmissibility was a maximum at the suspension resonant frequency, as expected. Excitations going through the undamped VOAS-2 were amplified almost 4 times at the resonant frequency of its suspension. Transmissibility across the cab suspension, at different locations on the frame, and between both B-Post directions and the cab mount were also studied.

Based on the three dynamic input signals, several conclusions can be drawn about the dynamic performance of VOAS-2 compared to VOAS-1. The resonant frequencies of VOAS-1 and VOAS-2 primary suspensions differed slightly, but not enough to significantly affect the ride quality of the vehicle. Also, with the low friction inherent in the design of VOAS-2, there is a strong reliance on the viscous dampers for reducing wheel hop and transient dynamics of the truck frame. Finally, based on the results of its dynamic performance, VOAS-2 would be a viable replacement for VOAS-1.

6.2 Recommendations for Future Research

This study answered all of the questions posed by the manufacturer at the beginning of the project. In the process of doing this work, however, several interesting phenomena were noticed and new questions developed. As an interest in seeing those questions answered, a few recommendations for future research in the area of heavy vehicle testing are outlined below:

1. Study the dynamic response of the frame in detail. This includes concentrating instrumentation along a single frame rail and observing frequencies around the resonance of the primary suspension, the cab, and the beaming mode of the frame.
2. Incorporate a system for applying excitations to the vehicle without requiring removal of the vehicle wheels.
3. Consider using vibration measurements at the B-Post in the cab as excitation for other studies at the Advanced Vehicle Dynamics Laboratory (AVDL), such as the seat suspension studies.
4. Possibly develop a semi-active or active control system to refine the optimized passive suspension, perhaps with the use of magnetorheological (MR) dampers.

References

1. Gillespie, Thomas D., "Fundamentals of Vehicle Dynamics," Society of Automotive Engineers, Inc., 1992, pp. 125-126, 146-148, 154-157, and 181-184.
2. Gillespie, Thomas D., "Heavy Truck Ride," Society of Automotive Engineers, Inc., 1985, pp. 5, 23, and 39.
3. Brady, Robert N., "Heavy-Duty Truck Suspension, Steering, and Braking Systems," Prentice Hall, 1989, pp. 27, 41, 73-74, and 96.
4. Milliken, William F., and Milliken, Douglas L., "Race Car Vehicle Dynamics," Society of Automotive Engineers, Inc., 1995, pp. 403, 613-614, and 721.
5. Letherwood, Michael D., and Gunter, David D., "Spatial multibody modeling and vehicle dynamics analysis of a high-mobility, heavy cargo transport truck with swing arm suspension," American Society of Mechanical Engineers, Design Engineering Division (Publication) De. v 101 1999. pp. 45-52.
6. Yang, Rakheja, and Stiharu, "Adapting an articulated vehicle to the drivers," American Society of Mechanical Engineers, Design Engineering Division (Publication) De. v 101 1999. pp. 1-13.
7. Cole, D J., and Cebon, D., "Influence of tractor-trailer interaction on assessment of road damaging performance," Proceedings of the Institution of Mechanical Engineers. Part D, Journal of Automobile Engineering. v 212 n 1 1998. pp. 1-10.
8. Borges, Steffen, Schardjin, and Argentino, "About the dynamics of a truck-trailer vehicle," Proceedings of the International Modal Analysis Conference - IMAC. v 2 1998. SEM, Bethel, CT, USA. pp. 1220-1226.

9. Field, Hurtado, Carne, and Dohrmann, “Structural dynamics modeling and testing of the Department of Energy tractor/trailer combination,” Proceedings of the International Modal Analysis Conference - IMAC. v 2 1997. SEM, Bethel, CT, USA. pp. 1994-2000.

10. Lee, Lim, and Kim, “Improving ride quality on the cab suspension of a heavy duty truck,” Commercial Vehicles and Highway Dynamics SAE Special Publications. v 1201 Oct 1996. SAE, Warrendale, PA, USA. pp. 11-15.

11. Knouff, B., and Hurtubise, D., “Advantages of structural composites in class 8 truck suspensions,” Commercial Vehicles and Highway Dynamics SAE Special Publications. v 1201 Oct 1996. SAE, Warrendale, PA, USA. pp. 57-62.

12. Suda, Yoshihiro, and Anderson, Ronald J., “Dynamic characteristics of unconventional, light-weight trucks for high-speed trains.,” Transportation Systems - 1992 American Society of Mechanical Engineers, Dynamic Systems and Control Division (Publication) DSC. Publ by ASME, New York, NY, USA. v 44. pp. 65-74.

13. Kutsche, Raulf, and Becher, “Optimized ride control of heavy vehicles with intelligent suspension control,” Heavy Vehicle and Highway Dynamics SAE Special Publications. v 1308 Nov 1997. SAE, Warrendale, PA, USA. pp. 63-67 973207.

14. Mraz, Stephen J., “It's all in the springs,” Machine Design. v 70 n 8 May 7 1998. pp. 80-82, 84, 86.

15. Tong, Rick T., and Amirouche, Farid, "Truck cab suspension design: Optimization and vibration control," Heavy Vehicle Systems. v 5 n 3-4 1998. pp. 236-260.

16. Tong, Amirouche, and Palkovics, "Ride control - a two state suspension design for cabs and seats," Vehicle System Dynamics. v 33 n SUPPL. 2000. pp. 578-589.

17. Wang, Bor-Tsuen, and Hu, Po-I, "Assessment of the ride quality of a truck-full trailer combination," Heavy Vehicle Systems. v 5 n 3-4 1998. pp. 208-235.

18. Forsen, Anders, "Road-induced longitudinal wheel forces in heavy vehicles," Heavy Duty Vehicle Braking and Steering SAE Special Publications. v 1307 Nov 1997. SAE, Warrendale, PA, USA. pp. 27-37 973260.

19. Blue, Douglas W., and Kulakowski, Bohdan T., "Computer optimization of heavy truck suspension parameters," Road Transport Technology Proceedings of the International Symposium on Heavy Vehicle Weights and Dimensions 1995. Int Forum Road Transp Technol, Ontario, Can.. pp. 517-523.

20. Oueslati, Rakheja, and Sankar, "Study of an active suspension for improved ride quality and reduced dynamic wheel loads," Road Transport Technology Proceedings of the International Symposium on Heavy Vehicle Weights and Dimensions 1995. Int Forum Road Transp Technol, Ontario, Can.. pp. 441-452.

21. Hinzburg, L L., and Nosencoff, M A., "Effect of chassis torsional stiffness and suspension roll stiffness distribution on truck handling," Proceedings of the Institution of Mechanical Engineers. Part D, Journal of Automobile Engineering. v 208 n 1 1994. pp. 69-70.

22. Meirovitch, Leonard, "Elements of Vibration Analysis," McGraw-Hill, Inc., 1986, pp. 30 and 31.

Appendix A

Kinematics Testing Procedure

A.1 Safety Issues

- Always wear safety glasses and gloves when using the impact wrench (hearing protection is suggested as well).
- Gloves are recommended when using the chain hoist.
- Gloves are also recommended during setup and while performing the tests.
- Always chock the front wheels once the vehicle is in position for testing, and before removing any of the wheels or tires.
- Charge the electromagnet on the chain hoist before using it. Push the battery test button on the electromagnet; if the gauge reads less than "Full", the battery needs charging. Plug the charger into the back of the electromagnet, when the light on the charger turns from yellow to green, the battery is fully charged.

A.2 State of the Test Bay

- Crossbeam should be unbolted from the rest of the structure and out of the way.
- Weight plates should be in their floor storage location, with the fifth wheel plate on top.
- Floor and path should be clear of all debris, hoses, cables, or other obstacles that may prevent the test vehicle from safely entering the facility.

A.3 Bring Test Vehicle into Facility

- Test vehicle should have enough fuel to ensure it does not run empty while in the facility.
- Mark locations on the floor to help you guide the vehicle as it is backed into place. Vehicle should be equal space between the two supports and the fifth wheel should be even with the overhead structure. At a later date, it is much easier to adjust the depth of the vehicle in the test rig than it is to adjust where it is located laterally.

A.4 Modifications to Test Vehicle Prior to Testing

- Remove the fifth wheel from the test vehicle, if it is so equipped. After the bolts have been removed and its air line is disconnected, use the hook on the chain hoist to lift the fifth wheel. Then, pull the vehicle forward, lower the fifth wheel onto a pallet, and move it out of the way. Pull the vehicle back into the proper location. Once the fifth wheel is removed, it is also much easier to reach the plumbing for the airsprings.
- Place the 20-ton jack stands under the vehicle frame, between the two drive axles. Bleed the air system slowly. One way to do this is to disconnect the actuation rod for the load-leveler and open the valve to let air escape.
- Remove the actuation rod for the load-leveler and store in a safe location. Secure the valve for the load-leveler at the mid-stroke (horizontal) position.
- Study the plumbing of the air lines for the airsprings; it is separate from the brake lines. For testing purposes, each drive axle must be on an independent air supply from the rest of the vehicle. As they are now, each side of the front and rear drive axle is connected through the load leveler. The easiest way to separate the systems is to use the two long lines, running from front drive axle to rear drive axle, on each frame-rail. Connect each one from one airspring to the other on the same drive axle.
- A regulated air supply hookup must be installed between the fitting and the airspring itself for each drive axle (on one side or the other). Install a tee at this location (3/8 in NPT) and then install the following, in order starting from the tee: a shut-off valve, a regulator, and a nipple for connecting an air hose. This allows each system to be brought up to pressure and then closed. Bring each system up to pressure to check for leaks. Remove the jack stands.
- Use the chain hoist to place the fifth wheel plate on the vehicle frame. The back edge of the fifth wheel plate should be installed 42 inches from the end of the frame. Align the 8 holes in the fifth wheel plate with the existing holes like the ones where the fifth wheel was mounted. Install the bolts and tighten them.
- Pick up the crossbeam with the chain hoist and place it on the fifth wheel plate. Loosely install all the bolts that tie the crossbeam into the rest of the structure. Use the regulated air supplies on the drive axles to lift the frame of the truck, if necessary. Loosely install all the clamps that attach the crossbeam to the fifth wheel plate. The vehicle may have to be rolled forward

or backward to align the holes. Tighten the clamps and then tighten the crossbeam to the rest of the structure.

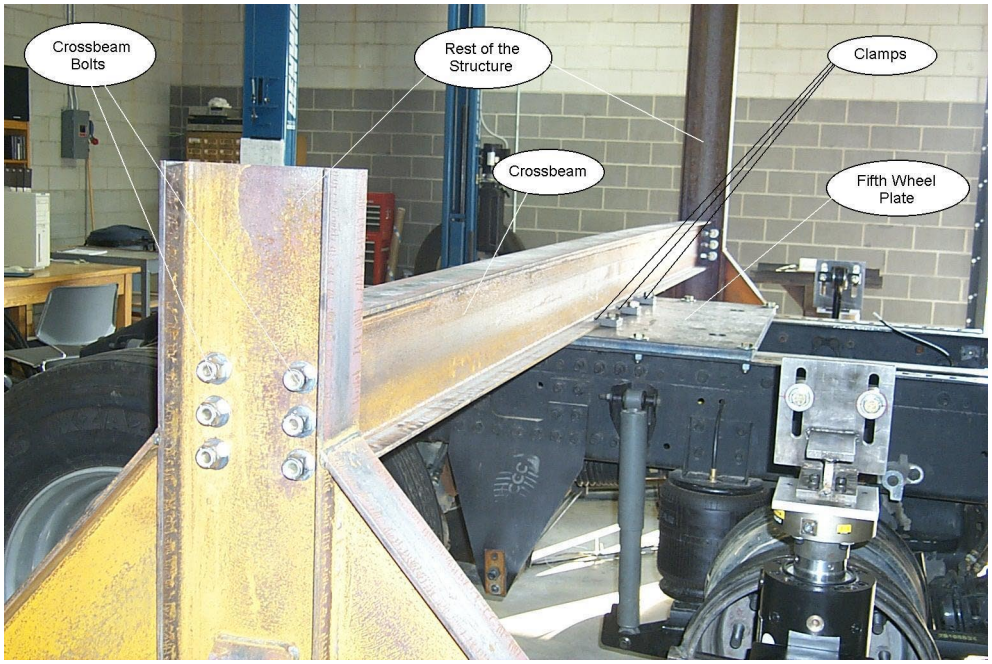

A.5 Choose a Drive Axle to Test

- From now on, "the axle" refers to the axle to be tested, as no other actions are performed on the other axle.
- Bleed the airsprings on the axle. Use the air jack to lift the suspension just enough that the tires barely touch the ground. Remove the wheels from that axle and store them out of the way. The impact wrench will have to be on the highest setting and it will still take some time on each lug nut. After removing the wheels, keep at least one lug nut hand tight against the brake drum on each axle until ready to assemble the actuation system.
- Support the axle at both ends before removing the air jack. The modified brake drums for dynamic testing work well if a piece of wood is placed between the axle and the modified drum.

A.6 Assemble the Actuation System

The following steps refer to each side of the axle. Perform the same task on each side, for each step, before continuing.

- Remove all lug nuts from the axle. Mount a modified brake drum for kinematics testing to the axle with the open side down (two bolt holes horizontal). The axle can be rotated by hand if the air brake is released (make sure front wheels are chocked before doing this). Only eight of the ten lug nuts will be accessible, but that is okay.
- Mount the shortened torque rod to the modified brake drum. Use the steel spacers and position the torque rod with the cut end facing down.

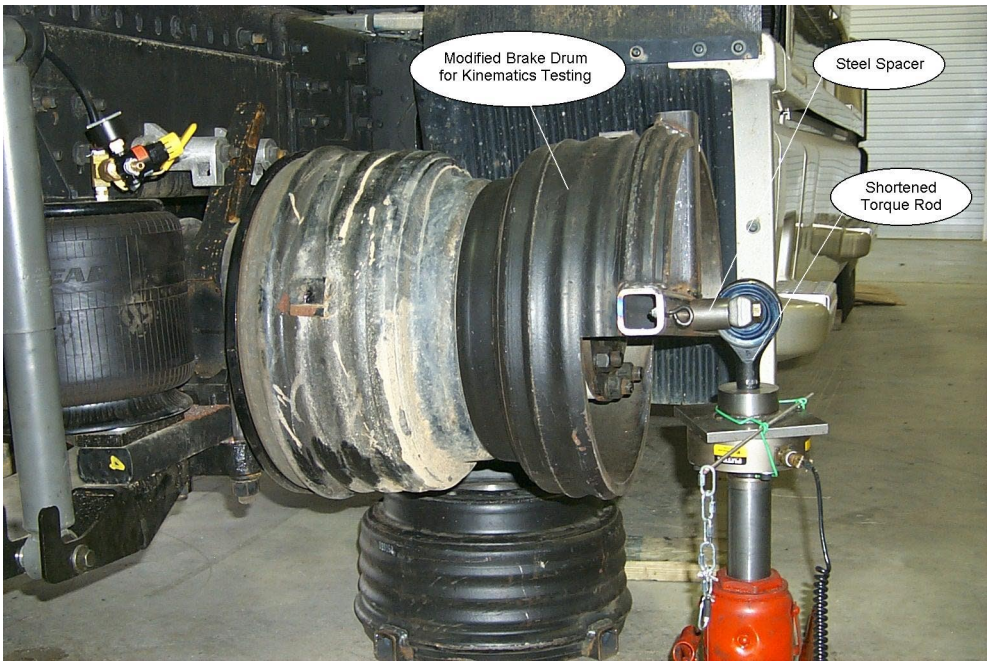

- Place one of the 1 in steel plates (not one of the weight plates) under the axle end. Set the ½ in rollers (5 of them) on the plate, parallel to the vehicle frame. Next, set the ¼ in plate (with LVDT mounting holes) on the rollers.
- Mount the load cell to the top of the modified hydraulic jack and mount the torque rod-to-load cell adapter to the load cell. Place these components on the ¼ in plate and lift the jack until the torque rod is fully seated in the adapter. The torque rod has to be straight down or it will be difficult to fit the adapter. Use a hammer to align the torque rod, if necessary.

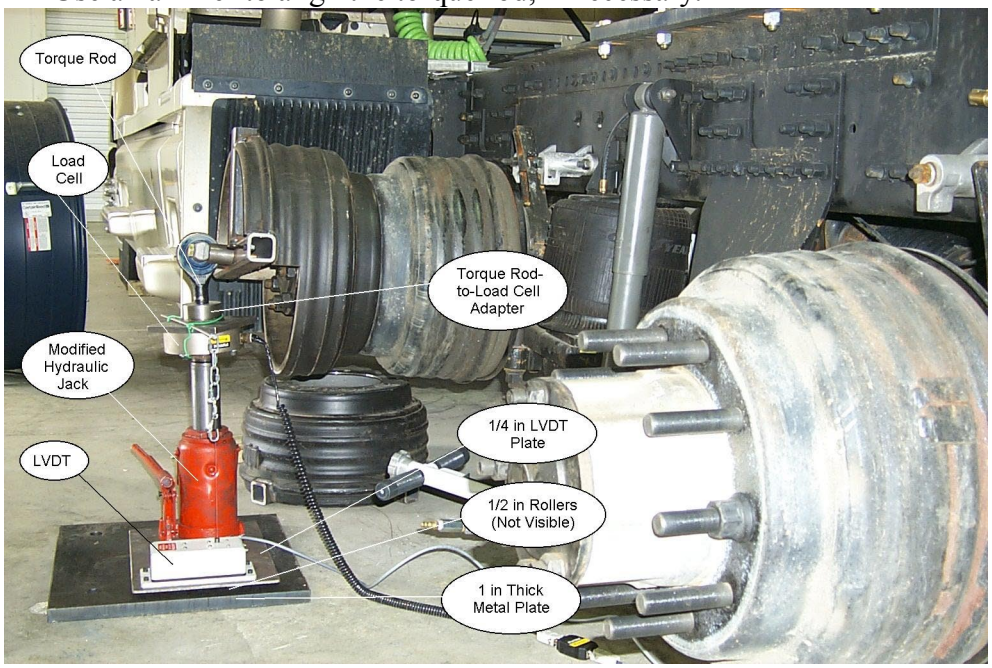

A.7 Instrument the Test Vehicle

- Mount an LVDT horizontally to the ¼ in plate on each side of the axle. Attach the string to the torque rod, adapter, or modified brake drum so that displacement of the hydraulic jack (and hence the end of axle, vertically) can be measured. (NOTE: Be careful that the LVDT string does not snap back into the LVDT after extending it.)
- Mount an LVDT vertically to a stand and attach the string to the center of the axle housing (or as close as possible). This will measure lateral displacement of the axle housing.

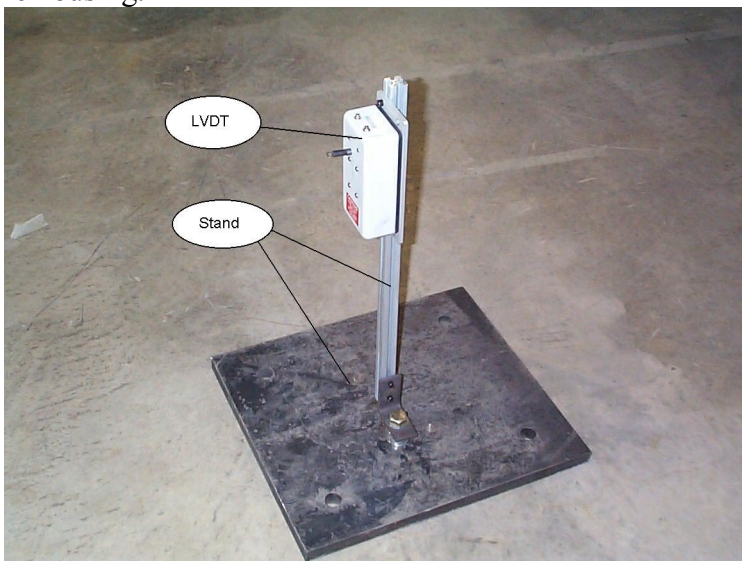

- For the roll steer tests, mount LVDTs to vertical stands and attach the strings to the modified brake drum on each side of the axle to measure displacement longitudinally.
- Hook up all cables for the LVDTs and the load cells, as well as their power supplies. Plug all the BNC connections into the box attached to the computer with the NIDAQ card.
- Set up the Labview code, input the sensitivity of each instrument, and test them. While plotting output, pull on the strings to check the LVDTs and push down on the load cells to check those.

A.8 Perform the Tests

These tests can be performed in any order. Each measurement point is the average of ten samples in five seconds.

a) Vertical Stiffness

1) Lift up each side of the axle with the hydraulic jacks until anything supporting the axle ends can be removed.
2) With the jacks even and with the suspension at ride height, set the air pressure of the suspension (this is the pressure when the axle is fully loaded and at ride height).
3) Lower the axle, 1 in at a time with each of the jacks, until the axle rests 2 in below ride height on both sides.

4) Record the first measurement point at this position. Vertical displacement (both sides), vertical force (both sides), and lateral displacement of the axle center are all measured statically at this point.
5) Raise the axle ¼ in on both sides and take another measurement.
6) Repeat this until the axle is 2 in above ride height (17 measurement points total).
7) Place supports under the axle ends and lower the axle onto them.
8) This test is complete.

b) Roll Stiffness

1) Repeat steps 1 and 2 from the Vertical Stiffness Test.
2) Record the distance between the vertical displacement LVDTs.
3) Raise the passenger side of the axle and lower the driver side, 1 in at a time with each jack. Do this until the axle is raised 2 in above ride height on the passenger side and 2 in below on the driver side (this is full roll, positive).

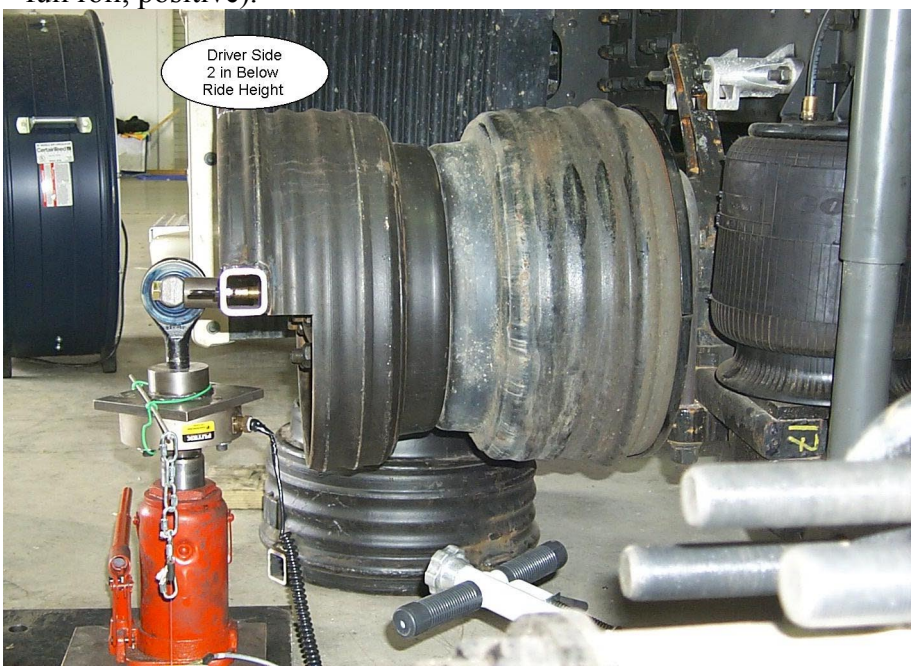

4) Record the first measurement point at this position. Vertical displacement (both sides), vertical force (both sides), and lateral displacement of the axle center are all measured statically at this point.
5) Lower the passenger side ¼ in, raise the driver side ¼ in, and take another measurement. Repeat this step until step 6, below, applies.
6) When the driver side is 2 in above ride height and the passenger side is 2 in below (this is full roll, negative), change the direction of the roll and continue taking measurements.
7) Proceed until the passenger side is 2 in above ride height and the driver is 2 in below (full roll, positive). Change the direction of the roll and continue taking measurements until step 8, below, applies.

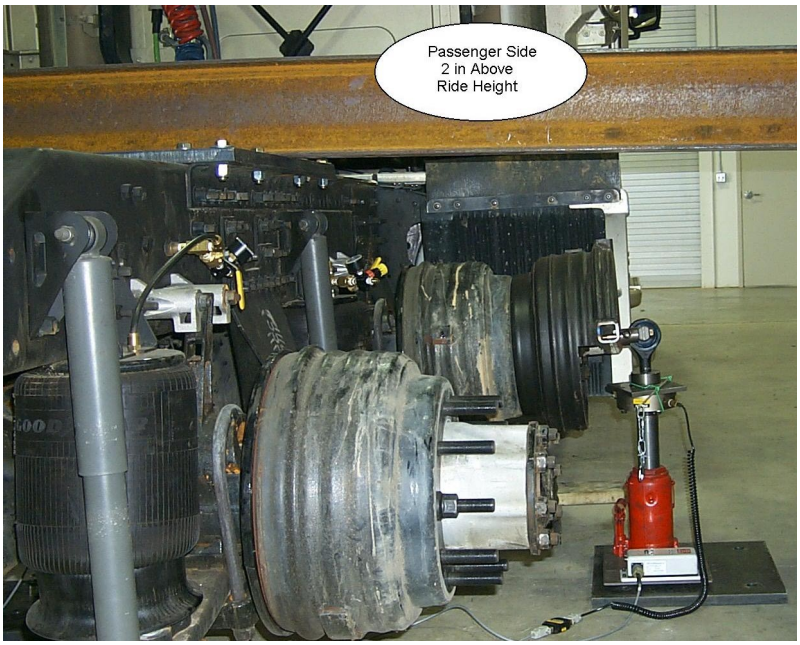

8) When the axle reaches ride height at each end (zero roll), take the last measurement (41 measurement points total).
9) Place supports under the axle ends and lower the axle onto them.
10) This test is complete.

c) Roll Steer

1) Repeat steps 1-3 from the Roll Stiffness Test.
2) Record the first measurement point at this position. Vertical displacement (both sides), vertical force (both sides), and longitudinal displacement (both sides) are all measured statically at this point.
3) Lower the passenger side 1 in, raise the driver side 1 in, and take another measurement. Repeat this step until step 4, below, applies.
4) When the driver side is 2 in above ride height and the passenger side is 2 in below (this is full roll, negative), change the direction of the roll and continue taking measurements.
5) Proceed until the passenger side is 2 in above ride height and the driver is 2 in below (full roll, positive). Change the direction of the roll and continue taking measurements until step 6, below, applies.
6) When the axle reaches ride height at each end (zero roll), take the last measurement (11 measurement points total).
7) Place supports under the axle ends and lower the axle onto them.
8) This test is complete.

A.9 Analyze the Data

The data analysis can be performed in any order. Microsoft Excel was used to perform the analysis on the data and to generate the plots for each test.

a) Vertical Stiffness

1) Each measurement point has its own file. So each one is opened and copied into a single spreadsheet.
2) The measurements are organized in columns, from dropping the suspension (rebound) to raising the suspension (jounce).
3) The data is converted from English to Metric units.
4) Using the data, the displacements and loads are referenced as a difference from those at ride height (zeroing ride height).
5) The average difference in displacement (between driver and passenger sides) is calculated at each measurement point.
6) The load is summed between driver and passenger sides.
7) The stiffness of the crossbeam is considered.
8) Finally, the data is plotted as the difference in total load (from ride height) with respect to the difference in displacement (from ride height). Vertical stiffness is the slope of this curve.

b) Roll Stiffness

1) Each measurement point has its own file. So each one is opened and copied into a single spreadsheet.
2) The measurements are organized in columns as the axle is rolled from a positive roll angle (passenger side above ride height and driver below), to negative roll, through positive roll again, and back to zero roll.
3) The actual roll angles are calculated.
4) The data is converted from English to Metric units.
5) The roll center height is calculated.
6) As referenced from ride height, the change in torque on the axle is calculated (zero roll is zero torque, maximum torque occurs at the extents of roll).
7) The change in torque is plotted against the roll angle. The slope of this curve is the roll stiffness. The plot will show a characteristic hysteresis loop as expected with a leaf spring.

c) Roll Steer

1) Each measurement point has its own file. So each one is opened and copied into a single spreadsheet.
2) The measurements are organized in columns as the axle is rolled from a positive roll angle (passenger side above ride height and driver side below), to negative roll, through positive roll again, and back to zero roll.
3) The roll and the yaw angles are calculated.
4) The data is converted from English to Metric units.

5) Roll steer is plotted as yaw angle versus roll angle.
6) Since the points measured in a roll steer test overlap some of those measured in a roll stiffness test, the data at those points are compared for repeatability. Repeatability is plotted as total load versus measurement point position for the two different tests.

A.10 Run More Tests or Return Vehicle to its Original Configuration and Remove from the Lab

Appendix B

Dynamic Testing Procedure

B.1 Safety Issues

- Always wear safety glasses and gloves when using the impact wrench (hearing protection is suggested as well).
- Gloves are recommended when using the chain hoist.
- Gloves are also recommended during setup and while performing the tests.
- Always chock the front wheels once the vehicle is in position for testing, and before removing any of the wheels or tires.
- Charge the electromagnet on the chain hoist before using it. Push the battery test button on the electromagnet; if the gauge reads less than "Full", the battery needs charging. Plug the charger into the back of the electromagnet, when the light on the charger turns from yellow to green, the battery is fully charged.

B.2 State of the Test Bay

- Crossbeam should be unbolted from the rest of the structure and out of the way.
- Weight plates should be in their floor storage location, with the fifth wheel plate on top.
- Floor and path should be clear of all debris, hoses, cables, or other obstacles that may prevent the test vehicle from safely entering the facility.

B.3 Bring Test Vehicle into Facility

- Test vehicle should have enough fuel to ensure it does not run empty while in the facility.
- Mark locations on the floor to help you guide the vehicle as it is backed into place. Vehicle should be equal space between the two supports and the fifth wheel should be even with the overhead structure. At a later date, it is much easier to adjust the depth of the vehicle in the test rig than it is to adjust where it is located laterally.

B.4 Modifications to Test Vehicle Prior to Testing

- Remove the fifth wheel from the test vehicle, if it is so equipped. After the bolts have been removed and its air line is disconnected, use the hook on the chain hoist to lift the fifth wheel. Then, pull the vehicle forward, lower the fifth wheel onto a pallet, and move it out of the way. Pull the vehicle back into the proper location. Once the fifth wheel is removed, it is also much easier to reach the plumbing for the airsprings.

- Place the 20-ton jack stands under the vehicle frame, between the two drive axles. Bleed the air system slowly. One way to do this is to disconnect the actuation rod for the load-leveler and open the valve to let air escape.
- Remove the actuation rod for the load-leveler and store in a safe location. Secure the valve for the load-leveler at the mid-stroke (horizontal) position.
- Study the plumbing of the air lines for the airsprings; it is separate from the brake lines. For testing purposes, each drive axle must be on an independent air supply from the rest of the vehicle. As they are now, each side of the front and rear drive axle is connected through the load leveler. The easiest way to separate the systems is to use the two long lines, running from front drive axle to rear drive axle, on each frame-rail. Connect each one from one airspring to the other on the same drive axle.
- A regulated air supply hookup must be installed between the fitting and the airspring itself for each drive axle (on one side or the other). Install a tee at this location (3/8 in NPT) and then install the following, in order starting from the tee: a shut-off valve, a regulator, and a nipple for connecting an air hose. This allows each system to be brought up to pressure and then closed. Bring each system up to pressure to check for leaks. Do not remove the jack stands at this time.
- Use the chain hoist to place the fifth wheel plate on the vehicle frame. The back edge of the fifth wheel plate should be installed 42 in from the end of the frame. Align the 8 holes in the fifth wheel plate with the existing holes like the ones where the fifth wheel was mounted. Install the bolts and tighten them.
- Pick up each weight plate individually with the chain hoist and place it on the fifth wheel plate. Take care to line up the four large holes; use a piece of material or something else as a pry-bar. Once several plates have been loaded, moving the ones on the bottom is nearly impossible. When all the plates are loaded, bolt them to the fifth wheel plate.

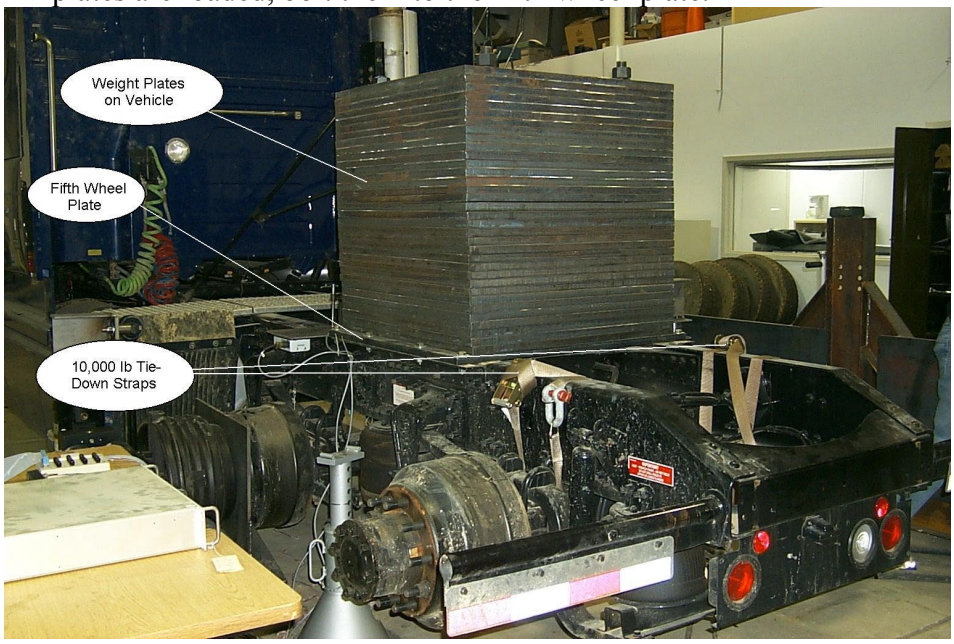

B.5 Choose a Drive Axle to Test

- Once the drive axle to be tested is chosen, go to the other drive axle (the one not being tested) and bleed its air system. Use the air jack to lift the suspension just enough that the tires barely touch the ground. Remove the wheels from that axle and store them out of the way. The impact wrench will have to be on the highest setting and it will still take some time on each lug nut. After removing the wheels, keep at least one lug nut hand tight against the brake drum on each axle end. Lift the axle up with the air jack until it is about 2 inches away from bottoming out. Use one 10,000 lb tie down strap to strap each side of the axle to the frame-rail. Secure the ends of each tie down strap and remove the air jack. No other action will be performed on this axle.
- Keep in mind that the vehicle frame and the significant additional weight are still supported by the jack stands. Go to the drive axle to be tested. Bleed its air system and follow the same procedures listed above for removing the wheels. Once they are removed, keep at least one lug nut hand tight against the brake drum on each axle end until ready to assemble the actuation system. Leave the air jack in place until that time.
- From now on, "the axle" refers to the axle to be tested, as no other actions are performed on the other axle.

B.6 Assemble Actuation System

The following steps refer to each side of the axle. Perform the same task on each side, for each step, before continuing.

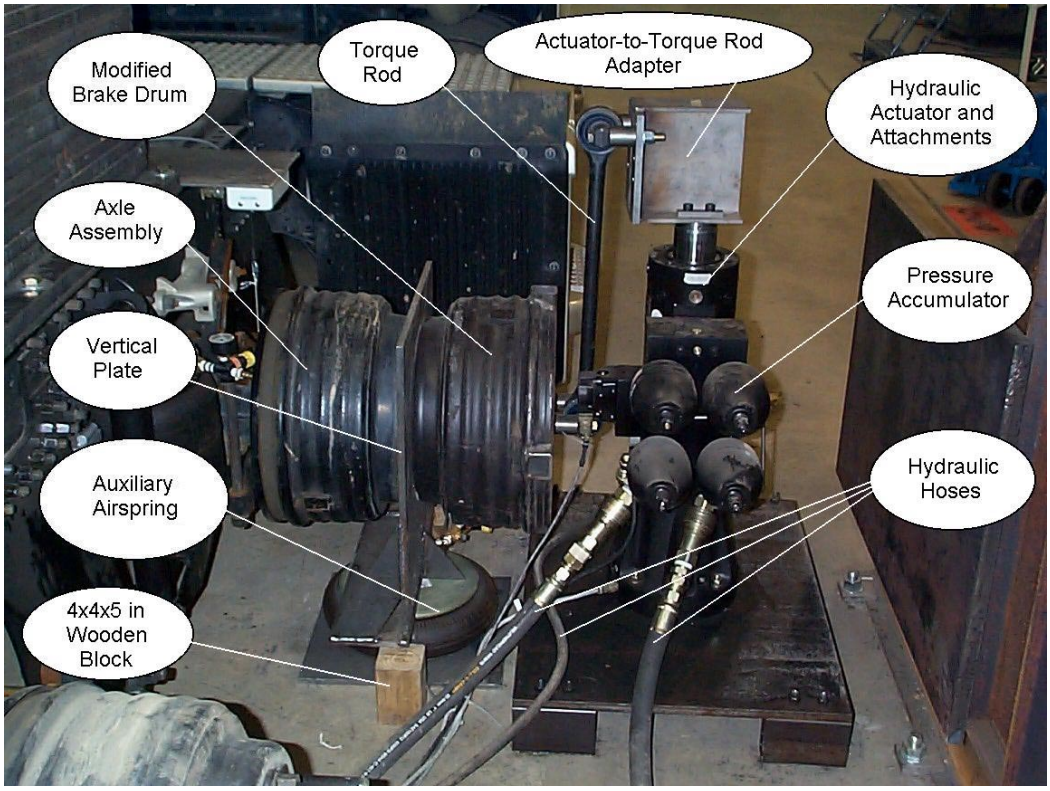

- Remove all lug nuts from the axle. Mount the auxiliary airspring and the vertical plate to which it is attached. The supports on the vertical plate face the vehicle frame. Use a small amount of air (there is no load) to lift the vertical plate to get it to align with the studs on the axle.
- Mount a modified brake drum for dynamic testing to the axle with the two boltholes horizontal. The axle can be rotated by hand if the air brake is released (make sure front wheels are chocked before doing this). Only eight of the ten lug nuts will be accessible, but that is okay.
- Once the modified brake drum and the auxiliary airspring are mounted, place two pieces of wood (4 in x 4 in stock, 5 in long) between the flange and the floor. When these four supports are in place (on both sides of the axle), the air jack can be removed.
- Mount the full-length torque rods to the modified brake drum. Use the steel spacers and position the torque rod up.
- Place hydraulic actuator in front of the axle end, with the pressure accumulators pointing toward the rear of the vehicle (this is so the fittings for the hydraulic hoses are pointed toward the pump).
- Hook up all three hydraulic hoses (1 pressure, 1 return, and 1 drain) to the actuator, taking care to make the right connections.
- Connect the three control and measurement cables to the actuator.
- Mount the actuator-to-torque rod adapter to the top of the hydraulic actuator.
- Turn on the power to the cabinet, and thus the 458 Hydraulic Controller.

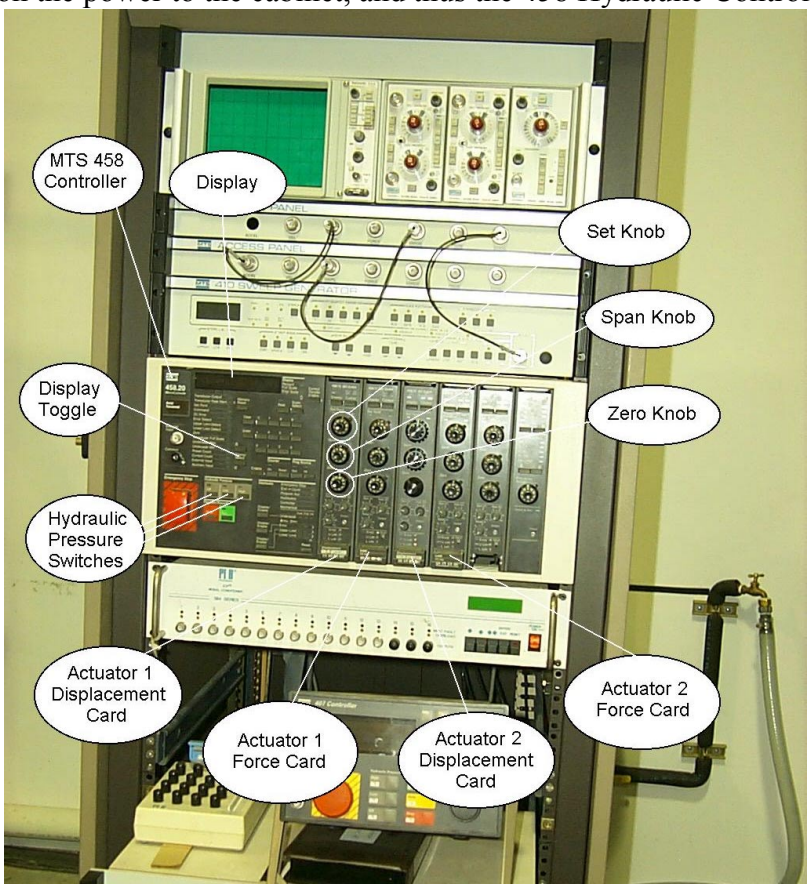

- Toggle the main display select to "DC Error" and select display on one of the actuator displacement modules. Use the "Set" knob on the actively displayed module to set the DC Error to zero (at least 0.000X). Do this for the other displacement module. This must be done BEFORE turning on the hydraulic pressure or the actuators will “jump”, along with the test vehicle.
- Use the controller to lift the actuators, and move their bases as necessary to line up the mounting holes of the torque rod with those of the actuator adapter. Install the bolts and metal spacers.
- When properly installed, the centerline of the actuators corresponds with the centerline of the torque rod, when viewed from the side of the vehicle. This correctly implies that the torque rod should be vertical in both planes, when referenced to the vehicle.

B.7 Instrument the Test Vehicle

- The hydraulic actuators are already instrumented to give displacement and load at each axle end (assuming all three cables are attached to each one).
- Install an LVDT on each frame-rail, directly above the axle. Use the ¼ in plate with the boltholes for an LVDT and use a C-clamp to hold the plate to the frame-rail. Position each LVDT with the string pointing down, 7 inches from the side of the frame. Attach the string to the axle to measure relative velocity between the frame and the axle. Since the LVDTs are installed upside-down, use a correction factor of "-1” in the Simulink model.

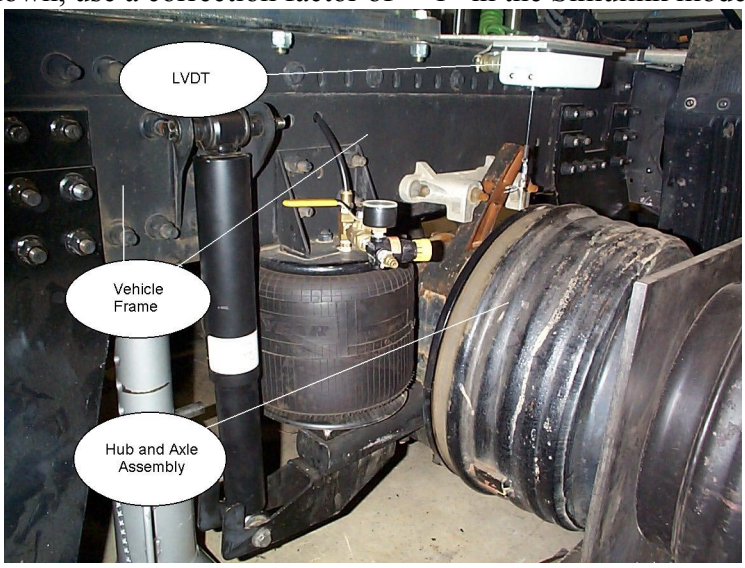

- There are several accelerometers installed on the vehicle. Any that are mounted upside-down will require a correction factor in the model. Two are mounted on the bottom of the frame-rail, one over each side of the axle. These accelerometers are located at the intersection of the frame flange center and the axle centerline. Two accelerometers are located at the cab mount, one mounted on the frame side and the other on the cab side (one directly above the other, upside-down). Align these on the vehicle centerline and as close to the rear-most edge of the cab at the cab suspension. Two accelerometers are mounted in the cab to take biaxial measurements (vertical and fore-and-aft).

Attach the biaxial accelerometers at the seat belt anchor after removing the plastic bolt cover.

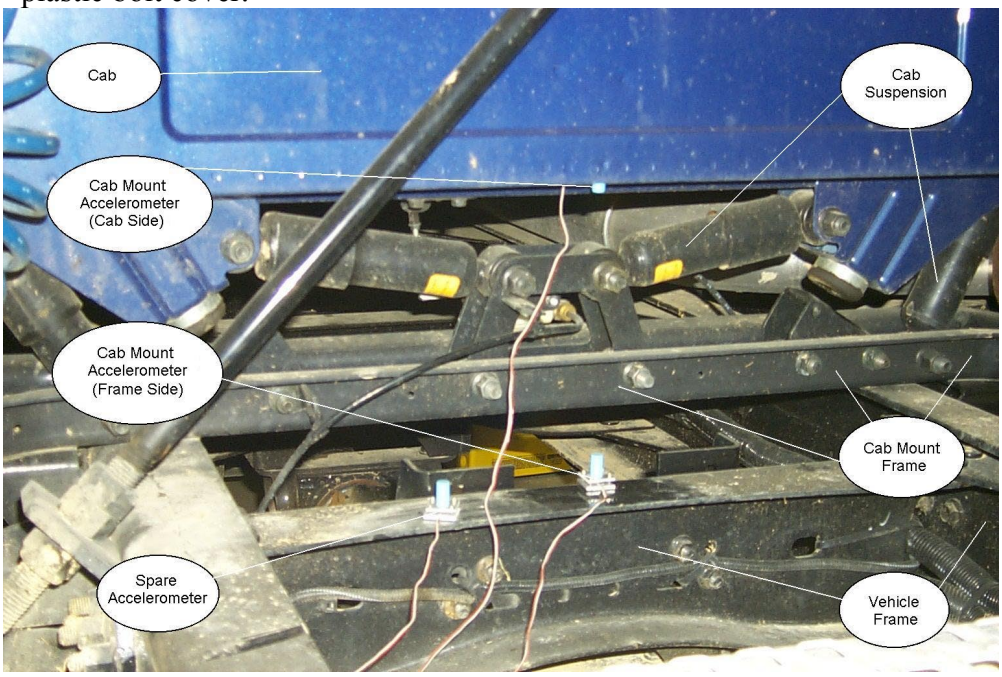

- Use the ICP signal conditioner to power the accelerometers and to gain their signals. To increase the resolution of the output, use a gain of 100 for each active channel.
- Route the BNC cables from the conditioner, the LVDTs, and from the 458 Controller to the dSpace AutoBox.
- Set up the Simulink model for each test signal with the proper sensitivity, position, and gain corrections for all the instruments. Make sure the signal gain is zero in the model so that the actuators do not receive a signal before they should. Test the output on each instrument.

B.8 Perform the Tests

These tests can be performed in any order, but the order listed here is suggested. All three tests can be run one after the other without starting over, but the ride height must be checked after each test. Each response is measured with a 200 Hz sampling frequency and the "ode5" solver in Matlab. For undamped tests, remove the dampers prior to testing.

1) Turn on the ventilation fans and start the vehicle. Run the vehicle until the air pressure is normal (120 psi). This is so that the response of the cab suspension will be accurate. Turn off the vehicle when 120 psi is reached.
2) Turn on the cabinet power to turn on the 458 controller and signal conditioner.
3) Set the DC Error of the hydraulic actuators (displacement) to zero and turn on the hydraulic pressure (low pressure first, then high pressure).
4) Raise the actuators until the pieces of wood can be removed from each side of the axle (be careful not to exceed 4000 lbs on either actuator). If the wooden

blocks are still immovable, add air to the auxiliary airsprings (without exceeding 100 psi).

5) Return the actuators to zero displacement (transducer output). Zero displacement is measured as 3 in from the top of the actuator to the bottom of the adapter.
6) Add air pressure on the auxiliary airsprings (80 psi max), but make sure the force on each actuator does not go below 400 lbs. If the load falls below 400 lbs, the actuators may move out of position.
7) Add air to the axle airsprings (up to 110 psi max) to bring the frame off of the jack stands. Check the load on the actuators by displaying the transducer output (on the 458 controller) on each actuator force module to ensure they do not become overloaded (4000 lbs max). Remove the jack stands.
8) Reset the actuators to zero displacement and set the air pressure on the auxiliary airsprings to 75 psi, on each side.
9) Measure from the bottom of the frame rail to the weld seam on both the front and the back of the axle housing. Average this number to get the ride height (for this study it was 181 mm or 7.125 in). Set the ride height of the axle by either adding or releasing air in the suspension.
10) Open the pure tone input Simulink file in Matlab, select "Tools", and then "RTW Build" to download the model to the AutoBox. Open the layout for the pure tone signal in dSpace Control Desk. Make sure the BNC box is plugged into the back of the AutoBox.
11) Set the waveform amplitude to 1.0, the waveform frequency to 1.0, and set the span to zero for both actuators (on the 458 controller).
12) Bring the input gain up to 0.25 and slowly increase the span on each actuator until motion of the vehicle is measurable (try to keep them as even as possible).
13) With an input gain of 1.0, the span of each actuator should be +/- 0.2 in (5.08 mm) for a 1 Hz pure tone signal.
14) Bring the input gain down to zero and close the layout, the system is ready for testing.

a) Chirp Signal

1) Check the ride height.
2) Open the chirp input Simulink file and build it into dSpace Control Desk. Set up the layout for the chirp signal in dSpace. Make sure the BNC box is plugged into the back of the AutoBox.
3) Bring the input gain up to 0.25 very slowly and check the vehicle motion.
4) When the signal pauses (for 4 seconds), start a new capture, 68 seconds long. Leave the auto-repeat option turned on.
5) View the signal in the window to make sure that it is complete (zero amplitudes on either side of the input signal in the input signal monitor window). When it is, slowly increase the gain to the maximum value for the specific test (for this study, we used 1.0, however, lower gains are recommended). Watch the vehicle closely to ensure that the gain

for the signal is not too high (excessive travel of the suspension or other phenomena that may be endanger bystanders or test equipment).

6) When a new signal starts, turn off the auto-repeat option and wait for the signal to finish. Slowly bring down the input gain to zero.
7) Save the capture as a new file and close the layout. This test is complete.

b) Hard Bump

11) Check the ride height.
12) Open the hard bump input Simulink file and build it into dSpace Control Desk. Set up the layout for the hard bump signal in dSpace. Make sure the BNC box is plugged into the back of the AutoBox.
13) Bring the input gain up to 0.05 very slowly and check the vehicle motion.
14) When the square wave is at zero, start a new capture, 60 seconds long. Leave the auto-repeat option turned on.
15) View the signal in the window to make sure that there is one complete wave. When there is, wait for the signal to start over. Quickly set the gain to 0.5, turn off auto-repeat, and wait for the signal to finish.
16) Slowly bring down the input gain to zero. Save the capture as a new file and close the layout. This test is complete.

c) **Pure Tone Signal(s)**

9) Check the ride height.
10) Open the pure tone input Simulink file and build it into dSpace Control Desk. Set up the layout for the pure tone signal in dSpace. Make sure the BNC box is plugged into the back of the AutoBox.
11) Bring the input gain up to 0.25 very slowly and check the vehicle motion.
12) Start a new capture, 10 seconds long. Turn the auto-repeat option off.
13) Bring the frequency up to 1.2 Hz, and the gain up to 1.0, slowly.
14) Collect a new capture and save it as a new file.
15) Increase the frequency to 1.3 Hz, leave the gain at 1.0, collect a new capture, and save it as a new file.
16) Increase the frequency to 1.4 Hz, leave the gain at 1.0, collect a new capture, and save it as a new file.
17) Increase the frequency to 1.45 Hz, leave the gain at 1.0, collect a new capture, and save it as a new file.
18) Reduce the gain to 0.9, increase the frequency to 1.5 Hz, collect a new capture, and save it as a new file.
19) Reduce the gain to 0.8, increase the frequency to 1.6 Hz, collect a new capture, and save it as a new file.
20) Increase the frequency to 1.65 Hz, leave the gain at 0.8, collect a new capture, and save it as a new file.
21) Increase the frequency to 1.7 Hz, leave the gain at 0.8, collect a new capture, and save it as a new file.

22) Increase the frequency to 1.8 Hz, leave the gain at 0.8, collect a new capture, and save it as a new file.
23) Reduce the gain to 0.75, increase the frequency to 3.0 Hz, collect a new capture, and save it as a new file.
24) Reduce the gain to 0.5, increase the frequency to 5.9 Hz, collect a new capture, and save it as a new file.
25) Reduce the gain to 0.25, increase the frequency to 8.8 Hz, collect a new capture, and save it as a new file.
26) Increase the frequency to 11.0 Hz, leave the gain at 0.25, collect a new capture, and save it as a new file.
27) Reduce the gain to 0.125, increase the frequency to 13.6 Hz, collect a new capture, and save it as a new file.
28) Reduce the gain to 0.080, increase the frequency to 16.5 Hz, collect a new capture, and save it as a new file.

B.9 Analyze the Data

The data analysis can be performed in any order. Matlab was used to perform the analysis on the data and to generate the plots for each test.

a) Chirp Signal

1) Load the chirp data file.
2) Determine Δt, the number of samples, and the period from the data.
3) Specify the number of FFT points and set up the frequency vector.
4) Convert the data from English to Metric units.
5) Rename the indices of the data file with descriptive names.
6) Calculate the frequency response of all the acceleration and relative velocity data.
7) Plot the input signal versus time.
8) Plot relative velocity and acceleration versus frequency.

b) Hard Bump Signal

1) Load the chirp data file.
2) Determine Δt from the data.
3) Convert the data from English to Metric units.
4) Rename the indices of the data file with descriptive names.
5) Plot the input signal, force, displacement, relative velocity, and acceleration versus time.

c) Pure Tone Signal

1) Load one of the pure tone data files.
2) Determine Δt from the data.
3) Convert the data from English to Metric units.
4) Rename the indices of the data file with descriptive names.
5) Plot the input signal, force, displacement, relative velocity, and acceleration versus time.

6) Repeat for each frequency.

B.10 Run More Tests or Return Vehicle to its Original Configuration and Remove from the Lab

Vita

Jeffrey L. Glass was born on November 3, 1977 in Staunton, Virginia. In 1995, he graduated first in his class at Fort Defiance High School. He went on to attend Virginia Tech, where in 1999, he earned a Bachelor of Science in Mechanical Engineering with honors. He chose to remain at Virginia Tech after graduating to pursue a Master of Science degree in Mechanical Engineering. His research for this degree took place in the Advanced Vehicle Dynamics Lab (AVDL) of Virginia Tech. In this lab, he studied the kinematics and dynamic analysis of heavy truck suspensions. He earned his M.S. degree in May 2001 and moved to Michigan shortly thereafter to begin working for General Motors.